

1992

Investigation of the pathways leading to reversible and irreversible inactivation of horseradish peroxidase.

Kathy J. Baynton
University of Windsor

Follow this and additional works at: <http://scholar.uwindsor.ca/etd>

Recommended Citation

Baynton, Kathy J., "Investigation of the pathways leading to reversible and irreversible inactivation of horseradish peroxidase." (1992). *Electronic Theses and Dissertations*. Paper 2510.

This online database contains the full-text of PhD dissertations and Masters' theses of University of Windsor students from 1954 forward. These documents are made available for personal study and research purposes only, in accordance with the Canadian Copyright Act and the Creative Commons license—CC BY-NC-ND (Attribution, Non-Commercial, No Derivative Works). Under this license, works must always be attributed to the copyright holder (original author), cannot be used for any commercial purposes, and may not be altered. Any other use would require the permission of the copyright holder. Students may inquire about withdrawing their dissertation and/or thesis from this database. For additional inquiries, please contact the repository administrator via email (scholarship@uwindsor.ca) or by telephone at 519-253-3000ext. 3208.



National Library
of Canada

Acquisitions and
Bibliographic Services Branch

395 Wellington Street
Ottawa, Ontario
K1A 0N4

Bibliothèque nationale
du Canada

Direction des acquisitions et
des services bibliographiques

395, rue Wellington
Ottawa (Ontario)
K1A 0N4

Your file *Votre référence*

Our file *Nôtre référence*

NOTICE

The quality of this microform is heavily dependent upon the quality of the original thesis submitted for microfilming. Every effort has been made to ensure the highest quality of reproduction possible.

If pages are missing, contact the university which granted the degree.

Some pages may have indistinct print especially if the original pages were typed with a poor typewriter ribbon or if the university sent us an inferior photocopy.

Reproduction in full or in part of this microform is governed by the Canadian Copyright Act, R.S.C. 1970, c. C-30, and subsequent amendments.

AVIS

La qualité de cette microforme dépend grandement de la qualité de la thèse soumise au microfilmage. Nous avons tout fait pour assurer une qualité supérieure de reproduction.

S'il manque des pages, veuillez communiquer avec l'université qui a conféré le grade.

La qualité d'impression de certaines pages peut laisser à désirer, surtout si les pages originales ont été dactylographiées à l'aide d'un ruban usé ou si l'université nous a fait parvenir une photocopie de qualité inférieure.

La reproduction, même partielle, de cette microforme est soumise à la Loi canadienne sur le droit d'auteur, SRC 1970, c. C-30, et ses amendements subséquents.

Canada

INVESTIGATION OF THE PATHWAYS LEADING TO
REVERSIBLE AND IRREVERSIBLE INACTIVATION OF
HORSERADISH PEROXIDASE

By

Kathy J. Baynton

A thesis submitted to the
Faculty of Graduate Studies and Research
through the Department of Chemistry and
Biochemistry
in partial fulfillment of the requirements for the
Degree of Master of Science
at the University of Windsor

Windsor, Ontario, Canada.
1992

(c) 1992 Kathy Baynton



National Library
of Canada

Bibliothèque nationale
du Canada

Acquisitions and
Bibliographic Services Branch

Direction des acquisitions et
des services bibliographiques

395 Wellington Street
Ottawa, Ontario
K1A 0N4

395, rue Wellington
Ottawa (Ontario)
K1A 0N4

Your file *Votre référence*

Our file *Notre référence*

The author has granted an irrevocable non-exclusive licence allowing the National Library of Canada to reproduce, loan, distribute or sell copies of his/her thesis by any means and in any form or format, making this thesis available to interested persons.

L'auteur a accordé une licence irrévocable et non exclusive permettant à la Bibliothèque nationale du Canada de reproduire, prêter, distribuer ou vendre des copies de sa thèse de quelque manière et sous quelque forme que ce soit pour mettre des exemplaires de cette thèse à la disposition des personnes intéressées.

The author retains ownership of the copyright in his/her thesis. Neither the thesis nor substantial extracts from it may be printed or otherwise reproduced without his/her permission.

L'auteur conserve la propriété du droit d'auteur qui protège sa thèse. Ni la thèse ni des extraits substantiels de celle-ci ne doivent être imprimés ou autrement reproduits sans son autorisation.

ISBN 0-315-78859-3

Canada

Name _____

Dissertation Abstracts International is arranged by broad, general subject categories. Please select the one subject which most nearly describes the content of your dissertation. Enter the corresponding four-digit code in the spaces provided.

0 4 8 7

U·M·I

SUBJECT TERM

SUBJECT CODE

Subject Categories

THE HUMANITIES AND SOCIAL SCIENCES

COMMUNICATIONS AND THE ARTS
 Architecture 0729
 Art History 0377
 Cinema 0900
 Dance 0378
 Fine Arts 0357
 Information Science 0722
 Journalism 0391
 Library Science 0399
 Mass Communications 0708
 Music 0413
 Speech Communication 0459
 Theater 0465

EDUCATION
 General 0515
 Administration 0514
 Adult and Continuing 0516
 Agricultural 0517
 Art 0273
 Bilingual and Multicultural 0282
 Business 0688
 Community College 0275
 Curriculum and Instruction 0727
 Early Childhood 0518
 Elementary 0524
 Finance 0277
 Guidance and Counseling 0519
 Health 0680
 Higher 0745
 History of 0520
 Home Economics 0278
 Industrial 0521
 Language and Literature 0279
 Mathematics 0280
 Music 0522
 Philosophy of 0998
 Physical 0523

Psychology 0525
 Reading 0535
 Religious 0527
 Sciences 0714
 Secondary 0533
 Social Sciences 0534
 Sociology of 0340
 Special 0529
 Teacher Training 0530
 Technology 0710
 Tests and Measurements 0288
 Vocational 0747

LANGUAGE, LITERATURE AND LINGUISTICS

Language
 General 0679
 Ancient 0289
 Linguistics 0290
 Modern 0291

Literature
 General 0401
 Classical 0294
 Comparative 0295
 Medieval 0297
 Modern 0298
 African 0316
 American 0591
 Asian 0305
 Canadian (English) 0352
 Canadian (French) 0355
 English 0593
 Germanic 0311
 Latin American 0312
 Middle Eastern 0315
 Romance 0313
 Slavic and East European 0314

PHILOSOPHY, RELIGION AND THEOLOGY

Philosophy 0422
 Religion
 General 0318
 Biblical Studies 0321
 Clergy 0319
 History of 0320
 Philosophy of 0322
 Theology 0469

SOCIAL SCIENCES

American Studies 0323
 Anthropology
 Archaeology 0324
 Cultural 0326
 Physical 0327

Business Administration
 General 0310
 Accounting 0272
 Banking 0770
 Management 0454
 Marketing 0338

Canadian Studies 0385

Economics
 General 0501
 Agricultural 0503
 Commerce-Business 0505
 Finance 0508
 History 0509
 Labor 0510
 Theory 0511

Folklore 0358

Geography 0366

Gerontology 0351

History
 General 0578

Ancient 0579
 Medieval 0581
 Modern 0582
 Black 0328
 African 0331
 Asia, Australia and Oceania 0332
 Canadian 0334
 European 0335
 Latin American 0336
 Middle Eastern 0333
 United States 0337
 History of Science 0585
 Law 0398

Political Science
 General 0615
 International Law and Relations 0616
 Public Administration 0617
 Recreation 0814
 Social Work 0452

Sociology
 General 0626
 Criminology and Penology 0627
 Demography 0938
 Ethnic and Racial Studies 0631
 Individual and Family Studies 0628
 Industrial and Labor Relations 0629
 Public and Social Welfare 0630
 Social Structure and Development 0700
 Theory and Methods 0344
 Transportation 0709
 Urban and Regional Planning 0999
 Women's Studies 0453

THE SCIENCES AND ENGINEERING

BIOLOGICAL SCIENCES

Agriculture
 General 0473
 Agronomy 0285
 Animal Culture and Nutrition 0475
 Animal Pathology 0476
 Food Science and Technology 0359
 Forestry and Wildlife 0478
 Plant Culture 0479
 Plant Pathology 0480
 Plant Physiology 0817
 Range Management 0777
 Wood Technology 0746

Biology
 General 0306
 Anatomy 0287
 Biostatistics 0308
 Botany 0309
 Cell 0379
 Ecology 0329
 Entomology 0353
 Genetics 0369
 Limnology 0793
 Microbiology 0410
 Molecular 0307
 Neuroscience 0317
 Oceanography 0416
 Physiology 0433
 Radiation 0821
 Veterinary Science 0778
 Zoology 0472

Biophysics
 General 0786
 Medical 0760

Geodesy 0370
 Geology 0372
 Geophysics 0373
 Hydrology 0388
 Mineralogy 0411
 Paleobotany 0345
 Paleocology 0426
 Paleontology 0418
 Paleozoology 0985
 Palynology 0427
 Physical Geography 0368
 Physical Oceanography 0415

HEALTH AND ENVIRONMENTAL SCIENCES

Environmental Sciences 0768

Health Sciences
 General 0566
 Audiology 0300
 Chemotherapy 0992
 Dentistry 0567
 Education 0350
 Hospital Management 0769
 Human Development 0758
 Immunology 0982
 Medicine and Surgery 0564
 Mental Health 0347
 Nursing 0569
 Nutrition 0570
 Obstetrics and Gynecology 0380
 Occupational Health and Therapy 0354
 Ophthalmology 0381
 Pathology 0571
 Pharmacology 0419
 Pharmacy 0572
 Physical Therapy 0382
 Public Health 0573
 Radiology 0574
 Recreation 0575

Speech Pathology 0460
 Toxicology 0383
 Home Economics 0386

PHYSICAL SCIENCES

Pure Sciences
Chemistry
 General 0485
 Agricultural 0749
 Analytical 0486
 Biochemistry 0487
 Inorganic 0488
 Nuclear 0738
 Organic 0490
 Pharmaceutical 0491
 Physical 0494
 Polymer 0495
 Radiation 0754
 Mathematics 0405

Physics
 General 0605
 Acoustics 0986
 Astronomy and Astrophysics 0606
 Atmospheric Science 0608
 Atomic 0748
 Electronics and Electricity 0607
 Elementary Particles and High Energy 0798
 Fluid and Plasma 0759
 Molecular 0609
 Nuclear 0610
 Optics 0752
 Radiation 0756
 Solid State 0611
 Statistics 0463

Applied Sciences
 Applied Mechanics 0346
 Computer Science 0984

Engineering
 General 0537
 Aerospace 0538
 Agricultural 0539
 Automotive 0540
 Biomedical 0541
 Chemical 0542
 Civil 0543
 Electronics and Electrical 0544
 Heat and Thermodynamics 0348
 Hydraulic 0545
 Industrial 0546
 Marine 0547
 Materials Science 0794
 Mechanical 0548
 Metallurgy 0743
 Mining 0551
 Nuclear 0552
 Packaging 0549
 Petroleum 0765
 Sanitary and Municipal 0554
 System Science 0790

Geotechnology 0428
 Operations Research 0796
 Plastics Technology 0795
 Textile Technology 0994

PSYCHOLOGY

General 0621
 Behavioral 0384
 Clinical 0622
 Developmental 0620
 Experimental 0623
 Industrial 0624
 Personality 0625
 Physiological 0989
 Psychobiology 0349
 Psychometrics 0632
 Social 0451

EARTH SCIENCES

Biogeochemistry 0425
 Geochemistry 0996



ABSTRACT

Verification of the purity of a commercial Horseradish peroxidase (HRP) preparation, kinetic analyses of two chromogenic assays and an investigation of the mechanisms of enzyme inactivation by two of its substrates, hydrogen peroxide (H_2O_2) and phenol, are described.

Isoelectricfocusing of Boehringer Mannheim Grad II HRP preparation revealed that it is composed of neutral isozymes B and C, as reported by the Manufacturer. No other contaminating isoenzymes were detected.

Kinetic analysis ($T=25^\circ C$, pH 7.4) of the 4-aminoantipyrine (AAP)/3,5-dichloro-2-hydroxybenzenesulfonic acid (HDCBS) chromogen system yielded K_{mapp} values for H_2O_2 , AAP and HDCBS of $41.0\mu M$, $3.94mM$ and $1.4mM$, respectively. Values of 800, 1,200 and $1,000min^{-1}$ were determined as a k_{cat} for H_2O_2 , AAP and HDCBS. Similar analyses performed on the AAP/phenol colourimetric assay demonstrated inactivation with increasing concentrations of AAP, suggesting two different mechanisms for these two systems during the formation of the final chromogenic product. Values of $157\mu M$ and $1.37mM$ were determined as the K_{mapp} for H_2O_2 and phenol, respectively. Values of 21,800 and $26,700min^{-1}$ were determined as the k_{cat} for both substrates, H_2O_2 and phenol.

Hydrogen peroxide, in the absence of donor substrates and at concentrations above $100\mu M$, inactivates HRP in a

time-dependent and irreversible mechanism-based suicide inactivation that does not require a pre-association of H_2O_2 with HRP before substrate turnover. Protection against inactivation is afforded in the presence of donor substrates. Inactivation curves of % remaining activity vs. time are biphasic in shape and are comprised of two sections: (i) an initial (fast) phase in which the majority of inactivation occurs very rapidly and exhibits a dependence, in terms of rate and magnitude of activity lost, on H_2O_2 concentration; (ii) a phase that follows from the initial phase, which appears to be neither exclusively an inactivation nor a period of recovery of enzyme activity. Inactivation data during the fast phase fit well to double-exponential decay curves and appeared to be second-order with respect to H_2O_2 and enzyme concentration (second-order inactivation rate constant, k_{app} , $0.023M^{-1}s^{-1}$). Kinetic parameters describing inactivation, dialysis data and spectrophotometric investigations indicate inactive enzyme intermediate formation, Compound P_{670} , to be predominant at H_2O_2 concentrations above 1.0mM. Below 1.0mM, Compound III formation appears to be predominant and its formation may be responsible for the rapid inactivation phase observed at all H_2O_2 concentrations.

Phenoxy radicals generated during the oxidation of phenol by HRP/ H_2O_2 also inactivate the enzyme in an irreversible, mechanism-based time-dependent inactivation

that follows a single-exponential decay. Inactivation is preceded by a slight activation of enzyme activity at low enzyme and low phenol concentrations; higher enzyme concentrations appears to offer some protection at higher phenol concentrations. A dependence of rate but not final magnitude of inactivation on phenol concentration is observed. A second-order inactivation rate constant ($T=25^{\circ}\text{C}$, pH 7.4) was determined to be $0.0193\text{M}^{-1}\text{s}^{-1}$.

**"When somebody's lost in thought, it's because
they are in unfamiliar territory"**

- anonymous

This work is dedicated both to the Baynton family and to my very, very good friends, A.C., E.S., and especially G.S. and G.H. who encouraged and supported my expeditions into the unknown "where no one has gone before" and who showed me the way when I became lost.

ACKNOWLEDGEMENTS

This "Opus Magnum" was made possible only as a result of the support and encouragement offered by a number of special individuals of whom I'd like to take this opportunity to thank. First, I would like to thank Dr. K.E. Taylor for taking me in as a young and nervous "summer student" and allowing me to "hang around" for so long. His continuous patience, understanding, guidance and support over the past 5 years has been invaluable; I have learned much from him that will never be forgotten. My thanks to Dr. B. Mutus and Dr. A. Warner for taking time from their hectic schedules to review this work and participate in my examination committee.

Many friendships, both inside and outside the laboratory have made endeavour of this project and my stay at the University of Windsor an experience I'll always recall with a warm feeling and a smile. In particular, I want to thank my lab-mates Dr. L. Al-Kassim and Marianne Lulic for their endless supply of friendly and professional support, advice and banter. A very special thanks to George Shimizu, Dr. E. Saravolac and Dr. Alu Chatterjee, without whose tireless offer of an ear to bend and a shoulder to cry on, I might have become truly insane. To the "brew crew" at the Gradhouse (you know who you are) for helping me in those moments when I needed to get a "little" crazy. Labo Lehn and Labo Fuchs for taking me in as a "fellow researcher", offering assistance and much needed beers at the drop of a hat. And finally, to Garry Hanan, for instilling in me both the true meaning of Carpe Deum and the will to dare to dream.

My thanks are extended to those organizations who most generously supported the continuation of this research project and my education. Financial gifts from the Institute for Chemical Science and Technology (ICST), the University Incentive Fund (URIF) of the Government of Ontario, the Rotary Club of Chatham, Ontario and Natural Sciences and Engineering Research Council (NSERC) of Canada made this work possible.

TABLE OF CONTENTS

ABSTRACT.....	iii
DEDICATION.....	vi
AKNOWLEDGEMENTS.....	vii
LIST OF TABLES.....	x
LIST OF FIGURES.....	xviii
LIST OF PLATES.....	xxv
ABBREVIATIONS.....	xxvi
CHAPTER	
1. INTRODUCTION.....	1
2. MATERIALS AND METHODS.....	28
3. RESULTS AND DISCUSSION	
3.1 Enzyme Characterization.....	48
3.2 Kinetic Investigation.....	51
3.2.1 Evaluation of AAP/HDCBS Assay.....	52
3.2.2 Evaluation of AAP/Phenol Assay.....	59
3.3 Inactivation of HRP	
3.3.1. Inactivation by H ₂ O ₂	68
3.3.1.1 Monitoring Spectral Changes.....	97
3.3.2. Inactivation by Phenoxy Radicals..	103
4. SUMMARY AND CONCLUSIONS.....	126
REFERENCES.....	131
APPENDIX A.....	136
APPENDIX B.....	139
APPENDIX C.....	147
APPENDIX D.....	150
APPENDIX E.....	152
APPENDIX F.....	154
APPENDIX G.....	155

APPENDIX H.....	170
APPENDIX I.....	181
VITA AUCTORIS.....	218

LIST OF TABLES

Table	Title	Page
1-1	Absorbance maxima and extinction coefficients of native HRP...	4
1-2	Comparative kinetic properties of native HRP isozymes	9
1-3	Rate constants and parameters describing the inactivation/catalytic pathways...	16
3-1	Observed and calculated rates (determined by Enzfitter™) vs. H ₂ O ₂ concentration (AAP/HDCBS assay)...	54
3-2	Observed and calculated rates (determined by Enzfitter™) vs. AAP concentration (AAP/HDCBS assay)...	55
3-3	Observed and calculated rates (determined by Enzfitter™) vs. HDCBS concentration (AAP/HDCBS assay)...	56
3-4	Kinetic constants of H ₂ O ₂ /AAP/HDCBS chromogen system...	57
3-5	Lack of influence of reaction rate on changing AAP concentration (AAP/Phenol Activity Assay)...	62
3-6	Observed and calculated rates (determined by Enzfitter™) vs. phenol concentration (AAP/Phenol activity assay)...	65
3-7	Observed and calculated rates (determined by Enzfitter™) vs. H ₂ O ₂ concentration (AAP/Phenol activity assay)...	66
3-8	Kinetic constants of H ₂ O ₂ /AAP/Phenol chromogen system...	67
3-9	% residual activity and total % inactivation of 100nM HRP after	75

	exposure to H ₂ O ₂ for 24 hours...	
3-10	% residual and irreversible activity at 48 hours...	75
3-11	Comparison of % residual activities of undialysed and dialysed 100nM HRP solutions...	78
3-12	% residual activity vs. time of triplicates from one experiment... [HRP]=100nM	80
3-13	Observed and calculated % remaining activity data vs. time used for double-exponential evaluation of inactivation...	85
3-14	Values of k _{obs} and their standard errors, representing both fast and slow inactivation phases...	87
3-15	Values of kinetic constants K _{iapp} and k _{inact} ...	88
3-16	Summary of intermediates implicated to be dominant,...	99
3-17	Summary of total % inactivation of various concentrations of HRP by enzyme-generated phenoxy radicals..	107
3-18	Example data set of observed and calculated fractional remaining activity vs. time used in single-exponential decay analysis...	112
3-19a,b	Values of k _{obs} calculated from single-exponential decay analysis for [HRP]=25nM and [H ₂ O ₂]=0.5mM (a) and 1.0mM (b).	114
3-20a,b	Values of k _{obs} calculated from single-exponential decay analysis for [HRP]=50nM and [H ₂ O ₂]=0.5mM (a) and 1.0mM (b).	116
3-21a,b	Values of k _{obs} calculated from single-exponential decay analysis for [HRP]=100nM and [H ₂ O ₂]=0.5mM (a) and 1.0mM (b).	118

3-22	Values of k_{app} , the second-order inactivation rate constant... (phenoxy-radical inactivation)	122
G1	Observed and calculated % remaining activity data vs. time used for double-exponential decay evaluation (100 μ M H_2O_2)	156
G2	Observed and calculated % remaining activity data vs. time used for single-exponential decay evaluation (100 μ M H_2O_2)	156
G3	Values of A_1 , A_2 , $-k_1$ and $-k_2$ and their standard error... (100 μ M H_2O_2)	157
G4	Observed and calculated % remaining activity data vs. time used for double-exponential decay evaluation (500 μ M H_2O_2)	158
G5	Observed and calculated % remaining activity data vs. time used for single-exponential decay evaluation (500 μ M H_2O_2)	158
G6	Values of A_1 , A_2 , $-k_1$ and $-k_2$ and their standard error... (500 μ M H_2O_2)	159
G7	Observed and calculated % remaining activity data vs. time used for double-exponential decay evaluation (750 μ M H_2O_2)	160
G8	Observed and calculated % remaining activity data vs. time used for single-exponential decay evaluation (750 μ M H_2O_2)	160
G9	Values of A_1 , A_2 , $-k_1$ and $-k_2$ and their standard error... (750 μ M H_2O_2)	161
G10	Observed and calculated % remaining activity data vs. time used for double-exponential decay evaluation (1.0mM H_2O_2)	162
G11	Observed and calculated % remaining activity data vs. time used for single-exponential decay evaluation (1.0mM H_2O_2)	162

G12	Values of A1, A2, -k ₁ and -k ₂ and their standard error... (1.0mM H ₂ O ₂)	163
G13	Observed and calculated % remaining activity data vs. time used for double-exponential decay evaluation (5.0mM H ₂ O ₂)	164
G14	Observed and calculated % remaining activity data vs. time used for single-exponential decay evaluation (5.0mM H ₂ O ₂)	164
G15	Values of A1, A2, -k ₁ and -k ₂ and their standard error... (5.0mM H ₂ O ₂)	165
G16	Observed and calculated % remaining activity data vs. time used for double-exponential decay evaluation (10.0mM H ₂ O ₂)	166
G17	Observed and calculated % remaining activity data vs. time used for single-exponential decay evaluation (10.0mM H ₂ O ₂)	166
G18	Values of A1, A2, -k ₁ and -k ₂ and their standard error... (10.0mM H ₂ O ₂)	167
G19	Observed and calculated % remaining activity data vs. time used for double-exponential decay evaluation (50.0mM H ₂ O ₂)	168
G20	Observed and calculated % remaining activity data vs. time used for single-exponential decay evaluation (50.0mM H ₂ O ₂)	168
G21	Values of A1, A2, -k ₁ and -k ₂ and their standard error... (50.0mM H ₂ O ₂)	169
H1	Absorbance changes occurring in the Soret upon exposure to 100μM H ₂ O ₂ ... ([HRP]=7.5μM).	171
H2	Absorbance changes occurring in the far red region upon exposure of 33μM HRP to 100μM H ₂ O ₂ ...	171
H3	Absorbance changes occurring in the Soret upon exposure to 1.0mM	173

	H ₂ O ₂ ... ([HRP]=7.5μM).	
H4	Absorbance changes occurring in the far red region upon exposure of 33μM HRP to 1.0mM H ₂ O ₂ ...	173
H5	Absorbance changes occurring in the Soret upon exposure to 10.0mM H ₂ O ₂ ... ([HRP]=7.5μM).	175
H6	Absorbance changes occurring in the far red region upon exposure of 33μM HRP to 10.0mM H ₂ O ₂ ...	175
H7	Absorbance changes occurring in the Soret upon exposure to 25.0mM H ₂ O ₂ ... ([HRP]=6.6μM).	177
H8	Absorbance changes occurring in the far red region upon exposure of 33μM HRP to 25.0mM H ₂ O ₂ ...	177
H9	Absorbance changes occurring in the Soret upon exposure to 50.0mM H ₂ O ₂ ... ([HRP]=6.6μM).	179
H10	Absorbance changes occurring in the far red region upon exposure of 33μM HRP to 50.0mM H ₂ O ₂ ...	179
I1a, b	Summary of the total % inactivation and the total H ₂ O ₂ consumed... (25nM HRP; phenoxy-radical inactivation (a) 0.5mM H ₂ O ₂ and (b) 1.0mM H ₂ O ₂).	182
I2a, b	Summary of the total % inactivation and the total H ₂ O ₂ consumed... (50nM HRP; phenoxy-radical inactivation (a) 0.5mM H ₂ O ₂ and (b) 1.0mM H ₂ O ₂).	183
I3a, b	Summary of the total % inactivation and the total H ₂ O ₂ consumed... (100nM HRP; phenoxy-radical inactivation (a) 0.5mM H ₂ O ₂ and (b) 1.0mM H ₂ O ₂).	184
I4	Observed and calculated % remaining activity data vs. time used for single-exponential decay analysis [HRP]=25nM; [H ₂ O ₂]=0.5mM; [phenol]=0.2mM...	188
I5	Observed and calculated % remaining activity data vs. time used for single-	189

	exponential decay analysis [HRP]=25nM; [H ₂ O ₂]=0.5mM; [phenol]=0.5mM...	
I6	Observed and calculated % remaining activity data vs. time used for single-exponential decay analysis [HRP]=25nM; [H ₂ O ₂]=0.5mM; [phenol]=0.75mM...	190
I7	Observed and calculated % remaining activity data vs. time used for single-exponential decay analysis [HRP]=25nM; [H ₂ O ₂]=0.5mM; [phenol]=1.0mM...	191
I8	Observed and calculated % remaining activity data vs. time used for single-exponential decay analysis [HRP]=25nM; [H ₂ O ₂]=0.5mM; [phenol]=2.0mM...	192
I9	Observed and calculated % remaining activity data vs. time used for single-exponential decay analysis [HRP]=25nM; [H ₂ O ₂]=1.0mM; [phenol]=0.2mM...	193
I10	Observed and calculated % remaining activity data vs. time used for single-exponential decay analysis [HRP]=25nM; [H ₂ O ₂]=1.0mM; [phenol]=0.5mM...	194
I11	Observed and calculated % remaining activity data vs. time used for single-exponential decay analysis [HRP]=25nM; [H ₂ O ₂]=1.0mM; [phenol]=0.75mM...	195
I12	Observed and calculated % remaining activity data vs. time used for single-exponential decay analysis [HRP]=25nM; [H ₂ O ₂]=1.0mM; [phenol]=1.0mM...	196
I13	Observed and calculated % remaining activity data vs. time used for single-exponential decay analysis [HRP]=25nM; [H ₂ O ₂]=1.0mM; [phenol]=2.0mM...	197
I14	Observed and calculated % remaining activity data vs. time used for single-exponential decay analysis [HRP]=50nM; [H ₂ O ₂]=0.5mM; [phenol]=0.2mM...	198
I15	Observed and calculated % remaining activity data vs. time used for single-exponential decay analysis [HRP]=50nM; [H ₂ O ₂]=0.5mM; [phenol]=0.5mM...	199

I16	Observed and calculated % remaining activity data vs. time used for single-exponential decay analysis [HRP]=50nM; [H ₂ O ₂]=0.5mM; [phenol]=0.75mM...	200
I17	Observed and calculated % remaining activity data vs. time used for single-exponential decay analysis [HRP]=50nM; [H ₂ O ₂]=0.5mM; [phenol]=1.0mM...	201
I18	Observed and calculated % remaining activity data vs. time used for single-exponential decay analysis [HRP]=50nM; [H ₂ O ₂]=0.5mM; [phenol]=2.0mM...	202
I19	Observed and calculated % remaining activity data vs. time used for single-exponential decay analysis [HRP]=50nM; [H ₂ O ₂]=1.0mM; [phenol]=0.2mM...	203
I20	Observed and calculated % remaining activity data vs. time used for single-exponential decay analysis [HRP]=50nM; [H ₂ O ₂]=1.0mM; [phenol]=0.5mM...	204
I21	Observed and calculated % remaining activity data vs. time used for single-exponential decay analysis [HRP]=50nM; [H ₂ O ₂]=1.0mM; [phenol]=0.75mM...	205
I22	Observed and calculated % remaining activity data vs. time used for single-exponential decay analysis [HRP]=50nM; [H ₂ O ₂]=1.0mM; [phenol]=1.0mM...	206
I23	Observed and calculated % remaining activity data vs. time used for single-exponential decay analysis [HRP]=50nM; [H ₂ O ₂]=1.0mM; [phenol]=2.0mM...	207
I24	Observed and calculated % remaining activity data vs. time used for single-exponential decay analysis [HRP]=100nM; [H ₂ O ₂]=0.5mM; [phenol]=0.2mM...	208
I25	Observed and calculated % remaining activity data vs. time used for single-exponential decay analysis [HRP]=100nM; [H ₂ O ₂]=0.5mM; [phenol]=0.5mM...	209
I26	Observed and calculated % remaining activity data vs. time used for single-	210

	exponential decay analysis [HRP]=100nM; [H ₂ O ₂]=0.5mM; [phenol]=0.75mM...	
I27	Observed and calculated % remaining activity data vs. time used for single- exponential decay analysis [HRP]=100nM; [H ₂ O ₂]=0.5mM; [phenol]=1.0mM...	211
I28	Observed and calculated % remaining activity data vs. time used for single- exponential decay analysis [HRP]=100nM; [H ₂ O ₂]=0.5mM; [phenol]=2.0mM...	212
I29	Observed and calculated % remaining activity data vs. time used for single- exponential decay analysis [HRP]=100nM; [H ₂ O ₂]=1.0mM; [phenol]=0.2mM...	213
I30	Observed and calculated % remaining activity data vs. time used for single- exponential decay analysis [HRP]=100nM; [H ₂ O ₂]=1.0mM; [phenol]=0.5mM...	214
I31	Observed and calculated % remaining activity data vs. time used for single- exponential decay analysis [HRP]=100nM; [H ₂ O ₂]=1.0mM; [phenol]=0.75mM...	215
I32	Observed and calculated % remaining activity data vs. time used for single- exponential decay analysis [HRP]=100nM; [H ₂ O ₂]=1.0mM; [phenol]=1.0mM...	216
I33	Observed and calculated % remaining activity data vs. time used for single- exponential decay analysis [HRP]=100nM; [H ₂ O ₂]=1.0mM; [phenol]=2.0mM...	217

LIST OF FIGURES

Figure	Title	Page
1-1	Model of heme crevice in native HRP...	2
1-2	Visible spectrum of a metallated porphyrin...	2
1-3	Curves exhibiting time- and H ₂ O ₂ -dependent inactivation of HRP	11
1-4	Scheme depicting partitioning of reaction pathways that exists at Compound I...	13
1-5	Scheme demonstrating the partitioning of possible reaction pathways at the level of Compound I-H ₂ O ₂ intermediate..	13
1-6	Reaction pathway scheme for enzyme-generated phenoxy radicals	20
1-7	Formation of the hydroperoxy radical from reaction between an enzyme-generated phenoxy radical and molecular oxygen	20
2-1	Visible spectrum of the characteristic alpha and beta bands of native HRP...	44
3-1	Plot of rate (μM/min.) vs. H ₂ O ₂ concentration (μM) values in Table 3-1.	54
3-2	Plot of rate (mM/min.) vs. AAP concentration (mM) values in Table 3-2.	55
3-3	Plot of rate (mM/min.) vs. HDCBS concentration (mM) values in Table 3-3.	56
3-4	Plot of rate (mM/min.) vs. phenol concentration (mM) values in Table 3-6.	65
3-5	Plot of rate (μM/min.) vs. H ₂ O ₂ concentration (μM) values in Table 3-7.	66
3-6	Donor-substrate protection of HRP	69

	against inactivation...	
3-7	Total absorbance change over time with addition of each new H ₂ O ₂ aliquot.	69
3-8	Time-dependent Inactivation of 100nM	73
3-9	Time-dependent Inactivation of 1μM HRP by H ₂ O ₂ ...	73
3-10	Plot of curves obtained from time-dependent inactivation data in Table 3-12.	80
3-11	Linearization of data presented in Table 3-12	82
3-12	A closer look at the values obtained within the first minute of exposure of HRP to H ₂ O ₂ ...	82
3-13	Plot of observed data in Table 3-13 fit to calculated double-exponential decay curve...	85
3-14	Least-squares linear regression plot of k _{obs} values...vs. H ₂ O ₂ concentration..	88
3-15	Appearance of absorbance maxima at 670nm...	99
3-16	Time-dependent inactivation of 50nM HRP by enzyme-generated phenoxy radicals...	104
3-17	An example of the semi-log plots obtained from ln % remaining activity vs. time data...	104
3-18	Comparison of time-dependent inactivation of 100nM HRP...	109
3-19	Visible spectrum of the product of HRP-catalyzed H ₂ O ₂ oxidation of phenol	109
3-20	Plot of experimental inactivation data fit to a single-exponential decay curve...	112
3-21a,b	Plots of k _{obs} vs. phenol concentration... ([HRP] = 25nM)	115

3-22a,b	Plots of k_{obs} vs. phenol concentration... ([HRP] = 25nM)	117
3-23a,b	Plots of k_{obs} vs. phenol concentration... ([HRP] = 25nM)	119
A1	Visible spectrum of native HRP	138
B1-1	Reaction scheme of AAP and phenol in the presence of HRP and H_2O_2 ...	141
B1-2	Peroxidase ping-pong mechanism...	141
B1-3	Reaction of AAP with oxidized HRP with Compounds I and II...	132
B1-4	Increase in absorbance at 510nm vs. time (HDCBS/AAP activity assay)	145
C1	Standard curve of absorbance at 510nm vs. hydrogen peroxide concentration...	149
D1	UV. absorption spectrum of 0.5mM solution of phenol...	151
G1	Plot of observed data fit to calculated double-exponential decay curve (100 μ M H_2O_2)...	157
G2	Plot of observed data fit to calculated double-exponential decay curve (500 μ M H_2O_2)...	159
G3	Plot of observed data fit to calculated double-exponential decay curve (750 μ M H_2O_2)...	161
G4	Plot of observed data fit to calculated double-exponential decay curve (1.0mM H_2O_2)...	163
G5	Plot of observed data fit to calculated double-exponential decay curve (5.0mM H_2O_2)...	165
G6	Plot of observed data fit to calculated double-exponential decay curve (10.0mM H_2O_2)...	167
G7	Plot of observed data fit to calculated double-exponential	169

	decay curve (50.0mM H ₂ O ₂)...	
H1	Development of an absorbance maximum at 406nm...(100μM H ₂ O ₂)...	172
H2	Development of absorbance maxima at 558 and 656...(100μM H ₂ O ₂)	172
H3	Development of an absorbance maximum at 406nm...(1.0mM H ₂ O ₂)...	174
H4	Development of absorbance maxima at 556 and 656...(1.0mM H ₂ O ₂)...	174
H5	Decay of absorbance maximum at 418nm...(10.0mM H ₂ O ₂)...	176
H6	Decay of absorbance maxima at 554 and 578nm and development...(10.0mM H ₂ O ₂)...	176
H7	Decay of absorbance maximum at 418nm...(25.0mM H ₂ O ₂)...	178
H8	Decay of absorbance maxima at 554 and 578nm and development...(25.0mM H ₂ O ₂)...	178
H9	Decay of absorbance maximum at 418nm...(50.0mM H ₂ O ₂)...	180
H10	Decay of absorbance maxima at 554 and 578nm and development...(50.0mM H ₂ O ₂)...	180
I1a, b	Time-dependent inactivation of 25nM HRP enzyme-generated phenoxy radicals...	185
I2a, b	Time-dependent inactivation of 50nM HRP enzyme-generated phenoxy radicals...	186
I3a, b	Time-dependent inactivation of 100nM HRP enzyme-generated phenoxy radicals...	187
I4	Plot of observed data in Table I4 fit to single-exponential decay curve ([HRP]=25nM; [H ₂ O ₂]=0.5mM; [phenol]=0.2mM...	188

I5	Plot of observed data in Table I5 fit to single-exponential decay curve ([HRP]=25nM; [H ₂ O ₂]=0.5mM; [phenol]=0.5mM...	189
I6	Plot of observed data in Table I6 fit to single-exponential decay curve ([HRP]=25nM; [H ₂ O ₂]=0.5mM; [phenol]=0.75mM...	190
I7	Plot of observed data in Table I7 fit to single-exponential decay curve ([HRP]=25nM; [H ₂ O ₂]=0.5mM; [phenol]=1.0mM...	191
I8	Plot of observed data in Table I8 fit to single-exponential decay curve ([HRP]=25nM; [H ₂ O ₂]=0.5mM; [phenol]=2.0mM...	192
I9	Plot of observed data in Table I9 fit to single-exponential decay curve ([HRP]=25nM; [H ₂ O ₂]=1.0mM; [phenol]=0.2mM...	193
I10	Plot of observed data in Table I10 fit to single-exponential decay curve ([HRP]=25nM; [H ₂ O ₂]=1.0mM; [phenol]=0.5mM...	194
I11	Plot of observed data in Table I11 fit to single-exponential decay curve ([HRP]=25nM; [H ₂ O ₂]=1.0mM; [phenol]=0.75mM...	195
I12	Plot of observed data in Table I12 fit to single-exponential decay curve ([HRP]=25nM; [H ₂ O ₂]=1.0mM; [phenol]=1.0mM...	196
I13	Plot of observed data in Table I13 fit to single-exponential decay curve ([HRP]=25nM; [H ₂ O ₂]=1.0mM; [phenol]=2.0mM...	197
I14	Plot of observed data in Table I14 fit to single-exponential decay curve ([HRP]=50nM; [H ₂ O ₂]=0.5mM; [phenol]=0.2mM...	198
I15	Plot of observed data in Table I15 fit to single-exponential decay	199

	curve ([HRP]=50nM; [H ₂ O ₂]=0.5mM; [phenol]=0.5mM...	
I16	Plot of observed data in Table I16 fit to single-exponential decay curve ([HRP]=50nM; [H ₂ O ₂]=0.5mM; [phenol]=0.75mM...	200
I17	Plot of observed data in Table I17 fit to single-exponential decay curve ([HRP]=50nM; [H ₂ O ₂]=0.5mM; [phenol]=1.0mM...	201
I18	Plot of observed data in Table I18 fit to single-exponential decay curve ([HRP]=50nM; [H ₂ O ₂]=0.5mM; [phenol]=2.0mM...	102
I19	Plot of observed data in Table I19 fit to single-exponential decay curve ([HRP]=50nM; [H ₂ O ₂]=1.0mM; [phenol]=0.2mM...	203
I20	Plot of observed data in Table I20 fit to single-exponential decay curve ([HRP]=50nM; [H ₂ O ₂]=1.0mM; [phenol]=0.5mM...	204
I21	Plot of observed data in Table I21 fit to single-exponential decay curve ([HRP]=50nM; [H ₂ O ₂]=1.0mM; [phenol]=0.75mM...	205
I22	Plot of observed data in Table I22 fit to single-exponential decay curve ([HRP]=50nM; [H ₂ O ₂]=1.0mM; [phenol]=1.0mM...	206
I23	Plot of observed data in Table I23 fit to single-exponential decay curve ([HRP]=50nM; [H ₂ O ₂]=1.0mM; [phenol]=2.0mM...	207
I24	Plot of observed data in Table I24 fit to single-exponential decay curve ([HRP]=100nM; [H ₂ O ₂]=0.5mM; [phenol]=0.2mM...	208
I25	Plot of observed data in Table I25 fit to single-exponential decay curve ([HRP]=100nM; [H ₂ O ₂]=0.5mM; [phenol]=0.5mM...	209

I26	Plot of observed data in Table I26 fit to single-exponential decay curve ([HRP]=100nM; [H ₂ O ₂]=0.5mM; [phenol]=0.75mM...	210
I27	Plot of observed data in Table I27 fit to single-exponential decay curve ([HRP]=100nM; [H ₂ O ₂]=0.5mM; [phenol]=1.0mM...	211
I28	Plot of observed data in Table I28 fit to single-exponential decay curve ([HRP]=100nM; [H ₂ O ₂]=0.5mM; [phenol]=2.0mM...	212
I29	Plot of observed data in Table I29 fit to single-exponential decay curve ([HRP]=100nM; [H ₂ O ₂]=1.0mM; [phenol]=0.2mM...	213
I30	Plot of observed data in Table I30 fit to single-exponential decay curve ([HRP]=100nM; [H ₂ O ₂]=1.0mM; [phenol]=0.5mM...	214
I31	Plot of observed data in Table I31 fit to single-exponential decay curve ([HRP]=100nM; [H ₂ O ₂]=1.0mM; [phenol]=0.75mM...	215
I32	Plot of observed data in Table I32 fit to single-exponential decay curve ([HRP]=100nM; [H ₂ O ₂]=1.0mM; [phenol]=1.0mM...	216
I33	Plot of observed data in Table I33 fit to single-exponential decay curve ([HRP]=100nM; [H ₂ O ₂]=1.0mM; [phenol]=2.0mM...	217

LIST OF PLATES

Plate	Description	Page
3-1	CBB.-stained 25% polyacryl- amide gel of Boehringer-Mannheim Grad II HRP preparation.	49

ABBREVIATIONS

AAP	4-aminoantipyrene
ABTS	2,2'-azino-bis(3-ethyl-benzthiazoline-6-sulphonic acid)
Abs.	absorbance
A.U.	absorbance units
α	alpha
BM.	Boehringer Mannheim Company
β	beta
CBB.	Coomassie brilliant blue
cm	centimeter
Cpd. I	Compound I
Cpd. II	Compound II
Cpd. III	Compound III
Cpd. IV	Compound IV
δ	delta
ϵ	extinction coefficient (units: concentration ⁻¹ cm ⁻¹)
FMN	flavin mononucleotide
g	gram
γ	gamma

H_2O_2	hydrogen peroxide
HDCBS	3,5-dichloro-2-hydroxybenzene-sulfonic acid
HRP	horseradish peroxidase
IEF	isoelectricfocusing
k_{app}	second-order inactivation rate constant (units: concentration ⁻¹ time ⁻¹)
k_{cat}	first-order rate constant (units: time ⁻¹)
k_{cat}/K_m	apparent second-order rate constant or specificity constant (units: concentration ⁻¹ time)
K_I	inactivator dissociation constant (units: concentration)
k_{inact} or k_i	limiting rate constant for inactivation (units: time ⁻¹)
k_{obs}	pseudo-first order inactivation rate constant (units: time ⁻¹)
K_m	Michaelis constant; substrate concentration at half-maximal reaction velocity (units: concentration)
L	litre
λ	lambda
M	molar
m	milli (10 ⁻³)
mg	milligram
mL	millilitre
mM	millimolar

mL	millilitre
mM	millimolar
MW.	molecular weight
MWCO.	molecular weight cut-off
min.	minute
n	nano (10^{-9})
ng	nanogram
nm	nanometre
nM	nanomolar
NaH_2PO_4	sodium dihydrogen phosphate (monobasic)
Na_2HPO_4	disodium hydrogen phosphate (dibasic)
NaPP	sodium phosphate buffer
pH	$-\log [\text{H}^+]$
p	pico
pI	isoelectric point
P_{670}	irreversibly inactivated HRP compound
RZ.	reinheitszahl; purity number; ratio of absorbance at 404nm:278nm
s or sec	seconds
TCA	trichloroacetic acid
TEMED	N,N,N',N'-tetramethylethylene diamine
μ	micro (10^{-6})

μg	microgram
μL	microlitre
μm	micrometre; micron
μM	micromolar
U	enzyme activity unit: $\mu\text{moles time}^{-1}$
uv.	ultraviolet
V	volts
v_i	initial velocity (units: absorbance units or concentration time^{-1})
V_{max}	maximum velocity; maximal rate of reaction at saturating substrate concentrations (units: concen- tration time^{-1})
[]	concentration

CHAPTER 1

INTRODUCTION

1.1 General

Horseradish peroxidase, a 40,000 dalton glycoprotein containing 2 calcium ions per molecule, is the most intensively investigated of all known peroxidases (Dunford and Stillman, 1976; Everse et al., 1990). Its broad spectrum of activity and lack of specificity towards the second donor substrate in the peroxidatic reaction, make it amenable to a number of applications ranging from enzyme markers in histo- and immunochemical techniques (Artiss et al., 1979; Conyers and Kidwell, 1991; Ngo and Lenhoff, 1980) to removal of toxic organics from industrial waste effluent (Dec and Bollag, 1990; Klibanov et al., 1980, 1981, 1983; Maloney et al., 1986; Nicell, J., 1991; Oberg et al., 1990).

Brown-coloured HRP contains a protoporphyrin IX (hemin) prosthetic group containing a penta-coordinate ferric iron (Fe III) (Figure 1-1). Interaction of the hemin with crucial amino acid groups in the hydrophobic heme "crevice" active site confers to HRP not only its activity (Ator and Ortiz de Montellano, 1987; Dawson, 1988; Ortiz de Montellano, 1987; Ortiz de Montellano et al., 1987; Sakurada et al., 1986) but also its characteristic visible absorption

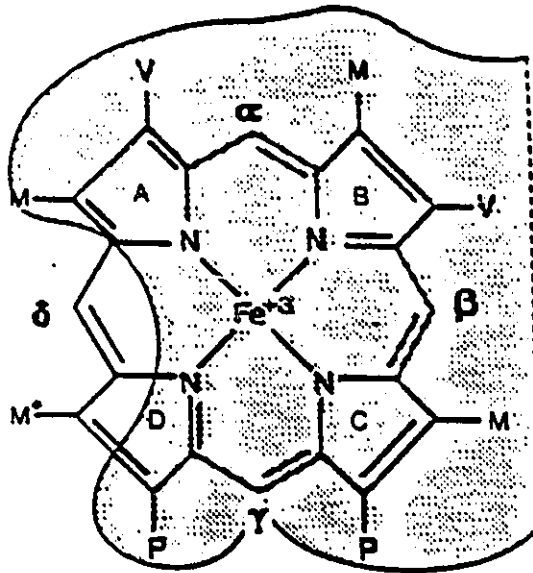


Figure 1-1 Model of the heme crevice in native HRP showing the 8-methyl (M^*) and δ -methylene bridge of the porphyrin ring where electron transfer between substrate and enzyme occurs (after Ortiz de Montellano, 1987). V=vinyl group ($\text{CH}_2=\text{CH}-$); P=propionic acid ($(\text{CH}_2)_2\text{CO}_2\text{H}$); A, B, C and D=pyrole.; α, β, γ and δ =methylene bridges.

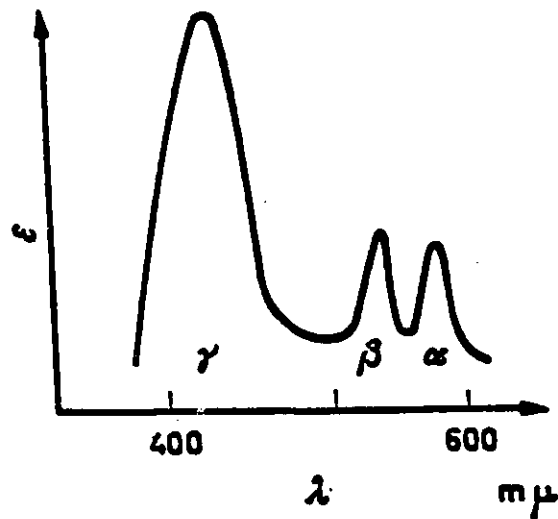


Figure 1-2 Visible spectrum of a metallated porphyrin in neutral or alkaline solution showing the bands observed in the native HRP spectrum. ϵ =extinction coefficient; λ =wavelength in millimicrons ($m\mu$) (Saunders et al., 1964).

spectrum (Figure 1-2). The α and β bands located towards the far red region of the visible spectrum (480-650nm) possess low extinction coefficients and are sometimes absent in the spectra of HRP's catalytic intermediates. The α band is situated between 550-650nm in conjunction with the β band, which is observed between 480-550nm (Saunders et al., 1964). The only universally observed absorption band in a hemoprotein visible spectrum is an intense, high energy absorption band possessing a molar extinction coefficient on the order of $10^5 \text{M}^{-1} \text{cm}^{-1}$: the γ or Soret band appearing around 400nm (Saunders et al., 1964). Monitoring isosbestic points between intermediate absorbance spectra and the appearance/disappearance of the bands towards the far red region over time are useful but rather ambiguous tools used frequently to identify and quantify the intermediates present during catalysis, and to determine reaction rate constants (Dunford and Stillman, 1976). Despite this ambiguity, identification of HRP's redox intermediates relies heavily on their characteristic visible spectra. Table 1-1 is a compilation of the absorption maxima and extinction coefficients taken from different authors, characterizing native HRP and its intermediates.

1.2 HRP Compounds and Overview of the Peroxidase Cycle

Exposure of native HRP to various oxidants and reductants quickly changes the iron's oxidation state,

HRP Compound	Absorbance Maxima	Extinction Coefficient ($M^{-1}cm^{-1}$)
Native	403	102,000
	498	11,250
	640	3,230
Cpd. I	400	53,000
	525	-
	577	-
	622	-
	651	3,000 (a)
Cpd. II	420	105,000
	527	9,500
	554	9,650
	660 (a)	3,000
Cpd. III (a)	416	97,000
	546	10,000
	583	8,700
	673	2,800
Cpd. IV (b) (F ₆₇₀) (c)	403	- (c)
	557	-
	560	4,000 (b)
	655	7,100 (b)
	670	3,000 (b)
	680	6,900 (b)

(a) Keilin and Hartree, 1951

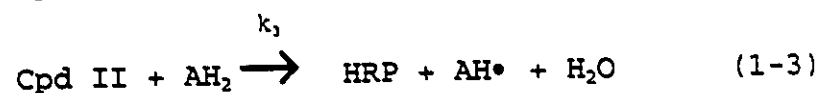
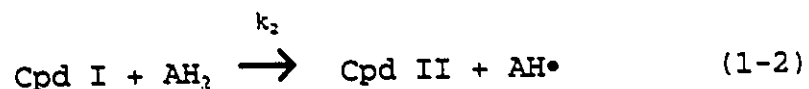
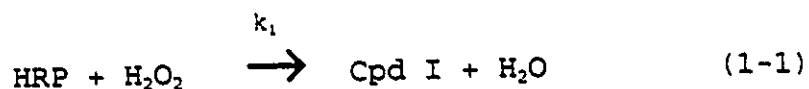
(b) Chance, 1949

(c) Yamazaki and Yokota, 1973

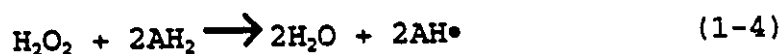
Table 1-1 Absorbance maxima and extinction coefficients of native HRP and its reaction intermediates (taken from Dunford and Stillman, 1976 except as noted).

generating reaction intermediates whose subsequent involvement in various reactions is dependent on the redox nature and concentration of substrates with respect to each other (Yamazaki and Yokota, 1973). In the peroxidatic reaction where sequential 1-electron oxidations of a variety of organic substrates is carried out in the presence of H_2O_2 , HRP has served as a model for all other peroxidases (Everse et al., 1990). The first obligatory step requires the entry and subsequent interaction of H_2O_2 or another organic peroxide at the iron atom of the porphyrin, resulting in the formation of the unstable iron-peroxide complex, Compound 0 (Baek and van Wart, 1989; 1992; Oberg et al., 1990). Subsequent 2-electron oxidation of the ferriheme occurs through a two-step heterolytic cleavage of H_2O_2 's O-O bond (Walsh, 1979) brought about by distal and proximal histidines 42 and 170, respectively, along with arginine 38 (Dawson, 1988; Poulos, 1987). A molecule of H_2O is released and green-coloured Compound I, containing two oxidizing equivalents more than ferric HRP (+5), is produced (Dunford and Stillman, 1976) in a second-order reaction possessing a rate constant (k_1) around $1.8-2.0 \times 10^7 M^{-1} sec^{-1}$ (25°C, neutral pH) (Dolman et al., 1975; Nakajima and Yamazaki, 1986). Compound I is reduced to pale red Compound II by 1 equivalent of endogenous or exogenous donor substrate (AH_2) through a 1-electron transfer to the porphyrin ring at the δ -mesocarbon and the 8-methyl group of

the heme (Ator and Ortiz de Montellano, 1987; Ator et al., 1987; Oberg et al., 1990; Ortiz de Montellano et al., 1988). Decay of I to II is second order with rate constants (k_2) ranging from rapid ($10^7 \text{M}^{-1} \text{sec}^{-1}$) to almost zero, depending on the hydrogen donor (Oberg et al., 1990). In the rate-limiting step, Compound II is reduced back to the native enzyme through the abstraction of an electron from another molecule of donor substrate (Dunford and Stillman, 1976). A simplified reaction scheme describing the peroxidatic cycle is (Everse et al., 1990):



where HRP represents the native, ferric enzyme, Cpd I and II compounds I and II, respectively, and AH_2 a donor substrate. Summing the above equations yields:



which suggests a reaction stoichiometry of 1 molecule of H_2O_2 for every 2 donor molecules oxidized. Under conditions of relatively low H_2O_2 and high donor concentrations, the passage of Compound I to Compound II becomes rate limiting and the integrity of cycling from native enzyme through to

compounds I and II back to native enzyme is maintained. This cycling is theoretically sustainable if sufficient donor substrate is available to protect HRP from oxidative attack by H_2O_2 (Arnao et al., 1990a,b) should the stoichiometric ratio predicted in equation 1-4 become greater than 0.5, and intermediates/products formed are not inhibitory to the enzyme (Dunford and Stillman, 1976).

1-2 Isoenzymes

The existence of multiple forms of HRP has been ascribed to microheterogeneity associated with the composition and orientation of post-translationally added carbohydrate residues, as well as heterogeneity arising from "artifacts" of enzymatic hydrolysis during the purification process (Everse et al., 1990). Kay et al. (1967) developed a classification system that is widely accepted and used to identify the 12 major isozyme classes known presently. The acidic isozymes (pI's = 3-4), designated A1-A3, exhibit similar kinetic properties distinct from the most prevalent isozymes, B and C (Kay et al., 1967). B and C are neutral to slightly basic, possessing pI's of approximately 8-9. The strongly basic isozymes with pI's of at least 10 are denoted D and E. Class E is further broken into isozymes E1-E6 (Aibara et al., 1981). B through E possess similar kinetic properties, placing them into a group kinetically distinct from the A isozymes.

Isoenzyme A3 possesses intermediate activity to classes A1/A2 and B/C in the oxidation of oxaloacetate and peroxidation of o-dianisidine (Kay et al., 1967) (Table 1-2). This has been ascribed to inactivation that occurs during catalysis (Kay et al., 1967). Inactivation was not observed with any of the other isozymes.

Most commercially available HRP preparations contain isozymes B and C (Dunford and Stillman, 1976; Everse et al., 1990). Acidic isozymes are generally easy to separate and are absent in most preparations. Both Boehringer Mannheim and Sigma Chemical Co. manufacture HRP preparations containing essentially isozyme C (designated HRP-C). There has been little evidence to indicate the presence of multiple components in most of the commercially pure HRP preparations (Everse et al., 1990; Kasinsky and Hackett, 1968). Support for this has come through the use of transient state kinetics. Multiple enzyme forms possessing different reactivities yet capable of catalyzing the same reaction tend to yield bi- or multi-phasic rather than typical pseudo-first order kinetic traces (Dunford and Stillman, 1976; Everse et al., 1990; Segel, 1975). This phenomenon has not yet been reported in commercial HRP preparations. However, absence of obvious bi- or multi-phasic behaviour does not preclude the presence of multiple components. Multiplicity may go undetected even if K_m and V_{max} values are very different among components. Minor

Isozyme	Specific Activity**	K _m *** (μ M)
A1	2.2	16.0
A2	2.3	18.8
A3	0.9	3.8
B	0.1	1.7
C	0.1	1.6

** moles of H₂O₂ consumed per minute per mole of HRP during o-dianisidine oxidation (Kay et al., 1967)

*** for H₂O₂ with o-dianisidine oxidation (Kay et al., 1967)

Table 1-2 Comparative kinetic properties of native HRP isoenzymes (Gonzalez et al., 1985).

components may be present in such minute quantities that they do not affect the overall kinetics of the major component to any significant degree. Equally, transient state kinetic properties of the minor components may be similar enough to those of the major component that little if any influence on the final results is observed (Dunford and Stillman, 1976; Segel, 1975).

Despite the reputed purity of most commercial HRP preparations, verification employing isoelectric-focusing (IEF) or column chromatography is advisable if one intends to perform any kind of detailed kinetic analyses.

1.4 HRP Inactivation Pathways

1.4.1 Inactivation by Hydrogen Peroxide

Exposure of Compound I to 1 equivalent of H_2O_2 in the absence of donor substrates results in a 2-electron reduction in a weak catalase reaction. A molecule of oxygen is produced along with ferric HRP, which is ready to take part in another round of catalysis (Arnao et al., 1990a). The second-order rate constant of this reaction is $500M^{-1}s^{-1}$ (pH 7.0, $T=25^\circ C$) (Hayashi and Yamazaki, 1979; Nakajima and Yamazaki, 1987). However, at H_2O_2 concentrations greater than 1 equivalent, in the presence or absence of donor substrates, HRP is inactivated in a time- and H_2O_2 -dependent manner (Figure 1-3) (Arnao et al., 1990b). The route of inactivation can proceed along one of two pathways which are

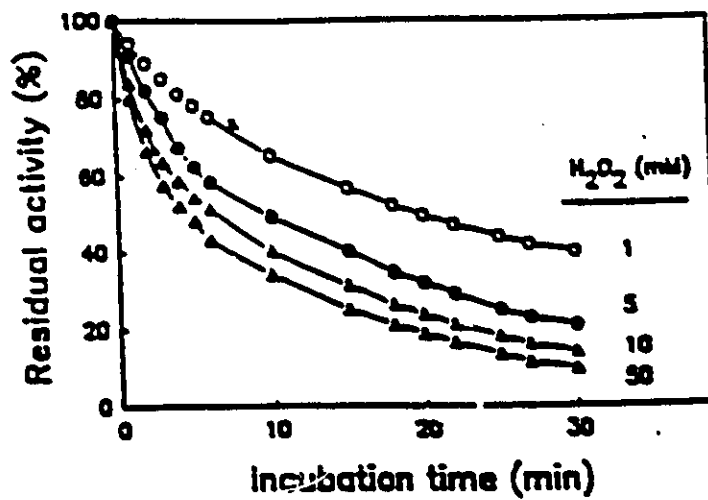


Figure 1-3 Curves exhibiting time- and H₂O₂-dependent inactivation of HRP (Sigma, type IX) ([HRP]=1μM; T=25°C, pH 6.3) (taken from Arnao et al., 1990b.)

suggested to be partitioned either at the level of Compound I in the presence of donor substrates (Arnao et al., 1990b; Nakajima and Yamazaki, 1987) (Figure 1-4), or at a Compound I-H₂O₂ intermediate, in the absence of donor substrates (Arnao et al., 1990a) (Figure 1-5). The present uncertainty surrounding the existence of Compound I-H₂O₂ (Baek and van Wart, 1992; Dunford and Stillman, 1976) and Compound II-H₂O₂ intermediates (Dunford and Stillman, 1976) and the reversibility of these pathways (Dunford and Stillman, 1976), however, does not necessarily render them mutually exclusive as suggested by the authors. One pathway involves obligatory production of Compound II in the familiar 1-electron reduction of Compound I by either a donor substrate (AH₂) or an extra equivalent of H₂O₂, which can play the role of reductant in the presence of Compound I's strong oxidative power and in the absence of traditional donor substrates (Arnao et al., 1990a; Hayashi and Yamazaki, 1979; Ortiz de Montellano, 1987). Further addition of H₂O₂ to Compound II in the presence and/or absence of donor substrates results in the formation of a red, relatively inert HRP-intermediate, Compound III (Everse et al., 1990). Under conditions of "excess" H₂O₂, Compound III's formation from Compound II is predominant over decay of Compound II back to the native enzyme (Nakajima and Yamazaki, 1987; Adediran and Lambeir, 1989). Compound III formation and accumulation is rapid ($k_c = 20M^{-1}s^{-1}$; Adediran and Lambeir,

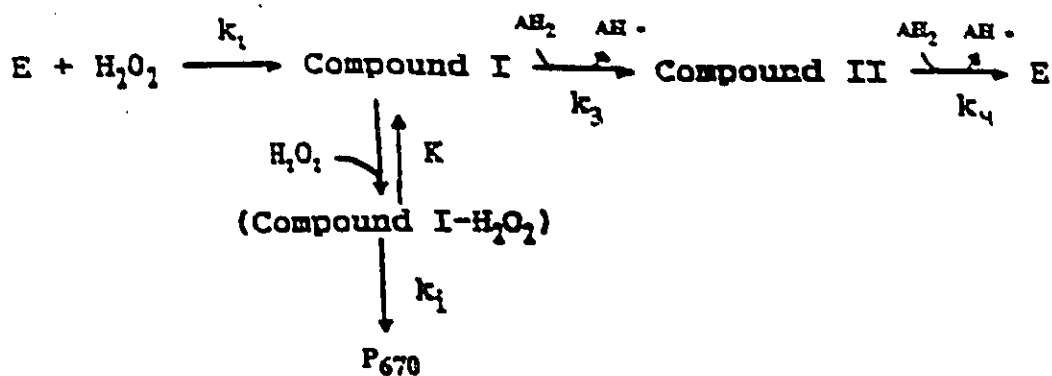


Figure 1-4 Scheme depicting partitioning of reaction pathways that exists at Compound I in the presence of donor substrates (AH₂) and greater than 1 equivalent of H₂O₂ (modified from Arnao et al., 1990a).

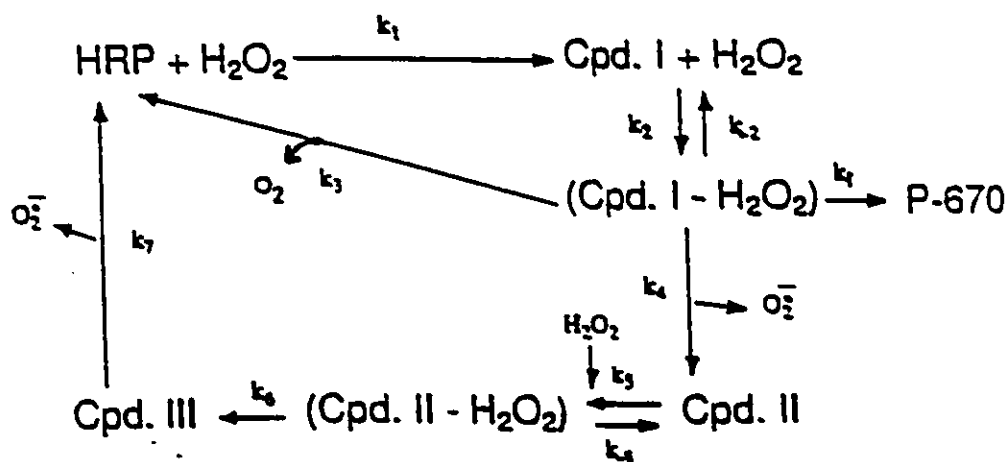


Figure 1-5 Scheme demonstrating the partitioning of possible reaction pathways at the level of a Compound I-H₂O₂ intermediate, in the absence of donor substrates: k₁-a mechanism-based inactivation leading to formation of Compound P₆₇₀; k₂-a weak catalase reaction regenerating native HRP, and; k₄+k₅+k₆-resulting in the formation of Compound III (modified from Arnao et al., 1990b).

1989), H_2O_2 -dependent (Noble and Gibson, 1970) and follows via one of two parallel and simultaneous pathways. They are distinguishable by superoxide scavenger tetranitromethane's (TNM) inhibitory effect over one path but not the other (Nakajima and Yamazaki, 1987; Adediran and Lambeir, 1989). In the predominant TNM sensitive pathway, the ferryl iron (IV) of Compound II is first reduced to ferric iron (III), resulting in a transient intermediate identical in nature to the native enzyme, along with production of a superoxide radical ($HO_2\cdot$). The second-order rate constant of this step, at $5^\circ C$, pH 7.0, is $2.1M^{-1}s^{-1}$ (Nakajima and Yamazaki, 1987). The ferric intermediate can either react with the superoxide radical to produce Compound III in another second-order process ($k=10^7M^{-1}s^{-1}$) (Adediran and Lambeir, 1989; Nakajima and Yamazaki, 1987) or it can react with a molecule of H_2O_2 , present in excess, producing Compound I (Nakajima and Yamazaki, 1987). From Compound I, either more Compound III can be formed or the second, slower pathway ($k_1 = 0.00392s^{-1}$; Arnao et al, 1990a) may be followed. Along this path, in the presence or absence of donor substrates, HRP "commits suicide" in a mechanism-based inactivation reaction characterized by a first-order, time-dependent loss of activity in which the enzyme half-life ($t_{1/2}$) is related to the rate constant of inactivation (k_1) by $t_{1/2}=0.693/k$ (Arnao et al., 1990a,b; Walsh, 1977a). Inactivation can result not only from excess H_2O_2 (Arnao et

al., 1990a,b; Bagger and Williams, 1971; Nakajima and Yamazaki, 1980) but other hydroperoxides as well (Chance, 1949; Marklund, 1973; Nakajima and Yamazaki, 1980); protection is afforded by high donor to peroxide concentrations (Arnao et al., 1990a,b; Dunford and Stillman, 1976). An irreversibly formed, green compound ("verdo-haemoprotein"), referred to as Compound IV or P₆₇₀ (due to the 670nm absorbance maximum witnessed in its presence), is produced via at least one intermediate (P₆₄₀) (Bagger and Williams, 1971; Nakajima and Yamazaki, 1980). It exhibits a visible absorption spectrum resembling protein-heme products of oxidative hemoglobin degradation in which the porphyrin ring has been irreversibly cleaved at one of the methylene bridges, generating a tetrapyrrole (Bagger and Williams, 1971; Brown et al, 1968; Smith et al., 1982). The choice of paths at the level of Compound I depends on the H₂O₂ concentration in the presence/absence of donor substrates (Arnao et al., 1990a,b). Upon obtaining most of the rate constants depicted in Figure 1-5 and Table 1-3, Arnao et al. (1990a) calculated several partition ratios based on the parameter r , described as the number of turnovers given by 1 mole of enzyme before inactivation: r_c is the ratio (k_3/k_1) of the rate constants leading to native enzyme (catalytic pathway) and Compound P₆₇₀, respectively, from a purported Compound I-H₂O₂ intermediate. A calculated value of 449 indicates the catalytic pathway would be favored over the

<u>Constant/Parameter</u>	<u>Value</u>	<u>Reference</u>
k_1	$2 \times 10^7 M^{-1} s^{-1}$	Yamazaki and Nakajima, 1986
k_2	$5 \times 10^2 M^{-1} s^{-1}$	Arnao et al., 1990a
k_{-2}	~ 0	"
k_3	$1.76 s^{-1}$	"
k_4	$7.85 \times 10^{-3} s^{-1}$	"
k_5	—	N/A
k_6	—	N/A
k_7	$20 M^{-1} s^{-1}$	Adediran and Lambeir, 1989
k_8	$4.18 \times 10^{-3} s^{-1}$	Nakajima and Yamazaki, 1987
k_9	$3.92 \times 10^{-3} s^{-1}$	Arnao et al., 1990a
$r_c (k_3/k_4)$	449	"
$r_{coIII} (k_7/k_8)$	2	"
$r_c + r_{coIII}$	451	"
r_c/r_{coIII}	225	"

N/A - not available

Table 1-3 Rate constants and parameters describing the inactivation/catalytic pathways of HRP, in the presence of H_2O_2 , referred to in Figure 1-5 and the text. All values were determined at 25°C, and neutral pH unless otherwise indicated.

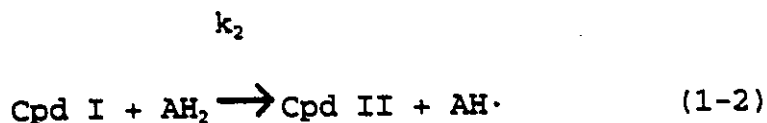
inactivation pathway under their experimental conditions; r_{CoIII} is the ratio (k_4/k_i) of rate constants describing the paths leading towards Compound III and Compound P_{670} formation, respectively. A determined value of 2.00 indicates that for every 2 catalytic turnovers producing Compound III, 1 inactivation would occur; the ratio r_c/r_{CoIII} indicates the number of catalytic cycles given by the enzyme behaving as a catalase to those in which Compound III would be generated. A value of 225 was determined under their conditions and indicates that the number of catalytic cycles given by the enzyme behaving as a catalase is approximately two orders of magnitude higher than those given by the pathway including Compound III. Upon addition of $r_c + r_{\text{CoIII}}$ values determined under their experimental conditions, they obtained a parameter which indicated that in a system containing only H_2O_2 and enzyme (Sigma, type IX) and under conditions of relatively high H_2O_2 (greater than 1 equivalent) ($T=25^\circ\text{C}$, pH 6.3), 451 catalytic turnovers involving both the catalytic and Compound III forming pathways would occur before one inactivation event would take place.

Generation of Compound III is accompanied by amino acid oxidation (Adediran and Lambair, 1989) and is thought to be an attempt by the enzyme to protect itself from fatal oxidative attack at the porphyrin ring under conditions of "excess" H_2O_2 (Bagger and Williams, 1971; Nakajima and

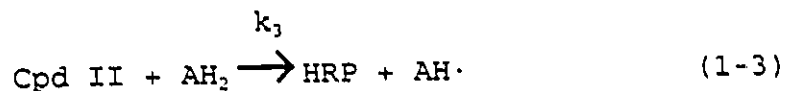
Yamazaki, 1987). Depletion of H₂O₂ results in slow re-generation of the native, active enzyme from Compound III with rate constant (k₇) of 4.18 x 10⁻³s⁻¹ (Nakajima and Yamazaki, 1987). Formation of Compound P₆₇₀ signals a failure of Compound III to prevent the self-induced death of HRP by its own substrate, H₂O₂, which it continues to turnover until it is no longer able (Arnao et al., 1990a,b; Bagger and Williams, 1971).

1.4.2 Inactivation by Enzyme-Generated Phenoxy Radicals

During the peroxidatic cycle, all neutrally charged phenolic donor substrates bind to Compound I in the vicinity of the heme 8-methyl group (Figure 1-1), assisted by hydrophobic interactions with the tyrosyl-185 residue (Sakurada et al., 1986). Irreversible oxidation occurs by a 1 electron abstraction generating Compound II and a neutral free radical (AH·) (Brewster et al., 1991):



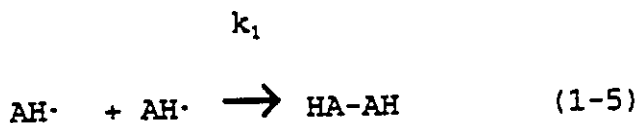
Compound II, in a similar but slower reaction, can react with a second donor molecule producing another free radical and regenerating native HRP (Job and Dunford, 1976; Shiga and Imaizumi, 1973; Yamazaki et al., 1960):



Once produced, the radicals diffuse away from the enzyme's active site (Danner et al., 1973; Yamazaki et al., 1960) and their chemical reactivity and structural characteristics determine the nature of the final products formed (Dunford and Stillman, 1976; Everse et al., 1990; Walsh, 1979; Yamazaki et al., 1960).

Phenoxy radicals are extremely reactive towards: (1) each other (Tripathi and Schuler, 1982; 1984; Walsh, 1979); (2) a molecule of phenol and/or product of phenol oxidation (Klibanov et al., 1980; 1981; 1983; Tripathi and Schuler, 1982); and/or, (3) the enzyme itself (Ma and Rokita, 1988; Klibanov et al., 1983; Lindsay et al., 1986).

Reactions between radicals produced in basic solutions and pulse radiolytically are extremely rapid, decaying with a half-life ($t_{1/2}$) of $\sim 2\mu\text{s}$ (Schuler et al, 1976; Tripathi and Schuler, 1984; Ye and Schuler, 1989). These predominantly second-order reactions exhibit rate constants approaching diffusion controlled limits - $2 \times 10^9 \text{M}^{-1}\text{s}^{-1}$ (Tripathi and Schuler, 1982; 1984; Ye and Schuler, 1989). The most common radical-radical reaction involves radical-radical coupling/combination (Figure 1-6):



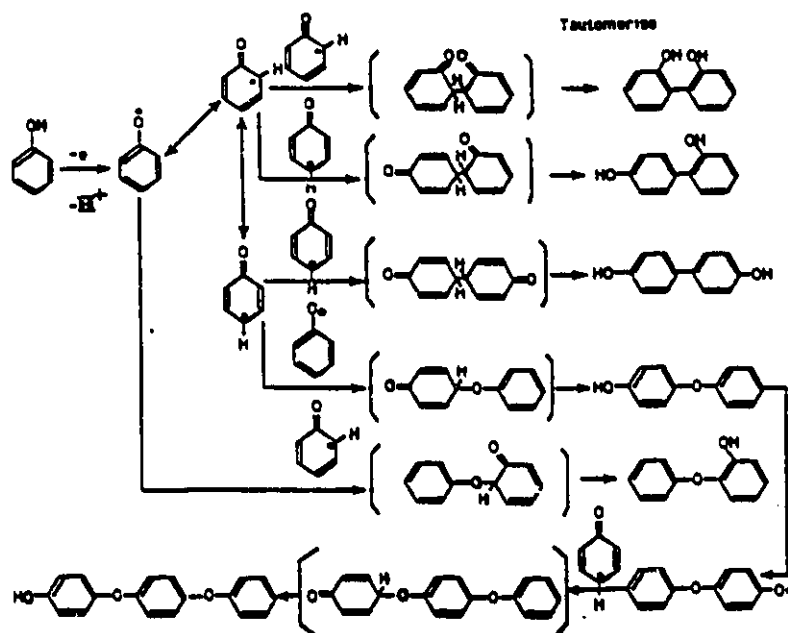


Figure 1-6 Reaction pathway scheme for enzyme-generated phenoxy radicals (after Huixian, 1991; unpublished)

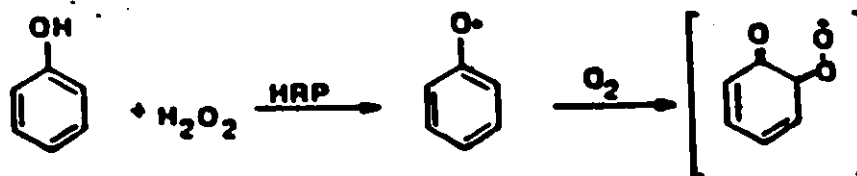


Figure 1-7 Formation of the hydroperoxy radical (in brackets) from reaction between an enzyme-generated phenoxy radical and molecular oxygen (Ma and Rokita, 1988).

producing any of 5 major products - o,o'-biphenol, p,p'-biphenol, o,p-biphenol, o-phenoxyphenol and p-phenoxyphenol - may be produced (Huixian, 1991; unpublished; Sawahata and Neal, 1982; Ye and Schuler, 1989). Most of these dimers are reasonably soluble in H₂O producing brownish-yellow coloured solutions (Huixian, 1991; unpublished; Ma and Rokita, 1988; Sawahata and Neal, 1982) and possess higher extinction coefficients than the parent phenol in the far uv. region (Huixian, 1991; unpublished). As these dimeric products accumulate to concentrations approaching those of free radicals, radical-directed secondary electron transfer reactions can occur, resulting in further oxidation and subsequent polymerization of products to trimers (Huixian, 1991; unpublished; Schuler et al., 1976; Tripathi and Schuler, 1984; Ye and Schuler, 1989) and more complex, insoluble oligomeric products that tend to precipitate out of solution (Huixian, 1991; unpublished; Klivanov et al., 1980; 1981; 1983). The enzyme is also capable of oxidizing some of the dimers, producing similarly complex and insoluble products (Klivanov et al., 1983; Nicell, 1991; Sawahata and Neal, 1982).

Another less common radical-radical reaction involves inter-radical electron transfer or disproportionation (Brewster et al., 1991; Tripathi and Schuler, 1982; Walsh, 1979; Ye and Schuler, 1989):

k_1



producing an oxidized species (A: hydroquinone) and another donor molecule capable of undergoing further enzymic oxidation/phenoxy radical attack (Ye and Schuler, 1989). Phenoxy radicals may also react with molecular oxygen producing another very oxidatively reactive intermediate, the peroxy radical (Figure 1-7) (Ma and Rokita, 1988; Ortiz de Montellano and Grab, 1986; Walsh, 1979).

At concentrations comparable to phenoxy radicals, phenol or products of radical-radical reactions may undergo phenoxy radical-mediated oxidative attack resulting in the production of further radical intermediates capable of reacting in radical-radical coupling/disproportionation reactions, ultimately producing products obtained from phenoxy radical-radical reactions (Huixian, 1991; unpublished; Klibanov et al., 1980; 1981; 1983 ; Sawahata and Neal, 1982; Schuler et al, 1976; Ye and Schuler, 1989). The pseudo-first order rate constant for radical-neutral species reactions is slower than radical-radical reactions - on the order of $2 \times 10^8 \text{M}^{-1}\text{s}^{-1}$ - reflecting the predominance of radical-radical reactions over secondary and tertiary radical reaction mechanisms (Ye and Schuler, 1989).

The enzyme itself may be attacked, in a phenoxy

radical-mediated time-dependent, mechanism-based inactivation reaction (Klibanov et al., 1983; Lindsay et al., 1986; Ortiz de Montellano and Grab, 1987; Ma and Rokita, 1982) dependent on both phenol and H_2O_2 concentrations, and potentiated by molecular oxygen (Ma and Rokita, 1982) (presumably through formation of peroxy radicals) (Ortiz de Montellano, 1986; Walsh, 1979). Inactivation is apparently first-order, exhibiting a value of 0.211min^{-1} in the absence of oxygen and 0.337min^{-1} in its presence (Ma and Rokita, 1982). Inactivation may occur at the active site in a manner analogous to that of azide, alkylhydrazine and phenyl-hydrazine mechanism-based inactivations, which are primarily the result of radical attack and association at the δ -meso carbon, followed by oxidative degradation of the porphyrin (Ator and Ortiz de Montellano, 1987; Ator et al., 1987; Ortiz de Montellano et al., 1988). Inactivation could also arise from radical oxidation of crucial amino acid groups located at the surface of the enzyme (Ator et al., 1987; Ator et Ortiz de Montellano, 1987; Ma and Rokita, 1988). The enzyme intermediate(s) involved in this particular inactivation mechanism is(are) not known (Ortiz de Montellano et al., 1988) and a systematic kinetic analysis has not yet been performed. What is known is that inactivation likely occurs somewhere at the level of Compound II since oxidation of phenol by Compound I is absolutely necessary to generate

radicals (Ortiz de Montellano et al., 1988). It is thought that Compound III, as with H_2O_2 inactivation, may be involved playing a similar protective role against oxidative, irreversible enzyme inactivation, perhaps involving the formation of an unreactive intermediate reminiscent of or identical to Compound P_{670} (Nicell, 1991).

1.5 Kinetic Considerations

There are certain pitfalls associated with attempts to gather accurate kinetic data of peroxidase reactions using traditional methods (Dunford and Stillman, 1976). The k values cited in the literature and representative of traditional rate constants, are not indicative of the true situation. HRP reaction intermediates, in particular Compounds I and II, react with their donor substrates in second-order fashion and do not form true Michaelis-Menten complexes. Compound I is not considered to be a true enzyme-peroxide complex, but rather an unstable derivative possessing an oxidized active site (Davies et al., 1976). Compound II, upon reacting with a donor, is described as a covalent compound distinct from a Michaelis-Menten complex (Dunford and Stillman, 1976). Therefore, Compounds I and II do not necessarily conform to Michaelis-Menten treatment (Dunford and Stillman, 1976).

There is evidence to suggest that when using proper substrates with the right redox potentials the three

reactions in the peroxidase cycle (1-1, 1-2 and 1-3) are irreversible and there remains the question of complex formation on the paths generating the HRP compounds (Dunford and Stillman, 1976; Everse et al., 1990). Quantitatively, it is impossible to know if 100% conversion of one intermediate has occurred to produce exclusively another intermediate. Kinetic evaluations are usually hampered by the abilities of Compounds I and II (in particular Compound I) to react with endogenous donors or oxidizable impurities that are capable of promoting their rapid and residual spontaneous decay. Impurities can be detected in buffers, H₂O₂ solutions, activity reagents and the enzyme preparations by running appropriate blank reactions (Dunford and Stillman, 1976). Light produced from spectrometers and the slow attack of enzyme molecules on each other have also been shown to accelerate spontaneous decay of both Compounds I and II (Everse et al., 1990).

Conventional treatment of results obtained in inactivation studies is precluded by the complexity associated with a 2 substrate system, the number of possible enzyme-intermediates involved and the apparent irreversible nature of both complex formation and inactivation itself (Marklund, 1973). HRP treads a fine line between catalysis and inhibition/inactivation. Substances acting as substrates at low concentrations can become inhibitors/inactivators when present at higher concentrations. To

circumvent this, substrates possessing this potential are often present in activity assay solutions at concentrations well below their K_m (non-saturating). Thus, kinetic parameters are more accurately described as apparent constants, but in practice, they are rarely cited as such (Ryu and Dordick, 1992). Adding further to the confusion, what was once thought to be a fairly well-understood mechanism in the peroxidase-oxidase reaction between HRP and nicotinamide adenine dinucleotide (NADH), has recently been shown to be much more complex, exhibiting periodic-chaotic sequences that involve at least five enzyme intermediates (Aguda and Larter, 1991). A similar complexity of mechanism, under the right conditions of substrate and enzyme concentrations, could in fact exist in the peroxidatic reaction.

Despite these obstacles, perfectly valid Michaelis-Menten K_m values may be defined for both oxidizing and reducing substrates. The use of pseudo-first order kinetics has assisted since neither knowledge of absolute molar absorptivities nor concentrations of reactants, products nor inert species contributing to the total absorbance is required during the first-order process. A serious and frequently encountered problem of pseudo-first order kinetic measurements is that they require large excesses of substrate which may accelerate the reaction to a point where the initial portion becomes too fast to follow (Dunford and

Stillman, 1976). However, the large molar absorptivities of peroxidases and huge absorbance changes that occur with the more sensitive chromogen systems used to measure HRP activity, make it possible to determine reasonably accurate and reproducible rate measurements as long as the enzyme concentration is kept low. This permits a somewhat more quantitative kinetic evaluation than could be achieved previously under first-order conditions, although strictly speaking, it should be borne in mind that such investigations are in reality still more qualitative than quantitative.

The purpose of this present study was to perform steady-state kinetic analyses in attempts to investigate two modes of HRP inactivation, namely H_2O_2 -mediated and enzyme-generated phenoxy radical-mediated inactivation.

CHAPTER 2

MATERIALS AND METHODS

2.1 MATERIALS

2.1.1 Enzymes

Horseradish peroxidase (HRP) ([Donor: Hydrogen-peroxide oxido-reductase; EC. 1.11.1.7] Grade II, RZ. 2) was obtained as a lyophilizate from Boehringer-Mannheim Canada, Dorval, PQ. This preparation consisted predominantly of the neutral isoenzyme C. The enzyme activity, as quoted from the supplier, is approximately 200 U/mg lyophilizate where one unit will catalyze the oxidation of one μ mole of guaiacol, in the presence of H_2O_2 , at 25°C, pH 7.5. Concentrated, aqueous stock solutions were prepared for subsequent dilutions and stored at 4°C.

Horseradish peroxidase isoenzymes (acidic [Type VII, RZ. 3.7; Type VIII, RZ. 3.2]; basic [Type IX, RZ. 3.2]), for isoelectric focusing gels (IEF), were obtained from Sigma Chemical Company, St. Louis, MO. Samples were stored at 4°C, in aqueous solutions until required.

Catalase (EC. 1.11.1.6, from bovine liver) was purchased from Sigma Chemical Co., St. Louis, MO. The quoted activity

from Sigma Chemical Co. is 9,700 U/mg solid and 15,700 U/mg protein, where one unit will decompose 1.0 μ mole of H_2O_2 per minute at 25° C, pH 7.0 while H_2O_2 concentrations fall from 10.3 to 9.2 mM. Enzyme was stored dessicated at 0°C until needed for dialysis.

The following pI protein standards for IEF were obtained from Sigma Chemical Co.: glucose oxidase (pI 4.2), soybean trypsin inhibitor (pI 4.6), B-lactoglobulin (pI 5.1), carbonic anhydrase (pI 5.4, 5.9), myoglobin (pI 6.8, 7.2) and lectin from Lens culinaris (pI 8.5).

2.1.2 Chemicals

2.1.2.1 Reagents for HRP Activity Assay, Hydrogen Peroxide (H_2O_2) Colourimetric Assay and HRP Inactivation Studies

3,5-dichloro-2-hydroxybenzenesulfonic acid (HDCBS), 4-aminoantiprene (AAP) and phenol crystals (purity of 99% or greater) were purchased from Aldrich Chemical Co., Milwaukee, WI. All solutions were prepared as needed in 0.1M sodium phosphate buffer pH 7.4 (NaPP) and stored in the dark at room temperature until needed. Hydrogen peroxide (60% w/v) was supplied by BDH Chemicals, Toronto. Stock solutions were prepared fresh daily. Disodium hydrogen phosphate (Na_2HPO_4) and sodium dihydrogen phosphate (NaH_2PO_4) for phosphate buffer were supplied by BDH chemicals.

2.1.2.2 Reagents for Isoelectric Focusing Gels (IEF)

Acrylamide, Bis (N,N'-methylene-bis-acrylamide), riboflavin-5'-phosphate (FMN), ammonium persulfate, TEMED (N,N,N',N'-tetramethylene-ethylenediamine) and ampholytes (Bio-Lyte 3/10) were purchased from Bio-Rad, Mississauga. BDH Chemicals supplied ethanol, acetic acid, nitric acid, sodium carbonate, glycerol, methanol and 5-sulfosalicylic acid (3-carboxy-4-hydroxy-benzenesulfonic acid). Formaldehyde, trichloroacetic acid (TCA), copper sulfate, potassium dichromate and silver nitrate were obtained from Aldrich. Coomassie Brilliant Blue G-250 (CBB) was purchased from Eastman Kodak, Rochester, NY.

2.1.3 Instrumentation/Equipment

All spectrophotometric measurements were performed on a Hewlett Packard Diode Array Spectrophotometer Model 8451. Dialyses were carried out using 42mm dialysis capsules and 12,000 - 14,000 MWCO membranes supplied by Diacell, Union Bridge, MD. Gel supports, 0.4 mm slab gel apparatus, power supply and Mini IEF Cell Model 111 were obtained from Bio-Rad.

2.2 METHODS

2.2.1 Preparation of Buffers

A 0.1M NaPP stock buffer was prepared from appropriate weights of Na_2HPO_4 (21g/L) (dibasic) and NaH_2PO_4 (2.64g/L) (monobasic). Solutions were prepared in distilled, deionized

water. Final pH determinations were made using a Fisher Scientific Accumet model 910 pH meter standardized with BDH and Fisher supplied standard buffers to ± 0.01 pH units at the appropriate temperature.

2.2.2 Enzyme Stock Solution Preparation

Dilutions of the stock solution prepared as described below were used for subsequent inactivation experiments.

2.2.2.1 Enzyme Purification

BM. HRP solutions were prepared in 0.1M sodium phosphate buffer (NaPP) pH 7.4. Dialyses were performed against distilled water for periods of time recommended by the dialysis cell manufacturer (Diacell) based on the volume of the solution. Enzyme purity was determined spectrophotometrically by the RZ. (reinheitszahl) defined as the ratio of absorbance at 404 and 278 nm.

2.2.2.2 Determination of HRP Concentration

Concentrations of HRP solutions were determined spectrophotometrically by measuring the protein heme which displays a characteristic absorbance maximum at 404 nm (the Soret band), and using an extinction coefficient (ϵ_{404}) of $102,000 \text{ M}^{-1}\text{cm}^{-1}$ (Everse et al., 1990) and molecular weight (MW) of 40,000 g/mole (Everse et al., 1990) (see Appendix A for sample calculation and visible spectrum of native enzyme).

2.2.2.3 Assay for HRP Activity

The assay described was developed by previous workers in the laboratory (Artiss et al, 1979). Initial velocities were determined in a 1.0mL assay mixture containing 250 μ L 9.6mM AAP (2.4mM final concentration), 500 μ L 18.0mM HDCBS (9.0mM final concentration), 130-150 μ L 0.1M NaPP and 20-50 μ L HRP solution (final concentration of 5-10nM). The reaction was initiated by adding 100 μ L of freshly prepared 1.0mM H₂O₂ solution (final concentration of 100 μ M). The appearance at 510nm of a chromogen ($\epsilon_{510nm} = 25,000 \text{ M}^{-1}\text{cm}^{-1}$ based on H₂O₂) formed from a reaction between AAP and HDCBS was monitored at room temperature for one minute in a plastic cuvette. Specific activities were typically 158.4 ± 17.9 U/mg peroxidase where one unit of peroxidase activity is that amount of peroxidase needed to convert one μ mole of H₂O₂ per minute at room temperature (see Appendix B for specific activity calculation and plot of $\Delta\text{Abs. } 510/\text{time}$).

2.2.3 Isoelectric Focusing Technique (IEF)

IEF was performed according to cell manufacturer instructions (Bio-Rad) and modified by B. Harake (PhD. thesis, 1991). This was done to detect the presence of isoenzymes (especially acidic) in the BM. HRP preparation.

The gels were prepared from the following stock solutions:

- A) Monomer Concentrate: 24.25% (w/v) acrylamide, 0.75%

(w/v) Bis (N,N'-methylene-bis-acrylamide) dissolved in distilled water and filtered with a 0.45 μ m filter. Stored for up to one month at 4°C.

B) FMN: 0.1% (w/v). Stored for one month in the dark at 4°C.

C) Ammonium Persulfate: 10% (w/v). Prepared fresh as needed.

For preparation of monomer-ampholyte solution (enough for two 125 x 65 x .4 mm gels) 5.5mL of distilled water, 2.0mL monomer concentrate, 2.0mL of 25% (w/v) glycerol and 0.5mL of broad range (pH 3-10) ampholytes (40% solution) were mixed separately and degassed for five minutes under vacuum. Catalyst solution was prepared by mixing together 20 μ L of 10% (w/v) ammonium persulfate, 50 μ L 0.1% (w/v) FMN and 5 μ L TEMED. The catalyst solution was added to the degassed monomer-ampholyte solution and swirled. This solution was pipetted immediately between the glass plate and the casting tray, and the entire slab was irradiated for 45 minutes. The glass plate was then turned glass side down on to the casting tray and irradiated for a further 15 minutes to eliminate any unpolymerized monomer on the gel surface.

Samples for IEF were prepared in distilled water and were layered in 2 μ L (typically 0.06-.4 μ g protein based on heme content) volumes on top of the gel by means of a 20 μ L Gilson Pipetman. Electrophoresis was run at 25°C for 15 minutes at stepped voltages of 100V and 200V respectively, followed by a

one hour run at 450V.

Proteins were stained using one of the techniques in the following sections.

2.2.3.1 Coomassie Brilliant Blue G-250 Stain (CBB)

Following Bio-Rad specifications for detection Method A, gels were immersed in a fixative solution consisting of 4% (w/v) sulfosalicylic acid, 12.5% (w/v) TCA and 30% (v/v) methanol for 30 minutes. The gel was then placed in a staining solution (filtered two times) containing 27% (v/v) ethanol, 10% (v/v) acetic acid, 0.04% (w/v) CBB and 0.5% (w/v) copper sulfate for 1-2 hours. Three washes of 15 minutes each, using a destaining solution comprised of 12% (v/v) ethanol, 7% (v/v) acetic acid and 0.5% (w/v) copper sulfate, were performed following staining. The gel was washed two more times for 15 minute periods in a second destaining solution of 25% (v/v) ethanol and 7% (v/v) acetic acid until the last traces of stain and copper sulfate were removed.

2.2.3.2 Silver Stain

According to the method of Neilson and Brown (1984), the gel was fixed for 30 minutes in 10% (w/v) TCA, washed three times for 10 minute periods with 10% (v/v) ethanol in 5% (v/v) acetic acid and then oxidized for 6 minutes with 3.4mM potassium dichromate in 3.2mM nitric acid. The oxidant solution was discarded and the gel washed three times (5

minutes each) with distilled water. The gel was then placed into a 12.0mM silver nitrate solution for 20 minutes and then washed two times for approximately 1 minute with distilled water. All of these steps were performed at room temperature accompanied by mild shaking. The gel was then incubated for 30 seconds at 40°C in a developer solution consisting of 0.28M sodium carbonate and 0.0185% (v/v) formaldehyde (added just prior to use). A second developer solution was added to the gel after discarding the first, and the gel was incubated for a further 5 minutes or until brown/black protein bands were discernible. Staining was stopped by replacing the developer solution with 5-10% (v/v) acetic acid solution.

2.2.4 Kinetic Evaluation of Horseradish Peroxidase

2.2.4.1 Kinetic Evaluation: HDCBS/AAP System

Kinetic evaluations of HRP with respect to H_2O_2 , HDCBS and AAP concentrations were performed to determine the K_m and V_{max} of each of these substrates. Knowledge of these values was necessary for optimizing methods used to determine residual enzyme activity during inactivation of HRP by H_2O_2 and phenoxy radicals, thereby minimizing potential interference by components arriving from the incubation samples into the activity assay mixture. Triplicate determinations monitoring reaction rates (appearance of product at 510nm) were performed at concentrations of the variable component ranging from 100 μ M to 10mM, while the other two assay components were kept at

constant and saturating concentrations (Section 2.2.2.3). Enzyme concentration was constant at approximately 20nM (20 pmoles). From plots of absorbance units vs. time, initial velocities were calculated (absorbance units [A.U.]/minute) and plotted against substrate concentration. Values for K_m and V_{max} were obtained from non-linear regression of the data sets using enzyme kinetics computer program ENZFITTER™. Calculated values observed for H_2O_2 were compared to values obtained from previous workers using this chromogen system. Values obtained for HDCBS and AAP were compared to values obtained from previous workers in this laboratory (Boss, 1986; Harake, 1988.)

2.2.4.2 Kinetic Evaluation: Phenol/AAP System

K_m and V_{max} values were determined for this chromogenic system which was used in place of the HDCBS/AAP system to determine remaining activity during phenoxy radical inactivation of HRP. Substitution of phenol for HDCBS as the partner to form a chromogen (absorbance maximum 510nm) with AAP eliminated the possibility of interferences arising from phenol present in samples removed from incubation solutions. Triplicate assays were performed as discussed above for the HDCBS/AAP system. Concentrations examined for H_2O_2 , phenol and AAP ranged from 1 μ M to 20mM at enzyme concentrations of 5 and 10nM, respectively. Components not being varied were held at constant and saturating concentrations. A plot of initial

velocities vs. substrate concentration was developed and evaluated by ENZFITTER™ using non-linear regression analysis to yield K_m and V_{max} values for each substrate. Component concentrations which yielded the fastest reaction velocity were also determined (see Appendix C for phenol/AAP activity reagent recipe).

An extinction coefficient was determined based on H_2O_2 concentration. Solutions were prepared containing in a 5mL total volume, 1.25mL 9.6mM AAP ([final] = 2.4mM), 0.133mL 0.375M phenol stock ([final] = 10mM), 0.4mL 0.1M NaPP and the appropriate volume of H_2O_2 from a 10mM stock to yield concentrations between 10 and 200 μ M. The solutions were made up to 5mL in distilled water. A volume of 900 μ L was measured into a semi-micro cuvette. A 100 μ L aliquot containing 100nM HRP (10nM [final]) was added to initiate the reaction. The increase in absorbance was monitored until it developed no further. The end-point value at 510nm was measured at this point. These end-point values were plotted against [H_2O_2] using a linear least squares treatment of the data (see Appendix C, Figure C1).

2.2.5 Inactivation Studies

2.2.5.1 Inactivation of HRP By H_2O_2 During Substrate Oxidation

Characterization of the behaviour of the BM. HRP during HDCBS/AAP oxidation, while successive aliquots of limiting amounts of H_2O_2 were added to the reaction mixture over time,

was undertaken as a preliminary experiment to compare with results obtained from similar experiments by Arnao et. al. (1990b) using the Sigma HRP and employing ABTS as the reductant. All measurements were performed in triplicate. Two concentrations of HRP and H_2O_2 were examined. To a plastic cuvette containing 9.0mM HDCBS and 2.4mM AAP (at saturating concentrations) in 1.0mL, a 20-50 μ L aliquot of enzyme diluted from a concentrated stock to yield final concentrations in the cuvette of 0.5 or 1.0nM (0.5 and 1.0 pmoles: concentrations similar to and 2-fold greater than those used by Arnao et al.) was added. The reaction was initiated by the addition of a 20 μ L aliquot of H_2O_2 yielding final concentrations, in 1.0mL, of 0.5 or 20 μ M respectively (0.5 and 20 nmoles: 1,000 to 20,000-fold molar excess over the enzyme). The reaction was allowed to proceed until no further increase in absorbance at 510nm with time was observed, indicating all H_2O_2 had been consumed. At this point, another aliquot of H_2O_2 was added to yield a concentration of 0.5 or 20 μ M in the cuvette, initiating further reaction. This procedure was repeated until no further increase in absorbance with time was observed upon subsequent addition of H_2O_2 . To confirm that the lack of increase in absorbance was due to enzyme inactivation by the accumulation of H_2O_2 and not due to the depletion of the donor substrates, HDCBS/AAP, a 20 μ L aliquot of a concentrated mixture of HDCBS/AAP yielding final concentrations of 9.0mM and 2.4mM, respectively, in a 1.0mL volume, was added to the

reaction mixture. Absence of increased absorbance with time corroborated complete inactivation of the enzyme. Presence of accumulated H_2O_2 as a result of the enzyme becoming inactivated and unable to use it for substrate turnover was further demonstrated by introducing an aliquot of HRP (0.5 or 1.0nM final) to the cuvette already containing excess H_2O_2 and HDCBS/AAP.

2.2.5.2 Time-Dependent Inactivation of HRP

Arnao et. al. (1990b) examined time-dependent inactivation of HRP (at a concentration of $1\mu M$) in the presence of H_2O_2 concentrations ranging from 1 to 50mM. Exposure of the enzyme to H_2O_2 lasted 30 minutes. Similar time-dependent inactivations were carried out in the present study using BM. HRP exposed to concentrations of H_2O_2 ranging from $100\mu M$ to 50mM. Inactivation was monitored for periods lasting from as little as 60 seconds to as long as 60 minutes. Triplicate test tubes representing given time periods of exposure of the enzyme to H_2O_2 were set up to contain the desired concentration of HRP in a 1.0mL final volume. Inactivation was initiated by the addition of an aliquot of H_2O_2 to the enzyme. As the desired time of exposure of enzyme to H_2O_2 approached (as monitored by a Micronta stop watch), a $20\mu L$ aliquot was withdrawn from the incubation sample and plunged exactly at the desired time into a plastic cuvette containing the activity assay components in a 1.0mL volume

(9.0mM HDCBS, 2.4mM AAP and 100 μ M H₂O₂). This diluted the enzyme-H₂O₂ sample, effectively halting the inactivation process and yielding a value that corresponded to the extent of inactivation achieved for that particular time of exposure of enzyme to a specific concentration of H₂O₂. Enzyme activity was determined from the rate of increase of absorbance at 510nm with time (A.U./minute). Control samples to which identical volumes of water were added to the enzyme in place of H₂O₂ were similarly assayed for activity at times corresponding to those at which the incubation samples had been tested for activity. This permitted % remaining activities at given times to be calculated. Various samples were incubated at room temperature for an additional 24 hour period and assayed to determine if any activity lost during the initial inactivation experiment had been recovered. Other samples were dialyzed, in the presence of catalase, for 20 minute and 24 hour periods in attempts to recover lost activity. Finally, samples exposed to H₂O₂ for 24 hours were dialyzed for 20 minute and 24 hour periods, in the presence of catalase, in attempts to recover lost activity.

Once time-dependent inactivation data had been obtained, rate constants of inactivation (k_{obs}) for each H₂O₂ concentration were determined by ENZFITTER™ fitting the data to both double and single exponential decay models.

2.2.5.3 Qualitative Investigation to Identify the Enzyme Intermediate Present During H₂O₂-Induced HRP Inactivation

A qualitative examination to identify the enzyme species present during the time-dependent inactivation of HRP by H₂O₂ was undertaken. The presence of a particular enzyme species could be indicated by spectrophotometrically monitoring changes that occurred in the native enzyme visible spectrum upon the addition of specific concentrations of H₂O₂. The Soret band (404nm) and the alpha (α) and beta (β) bands (640nm and 498nm, respectively) were monitored for any shifts (bathochromic or hypsochromic) and/or hyper/hypochromic effects upon addition of H₂O₂. Concentrations of H₂O₂ examined were 100μM to 100mM. Changes occurring in the Soret region were monitored from 350 to 450nm using enzyme concentrations from 2.3 to 15μM. Changes occurring in the alpha and beta bands were examined from 450 to 750nm, using enzyme concentrations from 23 to 46μM. Enzyme samples were monitored in a quartz cuvette for periods ranging from 60 seconds to as long as 72 hours. Spectra were measured at 30 second intervals (or as often as every 5 to 10 seconds for the 60 second experiment) until 60 seconds, at which time measurement intervals were increased to one measurement every 10 to 15 minutes. Plots of the spectra were overlaid on a spectrum of the native enzyme for comparison and the major absorbance peaks were recorded for each spectrum measured. Absorbance peaks identified during the experiment were compared to

literature values which stated the wavelengths where absorbance maxima (λ_{max}) are found in spectra obtained from "pure" HRP intermediates.

In order to compare the above spectra with actual HRP compounds and to determine the enzyme species from which compound P₆₇₀ develops, enzyme intermediates were prepared from the native enzyme using only H₂O₂. Spectra, as well as the wavelengths where absorbance maxima occurred were recorded once the intermediate had been generated. Presence of an intermediate was indicated by a stable visible absorption spectrum that underwent no further increase or decrease in absorbance at the characteristic wavelengths reported in the literature. Enzyme intermediates were prepared from a sample of native enzyme as follows (after Arnao et al., 1990; Saunders et al., 1964):

Compound I: To a 17.5 μ M HRP solution in a 1.0mL volume, 15 μ L of 1.0mM H₂O₂ stock solution was added (substoichiometric; 15 μ M). The presence of Cpd. I was confirmed by the presence of relatively stable absorbance maxima at 520 and 656nm (Dunford and Stillman, 1976; Keilin and Hartree, 1951), approximately 3 minutes after the addition of H₂O₂ to the enzyme.

Compound II: To a 1mL sample of 17.3 μ M native enzyme, 42.5 μ L of 1.0mM H₂O₂ (2.5-fold molar excess) was added. Approximately

3 minutes were required for complete conversion of native enzyme. Concentration of Cpd. II was approximated using an ϵ_{527} of $9,500\text{M}^{-1}/\text{cm}$ and an ϵ_{554} of $9,650\text{M}^{-1}/\text{cm}$ (Dunford and Stillman, 1976). Presence of Cpd. II was confirmed by the existence of stable absorbance maxima at 529 and 556nm.

Compound III: To the above solution of Cpd. II, $30\mu\text{L}$ of 100mM H_2O_2 (176-fold molar excess) was added and the development of the spectrum characteristic to Cpd. III was monitored for approximately 5 minutes. Presence of Cpd. III was confirmed by the appearance and stabilization of absorbance maxima at 546 and 580nm. Conversion of Cpd. II into Cpd. III was confirmed using ϵ_{546} of $10,000\text{M}^{-1}/\text{cm}$ (Keilin and Hartree, 1951).

Compound P_{670} /Compound IV: In the paper by Arnao et al. (1990a), it was suggested by results obtained during similar experiments that P_{670} might arise from/at the level of cpd. III. Therefore, $30\mu\text{l}$ of 1.0mM H_2O_2 (approximately 2-fold excess) was added to the above solution of Cpd. III. Presence of P_{670} was indicated by the gradual disappearance of the absorbance maxima at 546 and 580nm accompanied by the appearance of a peak which stabilized, approximately 2 to 3 minutes after the addition of H_2O_2 , at 670nm. Figure 2-1 shows the spectra of each pure HRP intermediate generated by the method outlined above.

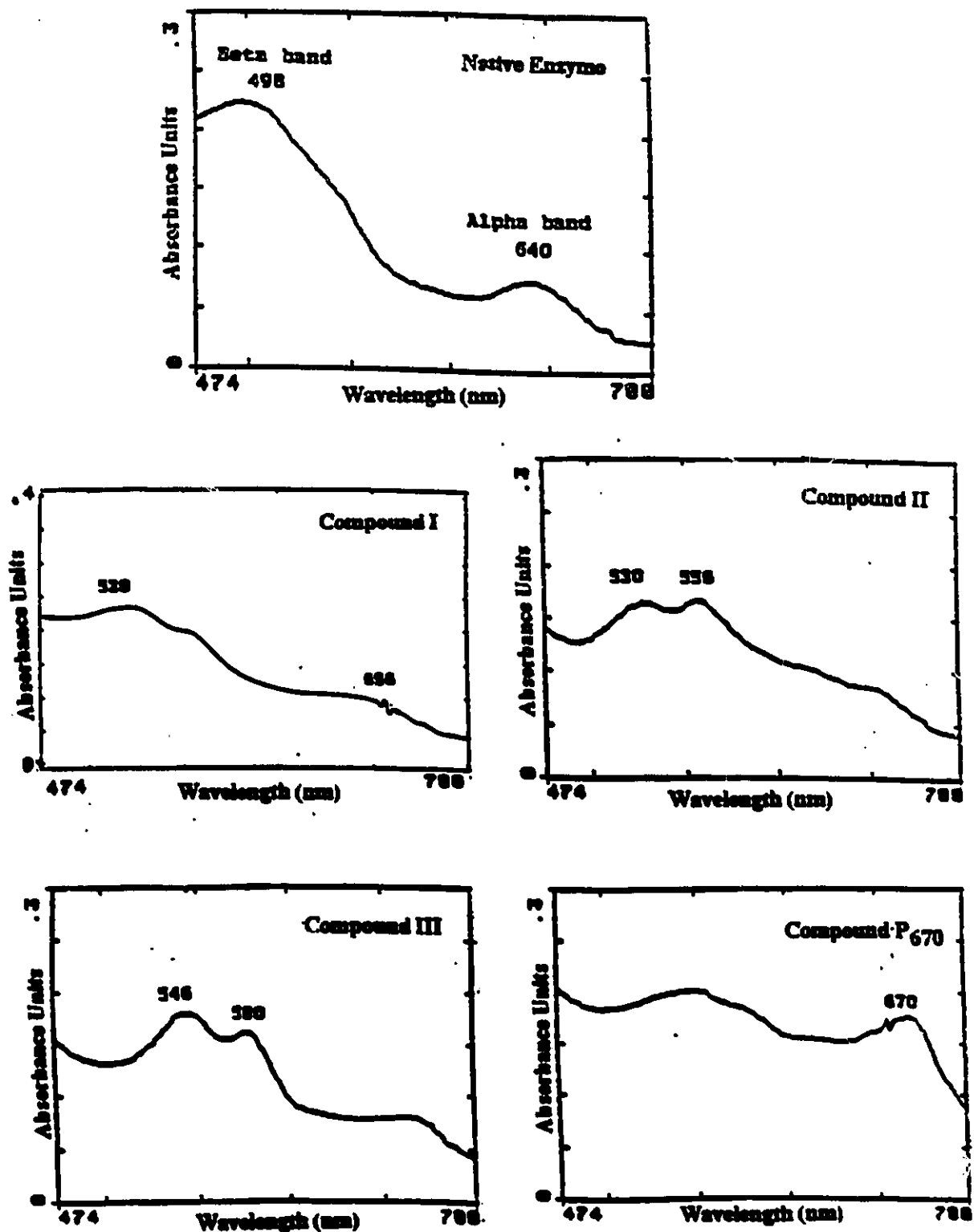


Figure 2-1 Visible spectrum of the characteristic alpha and beta bands of native HRP and its reaction intermediates (17.5 μ M HRP; T=25°C, pH 7.4)

2.2.5.4 Inactivation by Phenoxy Radicals

Experiments designed to measure the time-dependent inactivation of HRP by enzyme-generated phenoxy radicals at enzyme concentrations of 25, 50 and 100nM, H₂O₂ concentrations of 0.5 and 1.0mM and over a range of phenol concentrations from 0.2 to 5.0mM, were undertaken in the following manner. All measurements were performed in triplicate or duplicate. To test tubes containing 4mL of HRP of the appropriate concentration to yield the desired final concentration in a 5mL volume, and representing specific periods of time of exposure of enzyme to phenoxy radicals, phenol was added from a prepared stock solution just prior to addition of H₂O₂. Stock phenol concentrations were determined from the absorbance value at 272nm and an extinction coefficient of 1,300 M⁻¹/cm (see Appendix D for spectrum and calculation). H₂O₂ was added to initiate the inactivation process. The inactivation solutions were incubated at room temperature until just prior to measuring the activity. At this point, a 100 to 400μL aliquot of sample was removed and plunged into a 1mL plastic cuvette containing 600 to 900μL of the phenol/AAP activity reagent. Concentrations were adjusted to yield the desired final concentrations in the activity assay. The volume of sample removed from the incubation was such to yield final concentrations of enzyme in the cuvette (activity assay) of approximately 10nM (10 pmoles). This amount of enzyme yielded reliable activity results. Inactivation was effectively

halted by exposure of enzyme to excess amounts of substrates. An indication of the extent of inactivation for the incubation duration was obtained from the results of these assays. Activity was measured as the change in absorbance units per unit time (A.U./min.) at 510nm, and values obtained were divided by values representing the activity of the native enzyme incubated in the absence of both phenol and H₂O₂ for the same incubation period. From these values, percent remaining activities were calculated for each incubation span. Each phenol concentration was characterized for extent of enzyme inactivation for periods lasting for 20 minutes, 5 minutes and 1 minute respectively, at constant HRP and H₂O₂ concentrations. Control test tubes were set up to contain enzyme alone, enzyme plus phenol and enzyme plus H₂O₂. Rate constants of inactivation (k_{obs}) for each phenol concentration at specific HRP and H₂O₂ concentrations were calculated using ENZFITTER™ single-exponential decay program, from linearized plots of the data ($\ln \% \text{ remaining activity vs. time}$), and from half-life calculations using the equation $t_{1/2} = \ln 2/k$, which utilized data from plots of $\% \text{ remaining activity vs. time}$.

2.2.5.5 Hydrogen Peroxide Concentration Determinations

Consumption of H₂O₂ was monitored for each time interval to determine reaction stoichiometry and the point during the inactivation process where inactivation had overcome catalysis (as indicated by continuing decline in activity in the absence

of further H_2O_2 consumption). A reagent solution was developed by researchers in this laboratory (Taylor and Nicell, 1990; unpublished) which contained phenol (10mM final) and AAP (2.0mM final) at saturating concentrations so that the limiting component was the H_2O_2 arriving from the incubation solution. The extent of colour development at 510nm was dependent on the concentration of H_2O_2 . Maximum colour development was obtained within 5 minutes. The reagent solution contained 50nM HRP. All determinations were performed in duplicate and results had less than 0.1% error between samples. Volumes of 800 μ L were pre-measured into plastic cuvettes. 200 μ L samples were removed from the incubation solutions after the appropriate amount of time, and pipetted into the H_2O_2 reagent solution. A standard sample containing the amount of H_2O_2 originally present in the incubations at $t=0$ seconds (200 μ L of a 1.0 or 0.5mM H_2O_2 stock solution added to 800 μ L reagent) was set up and final H_2O_2 concentrations were determined by dividing the absorbance of the sample at 510nm by the absorbance of the standard at 510 nm (typically 0.75-0.8 absorbance units for a 1mM H_2O_2 sample) and multiplying this value by the concentration of the H_2O_2 in the standard. A blank cuvette was prepared by adding 200 μ L of NaPP buffer to 800 μ L of reagent solution (see Appendix E for sample calculations).

CHAPTER 3

RESULTS AND DISCUSSION

3.1 ENZYME CHARACTERIZATION

For the purposes of most kinetic experiments, only isozyme classes A, C and E are important (Dunford and Stillman, 1976). However, for inactivation studies supposed to characterize one specific, commercially obtained isoenzyme, it was necessary to establish the absence of other contaminating isoenzymes, in particular, A3, so that kinetic behaviour could be attributed to the isozyme of interest, C in this case. Plate 3-1 is the resultant CBB.-stained 25% polyacrylamide isoelectric focusing gel, containing ampholytes in the pH range of 3-10, performed on BM. HRP Grad II (predominantly HRP-C) from different lot numbers (lot number 12003025 in lane #6 and lot #112006949 in lane #5), along with commercially available pure isozymes (lane #3: acidic isozyme type VII; lane #4: acidic isozyme type VIII; lane #2: basic isozyme type IX). pI standards (described in Materials and Methods) were run concomitantly in lane #1 for qualitative comparison of pI's. The polarity of the gel from top to bottom is cathode (-) and anode (+), respectively. Based on the manufacturer's stated pI's, the order of the pI standards

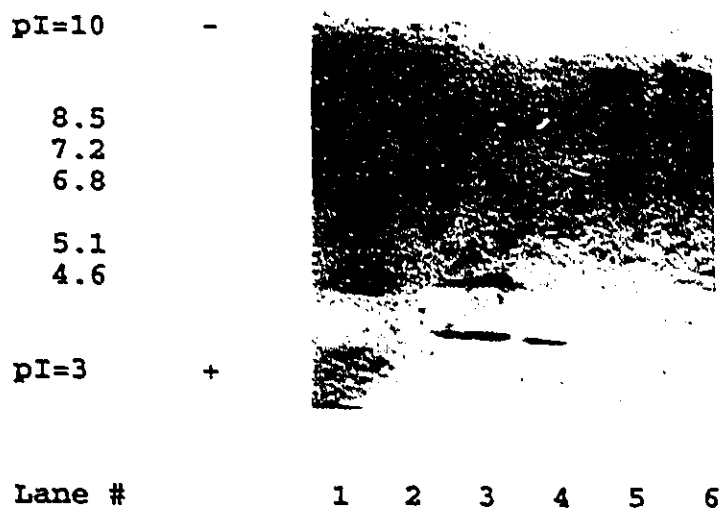


Plate 3-1 Coomassie BB.-stained 25% polyacrylamide gel of Boehringer-Mannheim Grad II HRP preparation. Presence of one band in lanes #5 and #6 that run close to Sigma basic isoenzyme negates the presence of contaminating isozymes.

- Legend:
- Lane #1: IEF standards
 - Lane #2: Sigma Type IX, basic isozyme (pI - 8)
 - Lane #3: Sigma Type VI, acidic isozyme (pI - 3-4)
 - Lane #4: Sigma Type VII, acidic isozyme (pI - 3-4)
 - Lane #5: BM. HRP, Grad II, lot #112006949
 - Lane #6: BM. HRP, Grad II, lot #12003025

(not all obvious) from top to bottom is lectin from Lens culinaris (pI 8.5), myoglobin (pI 7.2, 6.8), carbonic anhydrase (pI 5.9, 5.4), β -lactoglobulin (pI 5.1), soybean trypsin inhibitor (pI 4.6), and glucose oxidase (pI 4.2). Comparing lanes #3 and #4 (acidic isoenzymes; pI = 3.8 and 4.2) with lanes containing the BM. enzymes (lane #5 and 6, respectively), it can be seen that the BM. preparations exhibit a single protein band that migrated towards the cathode from the point of application, indicating the presence of predominantly neutral/basic isozymes. This is the expected pattern from a preparation containing the neutral to slightly basic isoenzymes B and C. There are no other detectable bands closer towards the cathode, nor towards the anode. This indicates that there are no extremely basic or acidic isozymes present in the BM. preparations, at least not at concentrations detectable by the CBE. stain technique employed (sensitive to as little as 1 μ g protein). From these results, it was assumed that if there were any acidic isozymes present in the BM. preparations, their concentrations were low enough to not significantly affect any subsequent transient-state inactivation kinetic investigations. Thus, subsequent results obtained from inactivation studies were attributed to HRP isozymes B and C, which have been shown to possess similar kinetic behaviour (Gonzalez-Vergara, 1985; Kay et. al, 1967).

3.2 KINETIC INVESTIGATION OF HORSERADISH PEROXIDASE

HRP's turnover number (how fast it produces one molecule of dye) depends only on the electron donor and its concentration. The colour formed and used to evaluate enzyme activity is highly dependent on this second, donor substrate. To obtain a reasonably accurate estimation of enzyme activity, it becomes extremely important that this component is not interfered with by the competitive substances (Conyers and Kidwell, 1991). However, HRP's oxidative unspecificity towards the donor substrate can result in just such a competition arising between the chromogen producing substrate and an interfering substance. Competition arises if the interfering substance is a better hydrogen donor than the substrate, or if it maintains the substrate in a perpetually reduced state (Artiss et al., 1981). Such negative interference ultimately reduces the effective concentration of the chromogen. This situation is further complicated if the interference forms a chromogen possessing a high extinction coefficient at an absorbance maximum close to the one being observed, yielding false high activities. Equally, the interference may exhibit both oxidized and reduced forms that do not contribute in any way to the final colour, resulting in false low activities (Artiss et al., 1981).

Interferences can be eliminated or minimized if the substrate, apart from exhibiting sensitivity, good stability and solubility of itself and its product, and small blank

reactions, is more reactive, demonstrating greater initial reaction velocities and affinity for the enzyme than the interference. It should not be so reactive that it inactivates the enzyme (Conyers and Kidwell, 1991; Sharp, 1972; Sharp et al., 1972).

Kinetic analyses were performed on the activity assays used to determine residual activity of HRP exposed to inactivating agents. Apparent kinetic constants obtained were used to optimize activity assay conditions serving to minimize possible interference arising from substances arriving in aliquots removed from the inactivation incubation solutions.

The reaction sequence characterizing both chromogenic assays used in this study involves the non-enzymatic coupling of enzyme-activated 4-aminoantipyrine (AAP; the "Trinder Reagent") with phenol or a sulphonated derivative of 2,4-dichlorophenol; in this case 3,5-dichloro-2-hydroxybenzene sulphonic acid (HDCBS). Activity assays employing the Trinder Reagent and a phenol have been successfully used in the determination of HRP activity by a number of researchers (Artiss et al, 1979; 1981; Boss, 1986; Conyers and Kidwell, 1991; Harake, 1988; Nicell, 1991; Peake et al., 1978; Porstmann et al., 1981; Purcell et al., 1978; Putz et al., 1976).

3.2.1 EVALUATION OF AAP/HDCBS ACTIVITY ASSAY

In end-point determination experiments comparing the

sensitivities of various chromogenic systems employing HRP/H₂O₂ and AAP plus a phenol, Artiss et. al. (1981) demonstrated that the combination of AAP/HDCBS, in a millimolar ratio of 2.4:9.0 respectively, at H₂O₂ concentrations between 3.5-176 μ M (T=37°C, pH 8.0), yielded the most sensitive and reproducible results. H₂O₂ concentrations beyond 0.3mM were later found to be inhibitory (Harake, 1988). Results obtained from this present study concur with those observed by previous researchers. At HRP, AAP, HDCBS and H₂O₂ concentrations of 10-20nM, 2.4mM, 9.0mM and 0.1mM, respectively (T=25°C and pH 7.4), linear, reliably fast and reproducible results were obtained with A.U./min. of 0.5-10 over 30-60 seconds. Standard errors were typically \pm 0.008-0.01 A.U./min. among triplicate samples. HRP activities, expressed as both specific activity and k_{cat} (Appendix F) were determined by dividing the change in A.U./min. by a pre-determined extinction coefficient of 25,000M⁻¹cm⁻¹ (based on H₂O₂ concentration) (Artiss et. al., 1981), and HRP concentrations based on heme content (Appendix A). Blank reactions demonstrated no detectable colour change during the assay period.

Observed and calculated rates determined by non-linear regression analysis performed by the ENZFITTER™ enzyme kinetics program for each substrate at constant and saturating concentrations of all other components, along with the corresponding plots, are shown in Tables 3-1, 3-2, 3-3 and

[H2O2] (μM)	Rate ($\mu\text{M}/\text{min.}$)	Calculated
1.00000E+01	1.79300E+01	3.14782E+01
3.00000E+01	7.36500E+01	6.78374E+01
5.00000E+01	9.32100E+01	8.82165E+01
7.00000E+01	1.04800E+02	1.01252E+02
9.00000E+01	1.10300E+02	1.10308E+02
1.00000E+02	1.11820E+02	1.13873E+02
1.10000E+02	1.12400E+02	1.16965E+02

Table 3-1 Observed and calculated rates (determined by Enzfitter™) vs. H_2O_2 concentration (AAP/HDCBS assay: [AAP]=2.4mM; [HDCBS]=9.0mM; [HRP]=20nM; T=25°C, pH 7.4)

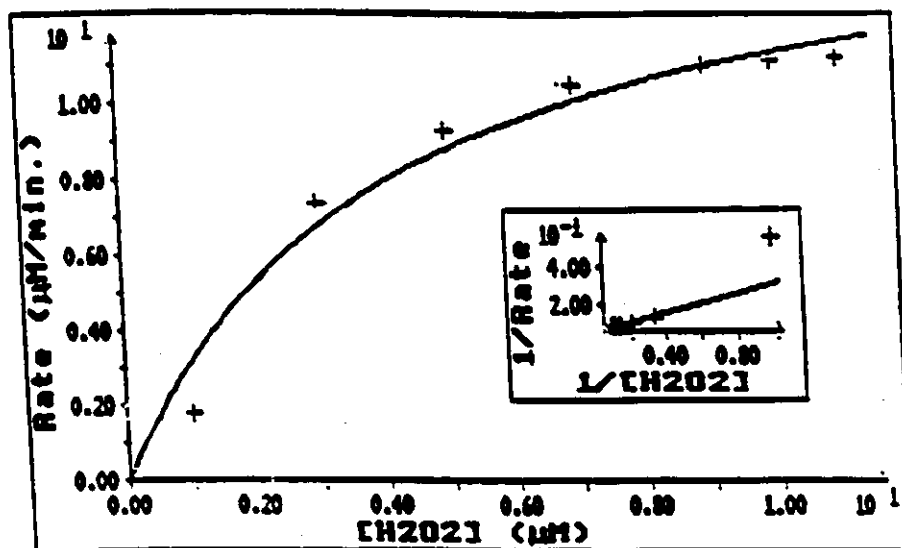


Figure 3-1 Plot of rate ($\mu\text{M}/\text{min.}$) vs. H_2O_2 concentration (μM) values in Table 3-1. Inset: Lineweaver-Burke representation of same data using parameters from non-linear regression analyses.

[AAP] (mM)	Rate (mM/min.)	Calculated
1.00000E+00	4.25000E+00	4.85691E+00
2.50000E+00	8.95000E+00	9.31598E+00
4.00000E+00	1.27000E+01	1.20912E+01
5.50000E+00	1.47000E+01	1.39848E+01
7.00000E+00	1.55000E+01	1.53594E+01
8.50000E+00	1.56000E+01	1.64026E+01

Table 3-2 Observed and calculated rates (determined by Enzfitter™) vs. AAP concentration (AAP/HDCBS assay: [H₂O₂] = 0.1mM; [HDCBS] = 9.5mM; [HRP] = 20nM; T = 25°C, pH 7.4).

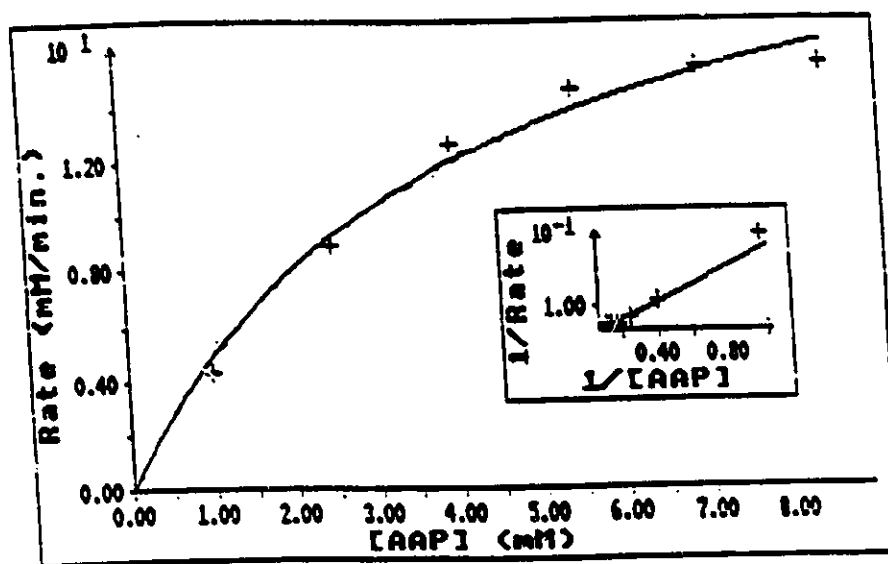


Figure 3-2 Plot of rate (mM/min.) vs. AAP concentration (mM) values in Table 3-2. Inset: Lineweaver-Burke representation of same data using parameters from non-linear regression analyses.

[HDCBS] (mM)	Rate (mM/min.)	Calculated
1.00000E+00	8.92000E+00	8.72927E+00
2.00000E+00	1.18900E+01	1.23178E+01
3.00000E+00	1.42700E+01	1.42737E+01
4.00000E+00	1.58400E+01	1.55047E+01
5.00000E+00	1.66800E+01	1.63508E+01
6.00000E+00	1.65800E+01	1.69681E+01

Table 3-3 Observed and calculated rates (determined by Enzfitter™) vs. HDCBS concentration (AAP/HDCBS assay: [H₂O₂]=0.1mM; [AAP]=2.4mM; [HRP]=20nM; T=25°C, pH 7.4)

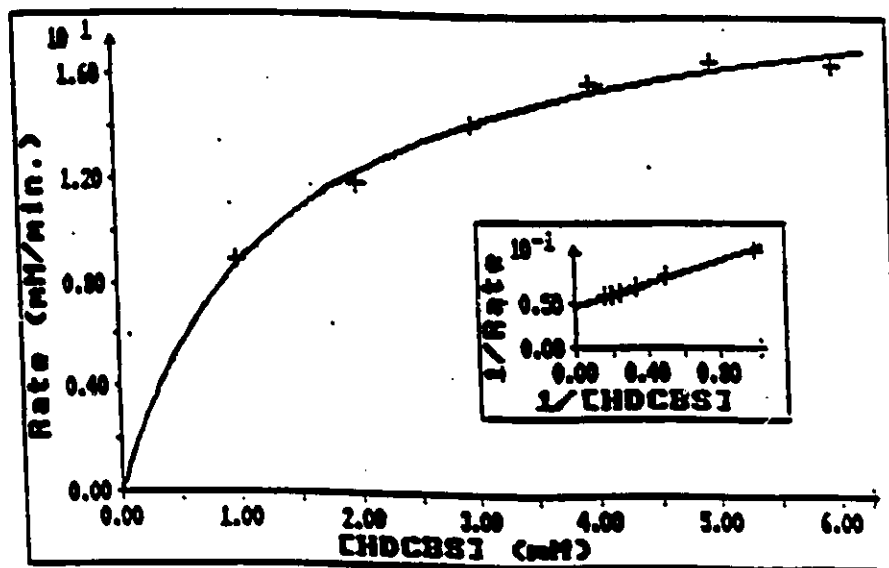


Figure 3-3 Plot of rate (mM/min.) vs. HDCBS concentration (mM) values in Table 3-3. Inset: Lineweaver-Burke representation of same data using parameters from non-linear regression analyses.

Substrate	K_m (mM)	V_{max} (mM/min. ⁻¹)	k_{cat}/K_m (mM ⁻¹ /min.)
H ₂ O ₂	$(41.01 \pm 1.15) \times 10^{-3}$	16.1 ± 1.67	19,512
AAP	3.94 ± 0.847	24.0 ± 2.21	304.6
HDCBS	1.40 ± 0.148	20.9 ± 0.669	714.3

Table 3-4 Kinetic constants of H₂O₂/AAP/HDCBS chromogen system: T=25°C, pH 7.4; [HRP]=20pmoles (20nM).

Figures 3-1, 3-2 and 3-3, respectively. Kinetic constants K_m , V_{max} (assumed to be apparent), determined by ENZFITTER™, and k_{cat}/K_m are shown for each substrate in Table 3-4. A K_m of $41.01 \pm 1.15 \mu\text{M}$ determined for H_2O_2 agrees reasonably well with values obtained by previous researchers working with this chromogen system: $25.1 \pm 4.1 \mu\text{M}$, pH 7.5, T = 25°C, BM. Grad I, II (Harake, 1988); $59.0 \pm 5 \mu\text{M}$, pH 7.4, T=25°C, BM. Grad I, II (immunoassay grades) (Boss, 1986). Despite general consensus that HDCBS is not a proper substrate, varying its concentration generated concentration-dependent rate curves. The K_m for HDCBS was determined to be $1.40 \pm 0.148\text{mM}$ and is similar to unpublished results obtained in this laboratory (T=25°C, pH 7.5) of 1.8-1.9mM (Lockstadt, 1987; unpublished). A K_m for AAP of 4.3mM (Lockstadt, 1987; unpublished) agrees well with the K_m determined from this study to be $3.94 \pm 0.847\text{mM}$. The millimolar ratio of H_2O_2 :AAP:HDCBS of 0.1:2.4:9.0 recommended by Artiss et. al. (1981) has all components but AAP at saturating concentrations well above their K_m 's. This ratio was maintained in activity assays used in this present study to evaluate residual enzyme activity during H_2O_2 inactivation investigations.

Based both on work performed in this laboratory (Lockstadt, 1987; unpublished), and on information available in the literature (Ryu and Dordick, 1992), AAP concentration may have been kept below its K_m to avoid possible enzyme inactivation. The intermediate of enzyme-activated AAP is a

reactive radical species (Griffin and Ting, 1978) possessing the potential to attack and inactivate the enzyme (Ma and Rokita, 1988; Sawahata and Neal, 1982). Kinetic investigations have shown that HRP incubated with H_2O_2 and AAP alone (0.1mM and 2.4mM, respectively) underwent inactivation (Lockstadt, 1987; unpublished). Based on these observations, it seemed best to keep the AAP concentrations low to ensure that any observed inactivation of HRP could be attributed almost entirely to the H_2O_2 in the incubation solutions and not to other possible mechanisms of inactivation existing in the assay solution.

3.2.2 EVALUATION OF AAP/PHENOL COLOURIMETRIC ASSAY

This chromogen system is effective but less sensitive compared with other AAP/phenol or phenol-derivative chromogen pairs used to evaluate HRP activity (Artiss et. al., 1981; Barham and Trinder, 1972; Porstmann et. al., 1981). Despite poorer limits of detection, it was ideal for measuring residual activity during enzyme-generated phenoxy radical inactivation. All substrates (with the possible exception of AAP) were present at saturating concentrations above their K_m . Replacing HDCBS with phenol reduced the possibility of competition arising between these two phenolic substrates upon addition of aliquots which were removed from incubation solutions containing enzyme, H_2O_2 and phenol and placed into the assay containing HDCBS. Phenol arriving in the aliquot

did not affect the reaction rate as long as phenol present in the activity assay was maintained at saturating concentrations. Linear and reproducible results were obtained at 25°C and pH 7.4, with standard errors among triplicates typically between ± 0.001 -0.3 A.U./min.

Gallati (1977) examined kinetics and optimal conditions of this same assay using small concentrations of HRP. His reaction scheme contrasts with other proposed schemes (Trinder, 1969; Barham and Trinder, 1972) in that it is the phenol, not AAP, which is enzymatically activated producing a quinone which undergoes non-enzymatic nucleophilic attack by AAP's amino group nitrogen, forming a red quinonimine. However, in contradiction to his own proposal, Gallati reported that a solution of phenol incubated with HRP/H₂O₂ in the absence of AAP, generated no colour upon addition of AAP. Samples removed from these solutions demonstrated varying degrees of inactivation, the extent of which depended on phenol concentration. Absence of colour formation (at 500nm) in solutions containing only HRP/H₂O₂ and phenol was attributed to the formation, from enzyme-generated phenoxy radicals, of products that were unreactive towards AAP and exhibited absorbance maxima distinct from 500nm. These radicals may have inactivated Gallati's enzyme, rendering it incapable of oxidizing AAP upon exposure.

This assay is employed by a Japanese company (Suntory) to evaluate HRP activity and recommended concentrations of H₂O₂,

AAP and phenol are 0.4, 0.84 and 10mM, respectively. Experiments examining concentrations of components that generated the fastest reaction rates and were saturating were performed in this study (data not shown) for use in subsequent kinetic analyses. Suitably rapid and reproducible reaction rates were obtained using millimolar concentrations of H₂O₂:AAP:phenol at 0.4:0.84:10, concurring with Suntory's recommendations. Assay solutions evaluating HRP inactivation by phenoxy radicals were prepared with components at these concentrations. In similar experiments, Gallati determined optimal phenol concentration to be 25mM under conditions of 2mM AAP and 0.75mM H₂O₂ and unknown enzyme concentrations (T=37°C, pH 7.4); essentially double the substrate concentration ratio used in this assay (0.75mM H₂O₂:2mM AAP:25mM phenol = ~2(0.4mM H₂O₂:0.84mM AAP:10mM phenol)).

In experiments examining dependence of the reaction rate on substrate concentration, Gallati observed that varying the concentration of AAP at saturating concentrations of H₂O₂ (0.75mM) and phenol (25mM) had no effect. A slight inhibitory effect was observed in this study at saturating concentrations of other components (phenol and H₂O₂) (Table 3-5), and is contrary to the results obtained from identical evaluations performed on the AAP/HDCBS system (Table 3-2; Figure 3-2). Independence of initial reaction rate on AAP concentration suggests that AAP is not recognized as a substrate by HRP, at least not in this chromogenic system, supporting Gallati's

[AAP] (mM)	[HRP] (nM)	Rate (A.U./min. ⁻¹)	
		[phenol] (mM)	
		5	10
0.05	5.0	0.54 ± 0.02	0.695 ± 0.02
0.075	"	0.54 ± 0.02	0.664 ± 0.02
0.01	"	0.50 ± 0.004	0.631 ± 0.053
0.15	"	0.49 ± 0.014	0.610 ± 0.053
0.05	10.0	1.20 ± 0.031	1.10 ± 0.17
0.075	"	0.93 ± 0.043	1.80 ± 0.16
0.10	"	0.853 ± 0.02	1.40 ± 0.25
0.15	"	0.75 ± 0.025	1.42 ± 0.07

Table 3-5 Inhibitory influence on reaction rate of changing AAP concentration (AAP/Phenol activity assay). [H₂O₂] = 0.4mM; T=25°C, pH 7.4.

hypothesis. Gallati's and the present results point to the existence of different reaction mechanisms in each assay system: the affinity of the enzyme for AAP may depend on the enzyme's affinity for the phenolic substrate. Phenol by itself, is a reasonable substrate (Ma and Rokita, 1988; Sawahata and Neal, 1982; present study) and may even be a better substrate than AAP. When present at saturating concentrations, phenol, once oxidized to its radical intermediate, may undergo radical-radical/phenol coupling that could be favored over chromogen formation with AAP and may somehow serve to protect against inactivation by AAP. However, from Table 3-5, at the high phenol concentration (10mM) and both enzyme concentrations (5 and 10nM), there is still some colour formation at the lowest AAP concentration, suggesting coupling with phenol can still occur. At both phenol concentrations, a slight decrease in reaction rate is observed with rising AAP concentration, suggesting AAP-induced enzyme inactivation may be occurring.

Decrease of reaction rate as a result of increasing AAP concentration made determination of optimal conditions for evaluating kinetic constants difficult. Ideally in kinetic determinations, all substrates, except for the one being examined, should be present at saturating concentrations (Fersht, 1977); AAP's behaviour made saturating conditions difficult to ascertain. As a result, assays were designed to yield fast and reproducible rates, with the focus on

maximizing phenol concentrations in order to minimize possible AAP-induced inactivation. AAP concentrations of 0.84mM generated fast, reproducible reaction rates without any obvious signs of inactivation at phenol and H₂O₂ concentrations of 10.0 and 0.4mM, respectively. This concentration of AAP was employed in the subsequent kinetic analyses. The fact that AAP was likely not present at saturating concentrations during these experiments renders the kinetic constants apparent rather than true qualitative determinants of kinetic behaviour.

Gallati obtained a K_m for phenol of 11.3mM, despite the difficulties encountered with AAP. This is approximately a 10-fold difference over our value of 1.37mM (Tables 3-6, 3-8; Figure 3-4). However, a temperature difference of 17°C existed between conditions used in this study and Gallati's. Substrate concentrations that are saturating at one temperature are not always saturating at another, rendering K_m a temperature dependent value. The V_{max} was calculated to be 0.267mM/min for phenol. A K_m for H₂O₂ was determined to be 162µM which does not agree very well with Gallati's K_m of 250µM (Tables 3-7 and 3-8; Figure 3-5). A V_{max} for H₂O₂ of 0.157mM/min. was determined. Despite the ambiguity introduced by AAP's lack of Michaelian behaviour, an assay was developed that minimized potential interference from substances arriving in the aliquots removed from the incubation solutions. For future investigations, a close examination of the mechanistic

[phenol] (mM)	Rate (mM/min.)	Calculated
2.00000E-01	3.83000E-02	3.39649E-02
5.00000E-01	7.43000E-02	7.12893E-02
7.50000E-01	9.16000E-02	9.43233E-02
1.00000E+00	1.12400E-01	1.12498E-01
2.50000E+00	1.69000E-01	1.72232E-01
5.00000E+00	2.16000E-01	2.09272E-01
1.00000E+01	2.21300E-01	2.34487E-01
1.50000E+01	2.59000E-01	2.44298E-01
2.00000E+01	2.44000E-01	2.49519E-01

Table 3-6 Observed and calculated rates (determined by Enzfitter™) vs. phenol concentration (AAP/Phenol activity assay: $[H_2O_2]=0.4\text{mM}$; $[AAP]=0.84\text{mM}$; $[HRP]=10\text{nM}$; $T=25^\circ$, pH 7.4)

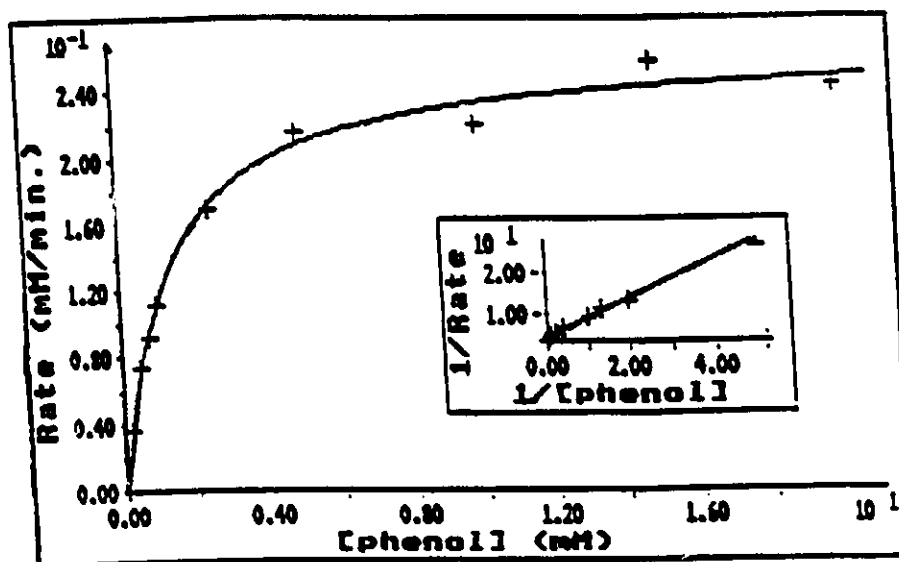


Figure 3-4 Plot of rate (mM/min.) vs. phenol concentration (mM) values in Table 3-6. Inset: Lineweaver-Burk representation of same data from non-linear regression analyses.

[H2O2] ($\mu\text{M}/\text{min}$)	Rate ($\mu\text{M}/\text{min}$)	Calculated
3.00000E+01	1.16000E+01	2.41118E+01
5.00000E+01	2.36900E+01	3.64811E+01
1.00000E+02	5.85000E+01	5.92945E+01
2.50000E+02	1.11190E+02	9.49029E+01
4.50000E+02	1.27800E+02	1.15445E+02
6.50000E+02	1.23600E+02	1.25928E+02
8.50000E+02	1.18200E+02	1.32288E+02

Table 3-7 Observed and calculated rates (determined by Enzfitter™) vs. H₂O₂ concentration (μM) (AAP/Phenol activity assay: [phenol]=10.0mM; [AAP]=0.84mM; [HRP]=10nM; T=25°, pH 7.4)

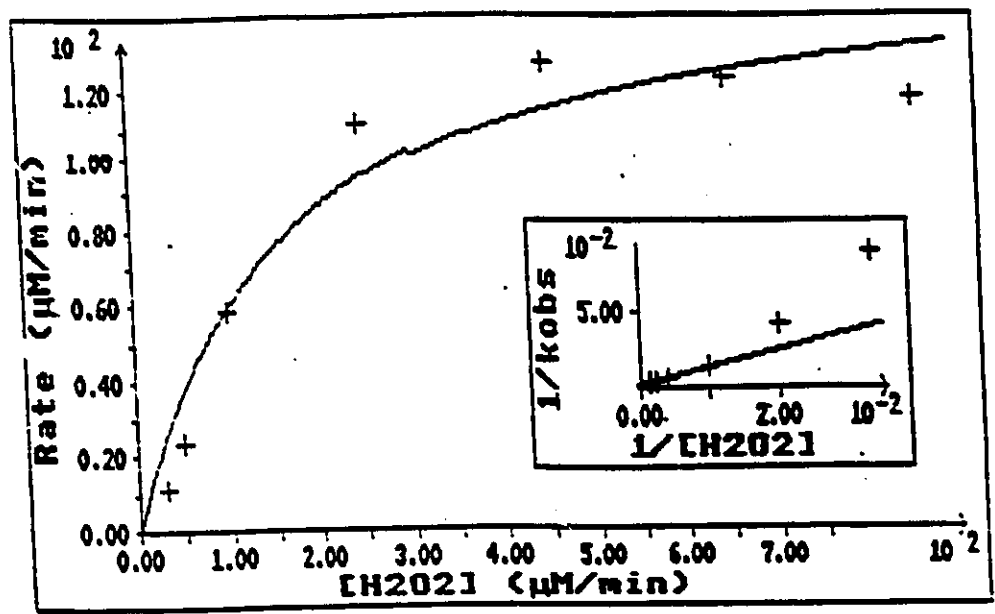


Figure 3-5 Plot of rate ($\mu\text{M}/\text{min}.$) vs. H₂O₂ concentration (μM) values in Table 3-7. Inset: Lineweaver-Burk representation of same data from non-linear regression analyses.

Substrate	K_m (mM)	V_{max} (mM/min.)	k_{cat}/k_m (mM ⁻¹ /min.)
phenol	1.37 ± 0.12	0.267 ± 0.001	19,490
H ₂ O ₂	$(162 \pm 54.4) \times 10^{-3}$	0.157 ± 0.017	136,250

Table 3-8 Kinetic constants of H₂O₂/AAP/Phenol chromogen system: [HRP]=10pmole (10nM); [AAP]=0.84mM; [phenol]=10.0mM; T=25°C, pH 7.4.

details involved in this and the AAP/HDCBS assay systems would be warranted. Also of interest would be to determine if AAP is enzymatically-activated into a radical intermediate capable of inactivating the enzyme.

3.3. Inactivation of HRP

3.3.1 Inactivation by H_2O_2

Hydrogen peroxide, the oxidant substrate of HRP in the peroxidase catalytic cycle, has been shown to inactivate the enzyme either in the absence of the protection afforded by reductant (H-donor) substrates, or in their presence, at concentrations determined to be "excess" (Bagger and Williams, 1971; Dunford and Stillman, 1976; Nakajima and Yamazaki, 1987; Arnao et al., 1990a, 1990b; Everse et al., 1990). Figure 3-6 demonstrates protection of HRP against H_2O_2 -induced inactivation in the presence of the donor substrates AAP and HDCBS. This is a typical plot illustrating the results obtained from one of many experiments in which single aliquots of H_2O_2 , yielding final concentrations of 5-20 μ M in 1mL (1000-2000 fold greater than enzyme concentration), were added to a system comprised of 9.0mM HDCBS, 2.4mM AAP and 0.5-1nM HRP (T=25°C, pH 7.4). Reaction progress was followed as the change in absorbance at 510nm vs. time. Aliquots (20 μ L) of 250-1000 μ M H_2O_2 solutions were added successively (arrows) to the assay solution when absorbance change ceased. In the experiment depicted by Figure 3-6, at least 10 aliquots were

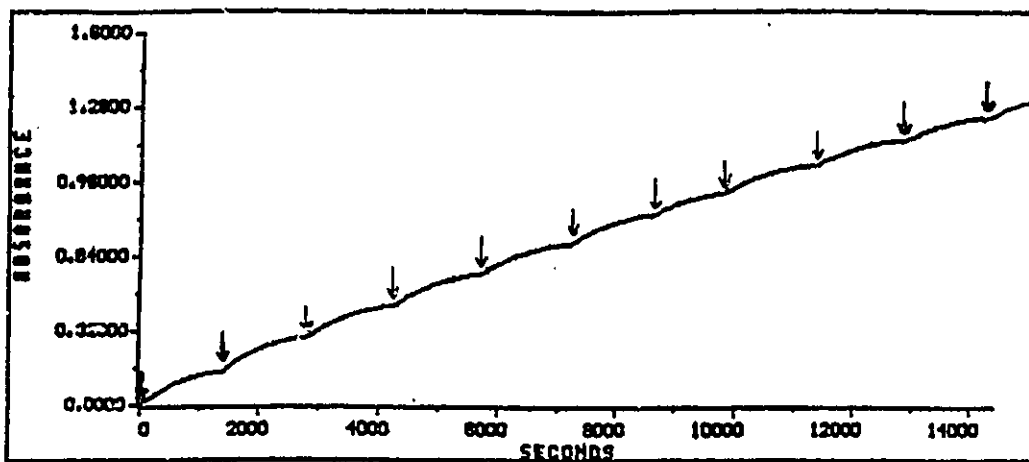


Figure 3-6 Donor-substrate protection of HRP against inactivation from addition of consecutive aliquots of H_2O_2 ($20\mu M$): $[HRP]=0.5nM$; $[AAP]=2.4mM$; $[HDCBS]=9.0mM$; $T=25^\circ C$, $pH 7.4$).

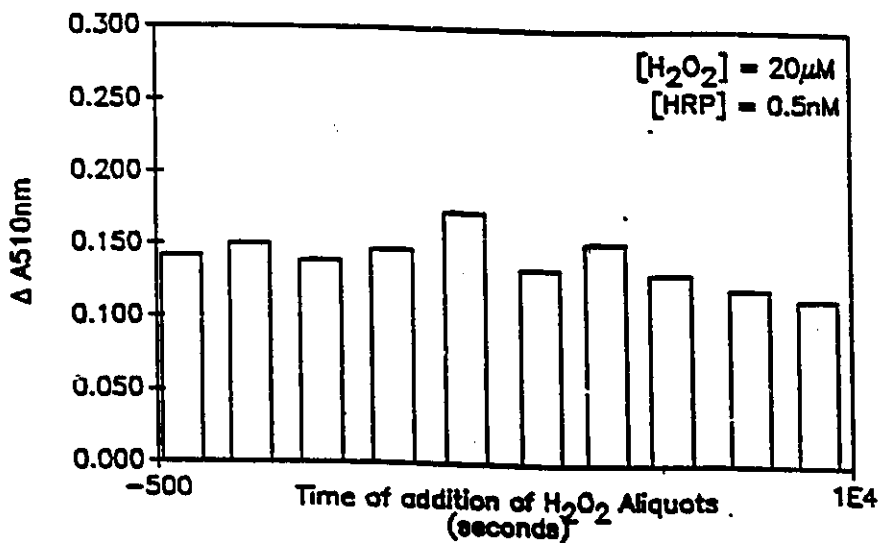


Figure 3-7 Total absorbance change over time with addition of each new H_2O_2 aliquot to system in Figure 3-6 (corrected for volume changes).

added over 4 hours before decrease in absorbance change was indicated. By this time, total concentrations of H_2O_2 in the reaction mixture were 50-200 μ M (corrected for dilution introduced with each aliquot). The levelling of these plots was due to the consumption of H_2O_2 and not to enzyme inactivation. Absorbance changes were also corrected for the volume introduced with each aliquot (20 μ L), so this decrease could not be attributed to increased assay volume, which would gradually reduce the effective concentration of assay components. Furthermore, this decrease was not the result of enzyme inactivation as addition of an aliquot of AAP/HDCBS, yielding final concentrations of 2.4/9.0mM (accounting for the volume of the system), permitted the reaction to resume as before. This pointed to consumption of one or both of the substrates (AAP/HDCBS) being responsible for what appeared to be a loss of enzyme activity.

Figure 3-7 is a bar diagram with each bar representing the total absorbance change observed for each individual curve comprising the overall plot shown in Figure 3-6. Changes have been corrected for the slight dilution introduced with each aliquot of H_2O_2 . As observed in Figure 3-6, except for the minute differences in bar height, no major decrease in absorbance change from the addition of one aliquot to the next is observed until the 9th or 10th aliquots. This again, was the result of AAP/HDCBS consumption, not enzyme inactivation.

Absence of inactivation in this system may be due to

protection of the enzyme by the donor substrates (AAP/HDCBS). This was likely accomplished by keeping the enzyme on the peroxidatic pathway, preventing the formation of either Compounds III or P₆₇₀ (Arnao et al., 1990b). Donor substrate protection of HRP against H₂O₂-mediated oxidative damage was observed by Nicell using the same AAP/HDCBS system (1991) and Arnao et al., using 2,2'-azinobis[3-ethylbenzthiazoline-6-sulphonic acid] (ABTS) as the chromogen (1990a). Arnao et al. observed decreasing consumption of H₂O₂ with time over a period of 2.5 hours and total concentration of 80µM H₂O₂. Decreasing absorbance was attributed to H₂O₂-mediated enzyme inactivation due to H₂O₂ accumulation, not ABTS depletion. However, the nature of their inactivating agent is questionable as they failed to test the residual activities of solutions containing HRP and the product of ABTS oxidation, the ABTS radical, which they could generate and isolate. It is apparent from this study (and Nicell, 1991) that the AAP/HDCBS system affords better protection against H₂O₂ inactivation than the ABTS system. Also, under these conditions and concentrations of components, the AAP/HDCBS system does not appear to generate either intermediates or products that are detrimental to the enzyme's activity.

Investigations in which HRP (100nM and 1µM) was incubated for 1 hour with various concentrations of H₂O₂ (1000nM-50.0mM) in the absence of donor substrates at 25°C, pH 7.4 were undertaken. Addition of H₂O₂ to an enzyme solution initiated

inactivation and aliquots were successively removed at specific times (usually every five to ten minutes) and tested for residual activity using the AAP/HDCBS colourimetric assay. Figures 3-8 and 3-9 demonstrate the typical curves of residual activity vs. time obtained for selected H_2O_2 concentrations and two concentrations of HRP (100nM and 1000nM). Inactivation was time-dependent and at all H_2O_2 concentrations, except those below 0.100mM (not shown), curves obtained exhibited "biphasic behaviour". These were distinct in shape from the time-dependent inactivation curves obtained by Arnao et al. (1990a) (Figure 1-3) who examined H_2O_2 concentrations identical to our upper range (>1.0mM) using HRP (Sigma, type IX) at a concentration of 1 μ M. Unlike the curves in Figure 1-3, inactivation curves in Figures 3-8 and 3-9 exhibit an initial rapid phase of inactivation characterized by the loss of substantial activity over a very short time (under 5 minutes), followed by a section where activity declines more slowly over time, if at all. At very destructive H_2O_2 concentrations (5mM-50mM; 50,000 to 500,000 fold excess over the enzyme present) initial velocity plots of absorbance change vs. time monitored over an hour, were linear. This indicated there was still some remaining activity (ie. not 100% inactivation) because simultaneously run blank reactions were always subtracted from activity determination values. Activities tested from samples containing low H_2O_2 concentrations (0.001mM; still ten-fold excess over the enzyme

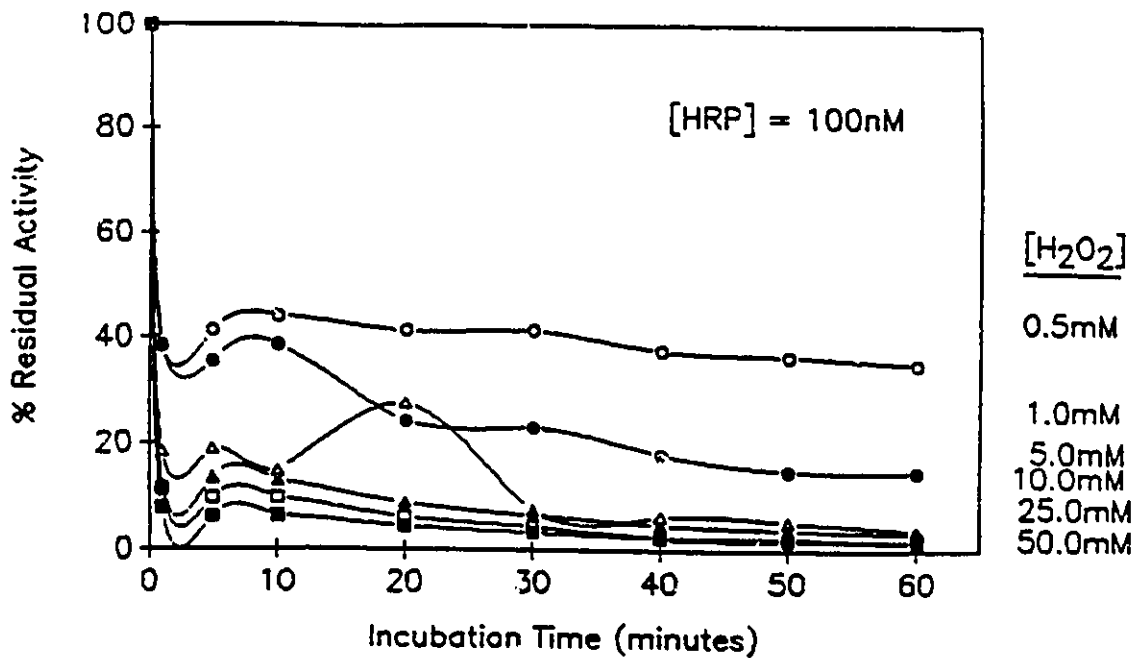


Figure 3-8 Time-dependent inactivation of 100nM HRP by H₂O₂ (T=25°C, pH 7.4).

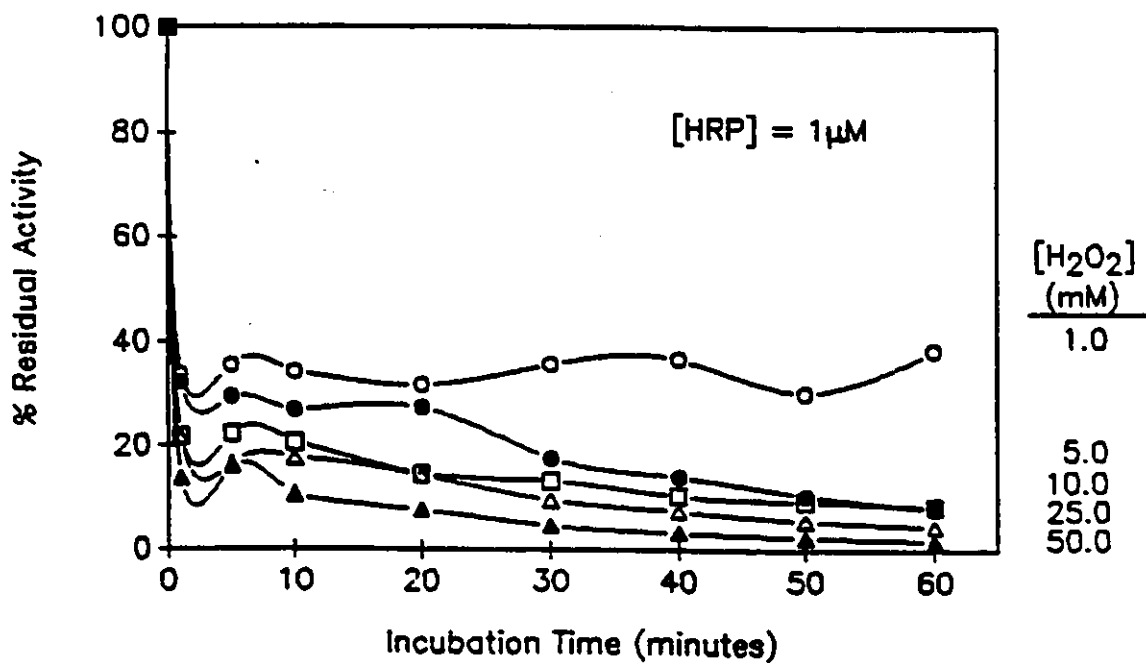


Figure 3-9 Time-dependent inactivation of 1µM HRP by H₂O₂ (T=25°C, pH 7.4).

concentration) left to incubate at 25°C for a total of 24 hours from the initial addition of H₂O₂, recovered full to progressively less activity as H₂O₂ concentrations increased. Substantial losses of activity were observed at H₂O₂ concentrations ranging from 0.20mM-50.0mM from the 60 minute reading to the 24 hour reading. Table 3-9 lists percent residual activities during 60 minutes of exposure of 100nM HRP to all H₂O₂ concentrations examined, as well as the last % residual activity value observed at the end of 60 minutes and 24 hours. From all data shown in Figures 3-8, 3-9 and Table 3-9, it appears that both rate and final extent of inactivation are dependent on H₂O₂ concentration, but not on a 10-fold difference of enzyme concentration.

Incubation experiments were then performed to determine if any activity lost over 60 minutes could be recovered by dialysis. This might indicate whether inactivation was reversible or irreversible, which in turn might yield possible clues to the catalytic pathway(s)/inter-mediate(s) involved. Solutions containing 1.0 and 0.1μM HRP were incubated with 0.5, 1.0, 5.0, 10.0, 25.0 and 50.0mM H₂O₂ and tested for residual activity as described earlier. Immediately after performing the activity test at 60 minutes, dialyses were carried out against a buffer (0.01M NaPP, pH 7.4) containing catalase to ensure complete destruction of any H₂O₂ that dialysed out of the incubation solutions. Dialysis progress was monitored every 15-30 minutes. All activity that could be

[H ₂ O ₂] (mM)	<u>% Residual Activity</u>					<u>Total % Inactivation</u>	
	<u>Incubation Duration (minutes)</u>					at 60min.	at 24 hrs.
	5	10	30	60	1440		
0.001	99.5	97.9	94.9	95.9	100	4.10	0.00
0.01	91.4	88.8	87.4	90.1	77.0	9.90	33.0
0.025	87.2	81.9	78.2	86.2	71.0	13.8	29.0
0.075	72.2	66.1	63.6	59.2	63.0	40.8	37.0
0.10	59.3	57.6	55.5	49.6	47.0	50.4	53.0
0.20	69.9	46.2	58.7	46.0	15.0	54.4	85.0
0.50	42.0	45.9	44.2	34.0	0.50	66.0	99.5
1.00	40.0	41.6	39.5	24.3	0.60	75.5	99.4
5.00	18.0	14.8	7.43	3.80	0.00	96.2	100
10.0	13.5	13.0	6.50	3.30	0.00	96.7	100
25.0	9.70	9.30	4.40	2.00	0.00	98.0	100
50.0	6.20	6.30	3.40	1.30	0.00	98.7	100

Table 3-9 % residual activity and total % inactivation of 100nM HRP after exposure to H₂O₂ for 24 hours (25°C, pH 7.4).

[HRP] (μ M)	[H ₂ O ₂] (mM)	<u>% Residual Activity (hours.)</u>				<u>% Irreversible Activity (at 48 hours)</u>
		1	3	24	48	
0.1	0.5	35.2	70.6	70.8	77.4	22.6
"	1.0	14.7	36.2	35.9	32.9	67.1
"	5.0	4.00	15.2	13.9	17.7	82.3
"	10.0	3.30	9.40	10.3	10.1	89.9
"	25.0	2.00	5.20	5.70	6.20	93.8
"	50.0	1.30	6.30	6.40	7.00	93.0
1.0	1.0	38.5	74.5	73.1	75.2	24.8
"	5.0	7.90	12.4	12.4	13.4	86.6
"	10.0	4.60	14.9	15.0	15.4	84.6
"	25.0	1.90	4.90	4.90	5.10	94.0
"	50.0	8.40	4.30	4.10	4.30	95.7

Table 3-10 % residual and irreversible activity at 48 hours of HRP samples incubated with H₂O₂ for sixty minutes, followed by 3 hour dialysis and further incubation for 24 and 48 hours (25°C, pH 7.4)

recovered was recovered within 3 hours. Samples incubated for 24-48 hours at room temperature following dialysis retained virtually the same activity observed immediately after dialysis. Table 3-10 lists % residual activities of 100nM HRP exposed to various concentrations of H_2O_2 during 1 hour of incubation, immediately following 3 hours of dialysis, and 24 and 48 hours after dialysis. Results show that no samples recover all lost activity, but for all samples, at least two-fold the activity observed prior to dialysis is recovered. At H_2O_2 concentrations below 10.0mM, the higher concentration enzyme is better protected against inactivation and recovers more activity; the exception being only at 50mM H_2O_2 . Protection is afforded only at H_2O_2 concentrations ≤ 1.0 mM; above 1.0mM, the enzyme is inactivated to the same extent, regardless of its concentration. Incomplete recovery of activity in solutions with or without dialysis points to the generation of both reversibly and irreversibly inactivated intermediates during inactivation. The number and nature of intermediates formed may depend upon H_2O_2 concentration, since total % inactivation becomes greater and % of activity recovered diminishes with rising H_2O_2 concentrations, irrespective of enzyme concentration. Table 3-11 is a compilation of data taken from Tables 3-9 (undialyzed samples) and 3-10 (dialyzed samples) for 100nM HRP. It reiterates that some but never all activity lost is recovered even when excess H_2O_2 is physically removed. Prior to dialysis (*), % residual

activities of both dialyzed and undialyzed samples exposed to the same H_2O_2 concentrations are similar. For most samples, 2-3 times the activity lost during the 60 minutes is recovered following dialysis (**). The similarity of % residual activities of dialyzed samples immediately following and 24 hours after dialysis indicates that all H_2O_2 that could be removed was removed.

The results of these dialysis experiments offers evidence to support the existence of a partitioning of pathways at one of the HRP intermediates (Arnao et al., 1990a,b). Two types of inactive intermediate are clearly generated in HRP solutions exposed to H_2O_2 : the amount of one generated relative to the other, a reflection of the pathway favored, seems to depend on H_2O_2 concentration. The greater the H_2O_2 concentration, the less activity recovered suggesting more irreversibly formed intermediate is present compared to reversibly formed intermediate. According to Arnao et al.'s partitioning model, H_2O_2 concentrations $\geq 1.0mM$ result in the formation of one molecule of irreversibly inactivated intermediate P_{670} for every two molecules of Compound III formed. At concentrations $>1.0mM$ (except for $1.0\mu M$ HRP), the % irreversible activity column in Table 3-10 suggests to the contrary that more P_{670} over Compound III may have been formed. Below $1.0mM$ for $100nM$ HRP and $\leq 1.0mM$ for $1.0\mu M$ HRP, substantial activity is recovered, suggesting that the pathway leading to Compound III formation is favored.

<u>[H₂O₂]</u> <u>(mM)</u>	<u>% Residual Activity</u>				
	<u>no dialysis</u>		<u>with dialysis</u>		
	<u>1 hour*</u>	<u>24 hours</u>	<u>1 hour*</u>	<u>3 hours**</u>	<u>24 hours***</u>
0.5	34.0	0.50	35.2	70.6	70.8
1.0	24.3	0.60	14.7	36.2	35.9
5.0	3.80	0.00	4.00	15.2	13.9
10.0	3.30	0.00	3.30	9.40	10.3
25.0	2.00	0.00	2.00	6.20	5.70
50.0	1.30	0.00	1.30	6.30	6.40

Table 3-11 Comparison of % residuals activities of undialysed and dialysed 100nM HRP solutions exposed for 1 hour to H₂O₂. At this time, all samples were tested for residual activity (*). Undialysed samples were left to incubate for 24 hours, at which time activity was tested. Dialysed samples were checked for activity immediately following 3 hours of dialysis (**), and 24 hours after dialysis (***) (25°C, pH 7.4).

Results of the 1 hour incubation experiments showed the majority of inactivation occurred well within the first five minutes of exposure of HRP to H_2O_2 . Experiments in which enzyme samples exposed to various concentrations of H_2O_2 were tested for residual activity every 5-10 seconds for one minute up to 5 minutes, then every 5-10 minutes for a total of 20-30 minutes, were undertaken to obtain more information during the rapid phase of inactivation. A summary of typical values obtained and averaged from several such experiments employing 100nM HRP is shown in Table 3-12 and graphically depicted in Figure 3-10. As with previous experiments, the magnitude of time-dependent inactivation demonstrated a H_2O_2 concentration dependence, with an exception being consistently observed at 0.75 and 1.0mM. The most extensive inactivation occurred well before 1 minute for all but the lowest H_2O_2 concentration (0.10mM). All plots, with this one exception, exhibited biphasicity. The shape of the 0.10mM curve may reflect a process in which a catalytic pathway involving a non-inactivating consumption of H_2O_2 is predominant over an inactivation pathway. Biphasic behaviour is retained upon linearization of the data (Figure 3-11). In attempts to qualitatively determine the order of the fast inactivation phase with respect to H_2O_2 concentration, values gathered over the first minute for concentrations $\leq 1.0mM$ were fit to a linear least-squares line (Figure 3-12). This generated a family of curves that were reasonably straight and exhibited

[H ₂ O ₂] (mM)	Incubation Duration (seconds)							Total % Inactivation
	5	10	30	60	300	900	1800	
0.10	96.0	97.0	87.0	83.0	69.0	71.7	72.0	28.0
0.25	95.0	94.0	79.0	54.0	54.2	51.0	40.0	60.4
0.50	93.0	90.0	79.0	55.0	46.0	39.0	35.0	64.7
0.75	78.0	75.0	54.0	35.0	30.0	30.0	31.0	69.0
1.00	84.0	73.0	51.0	38.0	34.0	39.0	35.0	65.0
5.00	67.0	56.0	31.0	15.0	14.3	15.2	15.0	85.0
10.0	24.0	20.0	21.0	14.0	15.0	14.0	12.0	88.0
50.0	7.50	7.50	6.90	6.10	6.20	5.30	4.43	95.6

Table 3-12 % residual activity vs. time of triplicates from one experiment in which 100nM HRP was exposed to H₂O₂ for 30 minutes (25°C, pH 7.4). Several values were obtained during the first minute and used to evaluate the rapid portions of inactivation curves observed in Figure 3-10 below.

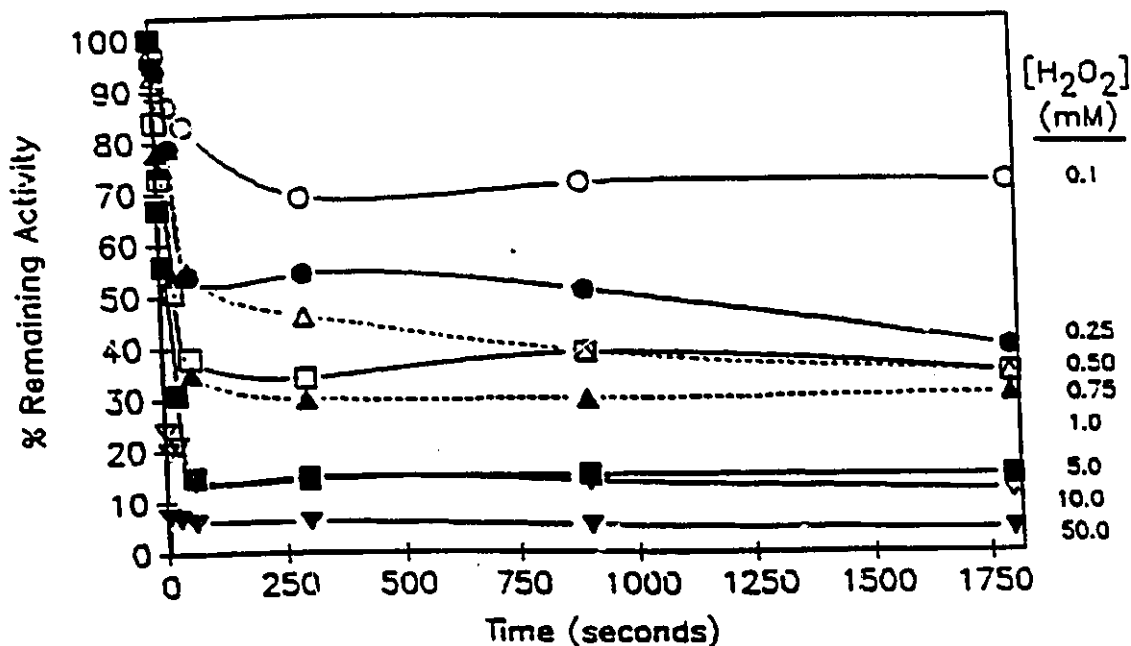


Figure 3-10 Plot of curves obtained from time-dependent inactivation data in Table 3-12.

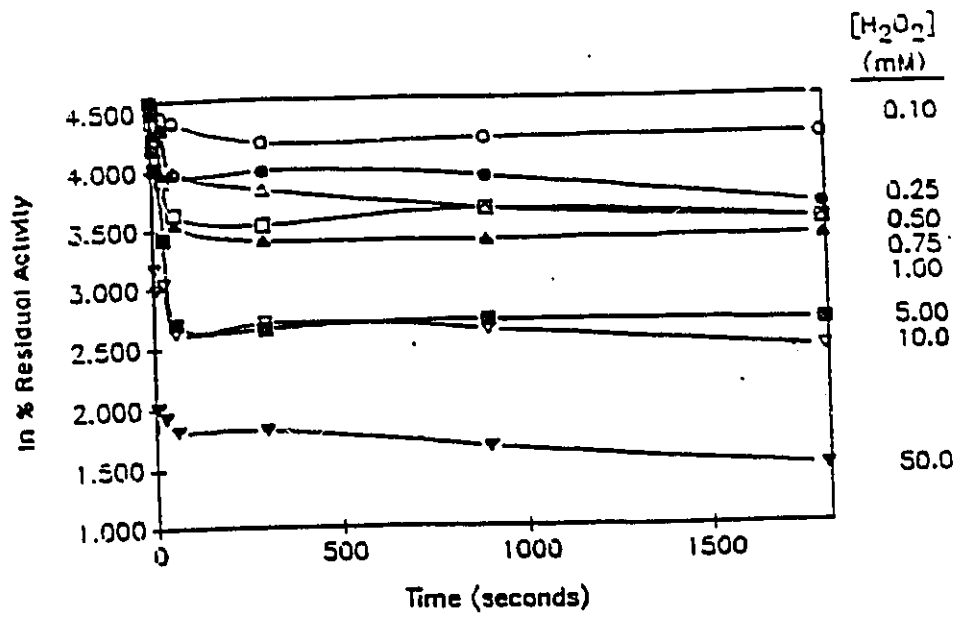


Figure 3-11 Linearization of data presented in Table 3-12.

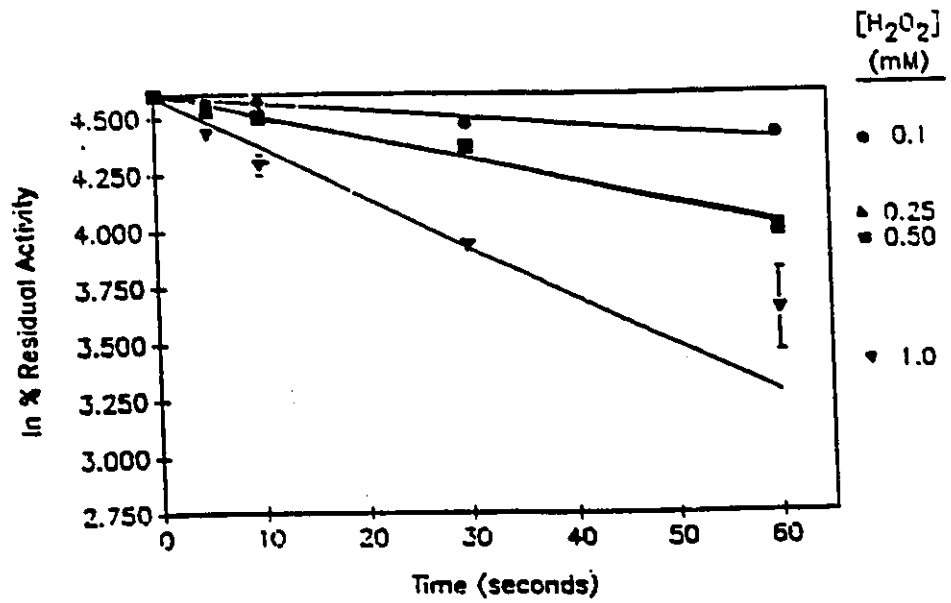


Figure 3-12 A closer look at the values obtained within the first minute of exposure of HRP to H_2O_2 . (Taken from Table 3-12).

correlation coefficients of at least 0.993. At H_2O_2 concentrations of 0.75 and 1.0mM H_2O_2 , only points obtained at 5 and 10 seconds were linear; examination of data beyond 10 seconds yielded terrible linear fits which indicated that the majority of inactivation occurred in under 10 seconds. An insufficient number of data points were gathered during this period of time from the higher concentration samples due to the inability of available equipment to follow the rapid phase of inactivation which appeared to be complete in less than 5 seconds. This precluded similar evaluations on these samples. From Figures 3-11 and 3-12, the slopes of the plots representing the rapid inactivation phase become steeper with increasing H_2O_2 concentration, pointing to a dependence of inactivation rate (of the rapid phase) on H_2O_2 concentration. Such a dependence was not observed from data obtained during the slow inactivation portions of the curves in Figures 3-11 and 3-12.

The reasonable linear fits of data obtained during the first minute at concentrations below 1.0mM hinted that inactivation was a mechanism-based, first-order process implying that H_2O_2 associates at the active site prior to partaking in a chemical step in which a covalent change (in the context of an irreversible change, such as an irreversible oxidation) is initiated (Walsh, 1979). In this system, substrate turnover is a necessary prerequisite for enzyme inactivation and it occurs through a transfer of oxidizing

equivalents. Based on the occurrence of these two events, the observed inactivation fulfills the criteria necessary for it to be considered a mechanism-based or suicide inactivation process (Walsh, 1977; 1979). This description concurs with that given to this inactivation by Arnao et al. (1990a).

The biphasic shapes of the curves obtained from the inactivation data led to the analysis, by the kinetics program ENZFITTER™, of the goodness of fit, in a manner similar to Arnao et al. (1990a), to an equation describing double-exponential decay:

$$y = A_1 \exp. (-k_1 t) + A_2 \exp (-k_2 t)$$

This equation is the sum of two unique and sequential single-exponential decay processes (Gentry, 1978). A_1 and A_2 are the positive constants representing the amplitude of inactivation demonstrated by each process. These had to be estimated in order for the data to be evaluated. Values for A_1 were given as % remaining activities representing the amplitude of the first decay process (the rapid phase) and were usually estimated between 20 and 30. Estimates for A_2 were taken as percent remaining activities at the inflection points of inactivation curves where the % remaining activity began to change little among subsequent readings (the slow phase). The parameter k represents the rate constant (k_{obs}) specific to each individual process comprising the whole.

Values for k were also estimated from the slopes of the lines in the semi-log plots (Figure 3-11) representing each inactivation phase (fast vs. slow) as determined above. Using these estimates and raw data (% remaining activity vs. time) collected during the first ten minutes of a twenty minute incubation (more than an adequate number of points to evaluate both processes), both a best fit line and inactivation rate constants for each process were calculated. Single-exponential decay analyses of data sets thought to represent each individual process were performed to corroborate results obtained from double-exponential decay evaluation. Observed and calculated data, values for A_1 , A_2 , k_1 and k_2 obtained from both analyses and plots of calculated double-exponential decay curves are given in Appendix G. All data, at all H_2O_2 concentrations, were successfully fitted to double-exponential decay curves in less than 4 chi-square iterations, with calculated values of percent remaining activity demonstrating good agreement with experimentally obtained values (Table 3-13, Figure 3-13). Similar agreements and curve fits were not obtained from single-exponential decay analyses. No inference as to the mechanism of inactivation could be made from either analyses, and because the data conformed much better to a double-exponential decay evaluation, subsequent kinetic analyses were performed using data obtained from double-exponential decay treatment only. Inactivation rate constants, k_{obs} , determined from both single- and double-

<u>Time (sec.)</u>	<u>% Remaining (Observed)</u>	<u>Calculated</u>
0	100	98.24
5	83.6	85.21
10	73.3	74.83
20	60.0	59.96
30	51.2	50.54
50	40.1	40.78
300	34.2	35.10
609	36.7	36.39

Table 3-13 Observed and calculated % remaining activity data vs. time used for double-exponential evaluation of inactivation from 1.0mM H₂O₂ of 100nM HRP (T=25°C, pH 7.4).

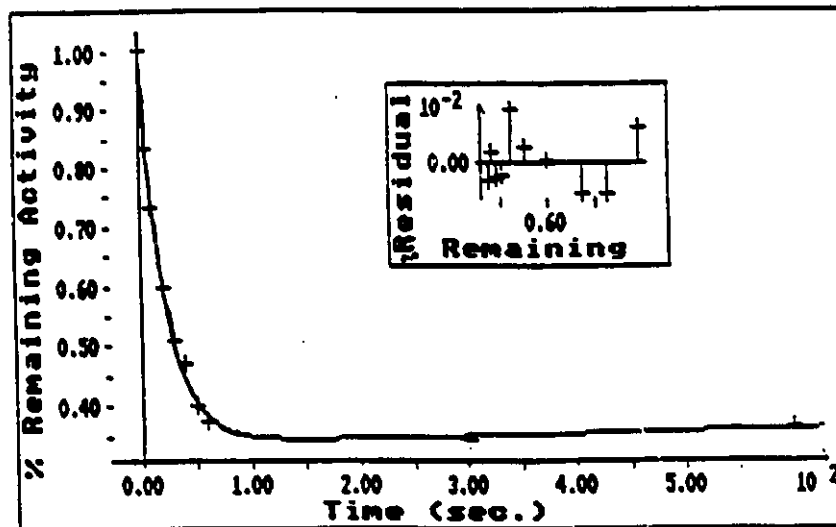


Figure 3-13 Plot of observed data in Table 3-13 fit to a calculated double-exponential decay curve (1.0mM H₂O₂).

exponential decay evaluations are shown in Table 3-14 for comparison. Values of k_{obs} obtained for the slow process were generally ill-behaved, exhibiting no clear dependence on H_2O_2 concentration, suggesting that more than just an inactivation process was occurring during this time. This rendered further kinetic analyses on the slow phase difficult and as a result, analyses were performed only upon k_{obs} values determined from the rapid phase of inactivation. A linear least-squares regression plot of k_{obs} (fast) values determined from double-exponential decay analysis vs. H_2O_2 concentration listed in Table 3-14 is presented in Figure 3-14. Values for H_2O_2 concentrations greater than 5mM exhibited increasingly larger error values, expressing the difficulty encountered in obtaining a sufficient number of data points for proper analysis during the fast inactivation phase, which was extremely rapid and practically complete by the time of the first activity reading at these higher concentrations. However, subsequent attempts to fit all data omitting these points decreased the correlation coefficient to 0.916; this became worse upon exclusion of all data above 1.0mM (values never dropped below 0.90). However, upon re-examination of Figure 3-10, it was noted that concentrations of 0.1mM did not exhibit the typical biphasic inactivation curves observed at higher H_2O_2 concentrations. If the rationale that what was being observed in this case (and perhaps at other slightly higher H_2O_2 concentrations such as 0.5mM) was not entirely the

[H ₂ O ₂] (mM)	Exponential Decay Process	k _{obs} (fast) (x10 ²) (min ⁻¹)	k _{obs} (slow) (x10 ²) (min ⁻¹)
0.1	double	1.80 ± 0.27	1.44 ± 0.76
"	single	0.38 ± 0.04	1.26 ± 0.99
0.5	double	1.87 ± 0.51	0.36 ± 5.10
"	single	0.76 ± 0.09	3.16 ± 0.43
0.75	double	3.73 ± 0.75	1.09 ± 4.32
"	single	1.89 ± 0.25	2.09 ± 1.45
1.00	double	4.54 ± 0.41	(-) 1.13 ± 1.50
"	single	7.19 ± 1.15	(-) 4.32 ± 6.08
5.00	double	7.19 ± 1.15	7.44 ± 6.48
"	single	3.70 ± 0.52	4.76 ± 3.26
10.00	double	68.4 ± 22.9	59.9 ± 34.6
"	single	23.5 ± 7.25	6.40 ± 3.66
50.00	double	116.6 ± 81.9	39.0 ± 36.1
"	single	48.9 ± 15.6	3.48 ± 2.17

Table 3-14 Values of k_{obs} and their standard errors, representing both fast and slow inactivation phases, obtained by single- and double-exponential decay analyses (see Appendix G). All values were obtained using 100nM HRP at 25°C, pH 7.4.

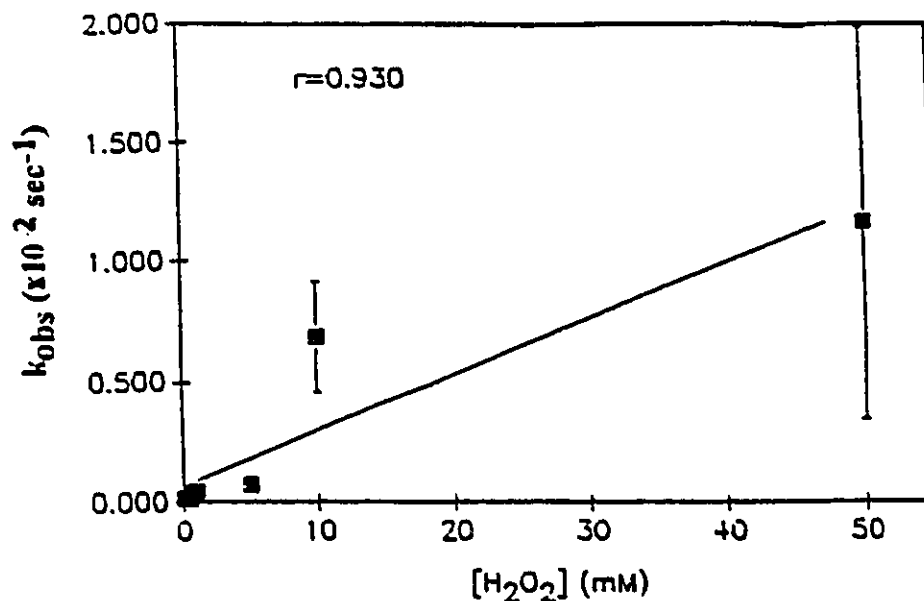


Figure 3-14 Least-squares linear regression plot of k_{obs} values obtained from double-exponential decay analysis shown in Table 3-14 vs. H_2O_2 concentration: [HRP]=100nM; T=25°C, pH 7.4.

Data	K_{Iapp} (mM)	k_{Inact} (sec ⁻¹)	Correlation Coefficient
entire set	0.33	0.068	0.744
- 50mM	0.24	0.054	0.731
-50 & 10mM	0.14	0.040	0.732
-50, 10 & 5mM	0.09	0.034	0.683
-0.10mM	22.3	0.94	0.96
-0.10 & 50mM	16.4	0.69	0.95
-0.10, 50 & 10mM	4.40	0.20	0.93

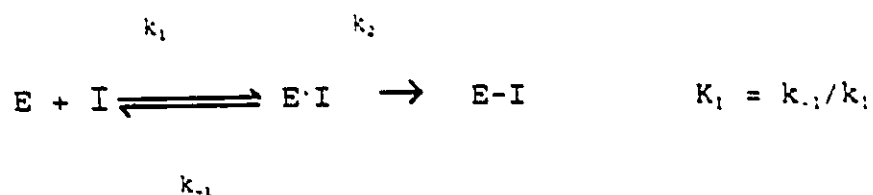
Table 3-15 Values of kinetic constants K_{Iapp} (inhibitor binding constant) and k_{Inact} (maximal rate of inactivation at saturating inhibitor concentrations) obtained from double reciprocal plots of k_{obs} vs. H_2O_2 data shown in Figure 3-14. Correlation coefficients from linear-least squares treatment of data are also indicated.

result of inactivation but also the depletion of available H_2O_2 , which was present in these solutions at concentrations representing $2K_m$, then this could possibly preclude using this point in "inactivation" analyses. Indeed, upon omission of this point in a linear least-squares analysis of fast process k_{obs} values, the correlation coefficient rises back to 0.925 (data not shown). A second-order inactivation rate constant (second-order in enzyme and H_2O_2 concentration: $k_{app} = k[enzyme][H_2O_2]$) was determined from the slope of the line in Figure 3-14 to be $0.023 \pm 0.0047M^{-1}s^{-1}$. The reasonable linear behaviour of all data points in this plot suggests that inactivation may in fact be second-order with respect to enzyme and H_2O_2 concentration (Adediran and Lambeir, 1989).

Therefore, it was clear that two complications were inherent to the data that could confound further kinetic analyses: (1) inactivation observed at and possibly higher than 0.10mM H_2O_2 may not be entirely due to inactivation per se, but a depletion of substrate (H_2O_2); (2) inactivation during the fast inactivation phase at concentrations above 1.0mM was too fast to be monitored with the equipment available, yielding what was probably an insufficient number of experimental values for proper analyses to be performed; However, the concentration range around 1.0mM was of greatest practical interest because this range tended to effect the most efficient dephenolization of waste water, the main focus of this group's research. In spite of these complications and

with them borne in mind, further analyses were performed on the data.

Secondary reciprocal plots of k_{obs} vs. inhibitor concentration yield two important kinetic parameters given in the following steady-state equation (Walsh, 1979):



Essentially a Lineweaver-Burk plot for the inhibitor, these plots describe pseudo-first order kinetics of inactivation resulting from a covalent reaction with the inhibitor pre-bound at the active site (Fersht, 1977; Walsh, 1977). The y-intercept gives the limiting rate constant (k_{inact} or k_2) or maximum rate of inactivation when all enzyme molecules are in the E·I complex. A finite vertical intercept indicates that the inactivation follows saturation kinetics and serves to further substantiate inactivation following from a pre-bound inactivator. A horizontal intercept of $-1/K_i$ gives the dissociation constant of the inactivator from E·I (the inhibitor binding constant K_{iapp}) yielding an idea of the enzyme's affinity for the inhibitor. Double-reciprocal plots were constructed from linear-least squares fits of double-exponentially obtained k_{obs} (fast) values presented in Table 3-14 in attempts to more closely examine the mechanism of

inactivation with respect to H_2O_2 concentration. Attempts to fit all data to a linear-least squares line gave reasonable estimates of inactivation constants $K_{i,app}$ and k_{inact} : 0.33mM and 0.068sec^{-1} ($t_{1/2} = 10.2\text{sec}$), respectively; but exhibited a low correlation coefficient of 0.744 (Table 3-15). Based on the previously discussed complications imposed by the data to this sort of kinetic analysis, attempts were made to fit data sets excluding either the k_{obs} values obtained at H_2O_2 concentrations above 1.0mM, or at 0.10mM, or excluding both (Table 3-15). Improvements in correlation coefficients were obtained upon omission of the 0.10mM value, but the inhibitor binding constants became worse. Exclusion of 0.10, 10 and 50mM k_{obs} values improved the correlation coefficient and the inhibitor binding constant value, although it was still relatively large (4.4mM). Taking this and the generally poor linear behaviour of the data into consideration, it is probable that H_2O_2 does not associate with HRP in the sense of a true association complex leading to a covalent interaction of enzyme with irreversible inhibitor. The k_{inact} value determined from the line excluding 0.10, 10 and 50mM k_{obs} values and including the other determined k_{inact} values could be used as qualitative evidence to verify the nature of inactivation observed in this study compared to inactivation observed by Arnao et al. (1990a). In spite of their questionable validity, all k_{inact} values in Table 3-15 indicate inactivation to be much faster than that observed by Arnao et

al. ($k_{inact} = 0.0039s^{-1}$). Despite computational difficulties, this difference is not surprising because the rates and final magnitudes of inactivation observed in this study were greater over shorter periods of time than those observed by Arnao et al. (compare Figures 1-3 and 3-10). However, the slower inactivation observed by Arnao et al. is somewhat odd because they examined inactivation at H_2O_2 concentrations $\geq 1.0mM$; concentrations that, in this study, resulted in incredibly fast inactivation. Discrepancies may be attributable to the different chromogen systems used to evaluate the residual enzyme activity (ABTS vs. AAP/HDCBS). Sigma type IX HRP comprised of basic isoenzymes was used in their study as opposed to the Boehringer Mannheim Grad II HRP containing isozyme C used in this study. Differences in behaviour towards H_2O_2 have been reported to exist among HRP isozymes (Section 1-2; Kay et al., 1967).

Despite the ambiguity of the data and differences in the assay systems used, it was still of interest to compare, qualitatively, inactivation results with those observed by Arnao et al. (1990a) since they are the only group to date to have examined inactivation of HRP by H_2O_2 in some detail. Parameters r_c , r_{coIII} and $r_c + r_{coIII}$ (Section 1.4.1; Table 1-3) were calculated for this system using k_3 and k_4 values obtained by Arnao et al. (at a pH of 6.3, using Sigma HRP and a range of H_2O_2 concentrations $\geq 1.0mM$; (1990a)). The k_{inact} used in these calculations was $0.2sec^{-1}$ determined from the double -

reciprocal plot of k_{obs} vs. H_2O_2 excluding k_{obs} values for 100 μ M, 10 and 50mM. Values of 8.8, 0.04 and 8.84 were determined for r_c , r_{coIII} and $r_c + r_{coIII}$, respectively. Compared to values determined by Arnao et al. (Table 1-3) and despite the poor behaviour of the data in kinetic analysis, these values in general point to inactivation being a more predominant process in this system than was observed in their system; in particular, the value of 0.04 for the parameter r_{coIII} suggests inactivation to be favored over the catalytic pathway leading to the formation of Compound III. Support for this is seen in the % irreversible activity column for H_2O_2 concentrations ≥ 1.0 mM in Table 3-10.

Despite the difficulties encountered in obtaining reliable quantitative data concerning the mechanism of H_2O_2 -mediated HRP inactivation, many interesting and useful qualitative details have been discovered that may be of use for future inactivation investigations and can be added to the meagre repertoire of information already known about this bizarre interplay of enzyme and its "Jekyll and Hyde-like" substrate:

1. Both irreversible and reversible inactivation mechanisms are responsible for the overall observed inactivation and this provides evidence in support of Arnao et al.'s partitioning model (1990a, b).

2. The rate and magnitude of inactivation, particularly during the initial rapid stages, are time-, and enzyme and H_2O_2 concentration dependent (second-order). Enzyme concentration may be an important factor in protection against inactivation at concentrations of H_2O_2 up to and including 1.0mM. Beyond this, extent of inactivation appears to be the same, irrespective of enzyme concentration.

3. The pathway favored in Arnao et al.'s partitioning model, which is reflected in the inactivation observed or the intermediates formed, also appears to be H_2O_2 concentration dependent. Below 1.0mM, perhaps even below 0.75mM, the formation of an intermediate (likely Compound III) which can recover some activity lost is predominant. Its formation diminishes but is still predominant as H_2O_2 concentrations approach 0.75 and 1.0mM. The irreversible inactivation pathway becomes the more favored path as concentrations rise above 1.0mM. The absence of apparent concentration dependence of inactivation at 0.75mM and 1.0mM suggests that this may be a "junction" where both pathways are more or less favored equally. The influence of less obvious factors may serve as determinants in the choice of pathway followed. These results provide evidence in support of Compound III as a protector against oxidative damage.

4. The good fits of % remaining activity vs. time during the

first 60 seconds of inactivation for all data to calculated values and plots suggests that the inactivation process as a whole, could be modelled after a double-exponential decay. Unfortunately, no direct mechanistic inference can be drawn from these analyses. The errors associated with calculated k_{obs} values are reasonable until 1.0mM H_2O_2 ; beyond this the inactivation process becomes too fast to be evaluated properly. Poor behaviour of data obtained during the slow process showed it to be more complex than either single- or double-exponential decay, and may reflect an equilibrium situation, rather than strictly inactivation per se, involving a number of HRP intermediates.

5. Reasonable linear fits of most k_{obs} vs. H_2O_2 concentration data offers more concrete support for inactivation being second-order rather than a first-order process with respect to H_2O_2 and enzyme concentrations, despite the fact that data collected: (1) at 0.10mM were not representative of inactivation exclusively; and, (2) above 1.0mM were insufficient to be properly analysed. As a result, inactivation rate constants were likely underestimates.

6. Double-reciprocal plots of k_{obs} vs. H_2O_2 concentration were ill-behaved and exhibited poor linear least-squares fits. This suggests that inactivation does not require a pre-association of H_2O_2 with the enzyme before the turnover event

resulting in inactivation.

7. Irreversible inactivation resulting in the generation of Compound P₆₇₀ has been described as slow (Arnao et al., 1990a; Nakajima and Yamazaki, 1980) compared to Compound III formation (20M⁻¹s⁻¹; Table 1-3; Adediran and Lambeir, 1989; Nakajima and Yamazaki, 1989) and results obtained from this study support this. Rapid formation of Compound III may account for the initial rapid drop of activity (the rapid inactivation phase) observed at all but the lowest H₂O₂ concentrations.

There is slightly more evidence provided from this study in favor of inactivation being a second-order rather than a first-order mechanism-based process as described by Arnao et al. (1990a). However, despite, in mechanistic terms, its questionable interaction with the enzyme prior to inactivation, the description of suicide substrate suits H₂O₂ rather well. Its turnover by the enzyme is necessary for inactivation to occur and irreversible inactivation has been suggested to occur at the active site (Marklund, 1973; Nakajima and Yamazaki, 1987; Ator et al., 1987). H₂O₂, like other mechanism-based inactivators, is known to behave as a substrate for a part of the catalytic cycle and an inactivator in others (Walsh, 1977). A "covalent" association or change occurs by way of an irreversible oxidation leading to subsequent inactivation. What is very clear from this study

is that this inactivation mechanism is very complex, involving a number of enzyme intermediates whose appearance coincides with H_2O_2 concentrations and the combination of two inactivation pathways. With equipment capable of efficiently monitoring rapid processes, it would be useful to define, more precisely than could be done in this study, the kinetic parameters characterizing this inactivation process. In particular, the determination of H_2O_2 concentrations causing one pathway to be favored over the other, and the extent of this favorability would be of interest, particularly in applications that require HRP maintain its catalytic integrity when exposed to higher than normally tolerated levels of H_2O_2 :

3.3.1.1 Monitoring Spectral Changes

Experiments were performed in attempts to identify, qualitatively, the HRP intermediate(s) present under conditions similar to those investigated during H_2O_2 -mediated HRP inactivation. Solutions of native enzyme, at concentrations of $10\mu M$ and $30\mu M$ to permit reliable monitoring of changes occurring in the Soret and far red regions (α and β bands), respectively, were exposed to various concentrations of H_2O_2 similar to those used in inactivation experiments ($100\mu M$ - $50mM$). Incubations were monitored spectrophotometrically for periods of 1-5 minutes. Plots of visible spectra recorded every 5 to 10 seconds for 1 minute, and every 30 seconds thereafter up to 5 minutes, were successively overlain

on a spectrum taken of the native enzyme prior to H_2O_2 addition ($t=0$ sec). Bands in the far red region are more distinct and were used to indicate the presence of intermediates (Table 1-1). Appendix H presents tables listing the absorbance maxima detected as distinct peaks measured at 10 second intervals over the reaction course. Plots showing decay and development of distinct absorbance maxima presented in these tables are also shown. Attempts to generate solutions exhibiting absorption spectra characteristic to each HRP compound were prepared from H_2O_2 only using literature-cited recipes (Arnao et al., 1990a; Dunford and Stillman, 1976). Spectra were recorded to assist in comparison of results and to enable the identification of intermediates present when accumulation of absorbance reached a maximum value (Figure 2-1).

Enormous differences in the magnitudes of extinction coefficients and the presence in solutions of greater than 1 intermediate contributing to the final spectrum (Dunford and Stillman, 1976) rendered it impossible to determine the exact origin of the observed absorption spectra as well as the relative concentrations of intermediates present. Therefore, no attempts were made to quantitate the amount of intermediate(s) present over time. Rather, approximations as to which intermediate was likely present based solely on the predominant absorbance maxima exhibited were made. Table 3-16 lists the intermediates estimated to be present at various H_2O_2 concentrations and the time during the incubation when the

[H ₂ O ₂] (mM)	Time at Maximum Accumulation of Absorbance (sec.)	Compound(s) Present
0.10	300	II
1.00	300	II
10.0	90	III/P ₆₇₀
25.0	60	III/P ₆₇₀
50.0	30	III/P ₆₇₀

Table 3-16 Summary of intermediates implicated to be dominant, based solely on comparisons of observed absorption spectra to literature citations, during exposure of solutions of HRP to concentrations of H₂O₂ investigated in time-dependent inactivation experiments: [HRP] = 30μM; T=25°C, pH 7.4.

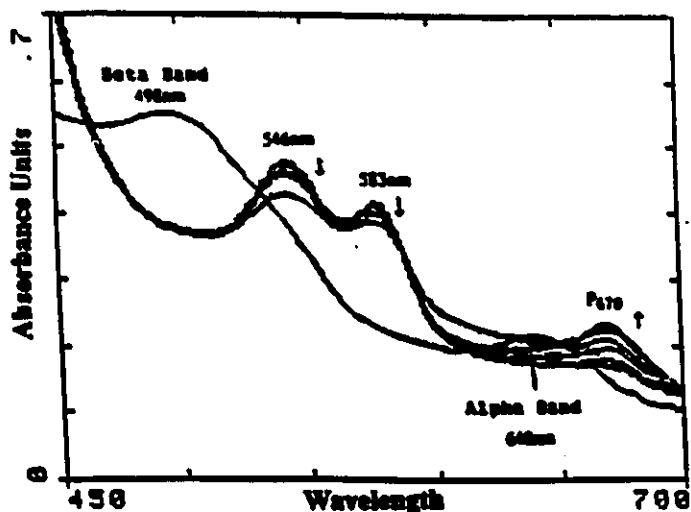


Figure 3-15 Appearance of absorbance maxima at 670nm from a spectrum characteristic of Compound III. [HRP]=30μM; [H₂O₂]=10mM; T=25°C, pH 7.4. Each plot a measurement taken every 10 seconds for a total of 60 seconds. A spectrum of the native enzyme, showing the alpha and beta bands is shown for comparison.

absorbance value(s) at the characteristic peaks was maximal. Spectra exhibiting absorbance maxima characteristic of Compound II became quickly predominant (within the first 5-10 seconds; Tables H2 and H4) at H_2O_2 concentrations of less than 1.0mM. At and above 1.0mM, spectra identified as belonging to Compound III formed rapidly (also within the first 5-10seconds) and remained predominant for the majority of the incubation period (Tables H6, H8 and H10). A peak recorded at 670nm was first detected at approximately 20-30seconds and developed slowly from Compound III's spectrum as the incubation proceeded. The time until its first detection decreased with rising H_2O_2 concentration. Peak development at 670nm was taken to indicate the formation of Compound P_{670} (Arnao et al., 1990a; Nakajima and Yamazaki, 1987). Absorbance accumulation at 670nm was accompanied by concomitant gradual decay of the peaks characteristic of Compound III in the far red region at 546 and 583nm (Figure 3-15). This phenomenon has been observed by several workers (Adediran and Lambeir, 1989; Arnao et al., 1990a; Bagger and Williams, 1971; Marklund, 1973; Nakajima and Yamazaki, 1987). Isosbestic points at approximately 590 and 498nm suggest that Compound P_{670} may form directly from Compound III. However, uncertainty exists in the origin of this spectrum being only Compound III; Compounds I and II could also be present at low concentrations and contributing to this spectrum. There is already strong evidence to suggest that P_{670} forms from Compound I generated in

solutions of Compound III as a result from interactions between the ferric intermediate on the path to Cpd. III formation and excess H_2O_2 (Arnao et al., 1990a,b; Nakajima and Yamazaki, 1987; Adediran and Lambeir, 1989). Once formed, Compound I then may react with excess H_2O_2 generating Compound P_{670} (Arnao et al., 1990a; Nakajima and Yamazaki, 1987). Solutions exhibiting a 670nm peak were a bright green colour similar to that observed in Chance's solutions of Compound IV (1949), reported now to have been the first evidence of Compound P_{670} 's existence (Bagger and Williams, 1971; Nakajima and Yamazaki, 1980).

Extensive bubble production was observed during P_{670} accumulation and with prolonged exposure beyond 5 minutes, solutions underwent a complete loss of visible spectrum. This was observed by Bagger and Williams (1971) and Marklund (1973) and is apparently indicative of oxidative damage at the porphyrin resulting in ring cleavage to a linear tetrapyrrole (Brown et al., 1968; Bagger and Williams, 1971).

These results, though qualitative, corroborate reasonably well with results of inactivation experiments. At low H_2O_2 concentrations (below 1.0mM), evidence for the favored formation of Compound III over P_{670} is supported by an absence of the 670nm absorbance maximum in these solutions. Despite Compound P_{670} 's low extinction coefficient (Table 1-1) which makes its presence difficult to detect at reasonable concentrations, negligible formation of P_{670} was indicated

earlier by the substantial recovery of activity lost upon dialysis (Table 3-10). The predominance of a Compound II-like spectrum in these solutions may result from the reaction of Compound III's ferric intermediate with H_2O_2 to yield Compound I (as described earlier in section 1.3) which is unstable and quickly forms II. At higher H_2O_2 concentrations ($\geq 1.0mM$), evidence suggests that the slower irreversible inactivation pathway is now favored (increase % irreversible activity in Table 3-10) and becomes even more favored as H_2O_2 concentration rises, with 25 inactivations occurring to every one pathway generating Compound III (present study, Section 3.1.1; Arnao et al., 1990a). Enough Compound III would likely still be formed to account for the huge decreases in activity observed during the first few seconds of inactivation at these H_2O_2 concentrations.

After initial and rapid generation of Compound III (the rapid inactivation phase), perhaps a cycling of Compound III's ferric intermediate forming Compound I (Nakajima and Yamazaki, 1987) from which two possible pathways can be followed producing a number of intermediates, might account for the unusual behaviour of the data obtained during the slow phase of inactivation. It would be of interest to re-examine these pathways in detail to derive more precise kinetic information and in so doing, determine the approximate amounts and types of intermediates formed under specific conditions of H_2O_2 concentration.

3.3.2 Inactivation by Enzyme-Generated Phenoxy Radicals

The first workers to conduct a detailed investigation of HRP inactivation by phenoxy radicals generated from enzyme-catalyzed oxidation of phenol in the presence of H_2O_2 were Ma and Rokita (1988). The occurrence of this type of inactivation had been hinted at previously (Ortiz de Montellano and Grab, 1987). Inactivation was determined to be both phenol and H_2O_2 -concentration dependent, requiring substrate turnover and retention of the radical at the enzyme's active site. Molecular oxygen potentiated inactivation. Possible reaction mechanisms or enzyme intermediates generated were not addressed.

Inactivation of HRP by enzyme-generated phenoxy radicals was examined under aerobic conditions to determine the effects of enzyme, H_2O_2 , and phenol concentrations. All reactions were carried out at 25°C and pH 7.4. To solutions containing HRP and phenol, an aliquot of H_2O_2 was added to initiate the reaction generating phenoxy radicals. Incubations were monitored for a total time of 20 minutes. Samples were removed at specific times and tested for remaining activity using the AAP/phenol activity assay, compared to a control containing identical enzyme concentrations minus both phenol and H_2O_2 . All plots of absorbance vs. time were linear except in cases of complete enzyme inactivation. Figure 3-16 demonstrates the typical inactivation curves observed at most phenol, H_2O_2 , and enzyme concentrations. The lines shown are

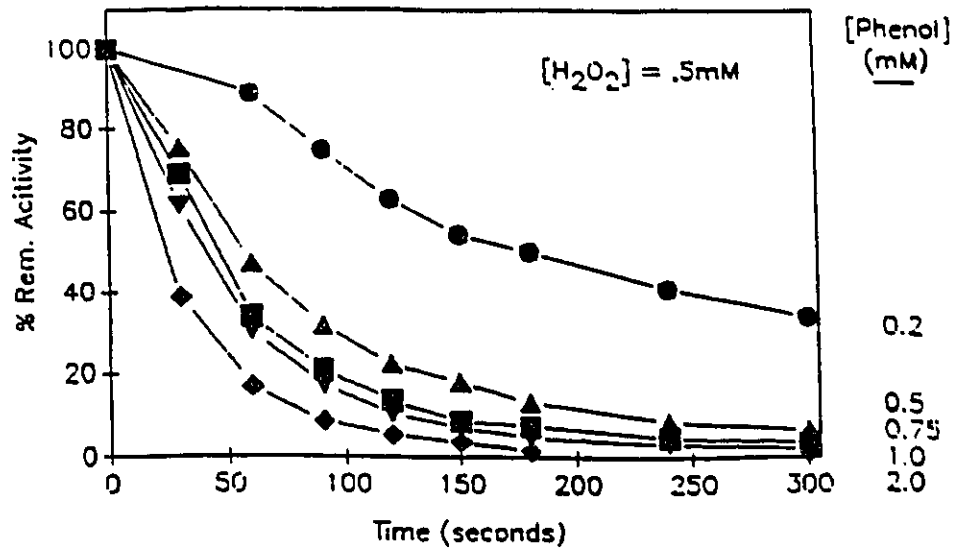


Figure 3-16 Time-dependent inactivation of 50nM HRP by enzyme-generated phenoxy radicals at various concentrations of phenol. [H₂O₂]=0.5mM; T=25°C, pH 7.4. Curves shown are arbitrarily drawn to join the data points.

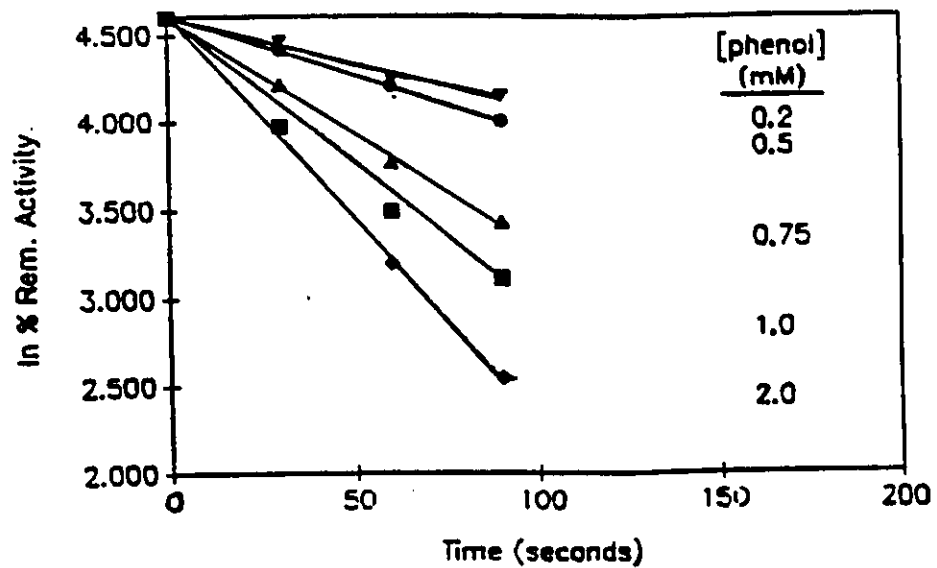


Figure 3-17 An example of the semi-log plots obtained from ln % remaining activity vs. time data collected during the first 60-90 seconds. [HRP]=25nM; [H₂O₂]=0.5mM; T=25°C, pH 7.4.

arbitrary but in general, these curves followed time-dependent single-exponential decay. Inactivation at all combinations of enzyme, phenol and H_2O_2 concentrations was complete by a maximum of 5 minutes. Residual activities at all enzyme concentrations and at phenol concentrations of $>0.2mM$ were below 10% by 5 minutes. At phenol concentrations greater than $0.2mM$ and all concentrations of enzyme and H_2O_2 , inactivation during the first 100 seconds happened faster than inactivation during the last 400 seconds. Inactivation at $0.2mM$ phenol appeared to be almost linear with time and the % remaining activity at 30 seconds was very often, greater than the 100% control value, particularly at the lower phenol concentrations ($\leq 0.5mM$). Values decreased with increasing phenol concentrations until, at phenol concentrations of $0.75-1.0mM$, the first reading at 30 seconds was below 100%. This was likely attributable to a phenoxy-radical mediated-activation process. Monophenol potentiation of oxidation rates of several substrates in reactions catalyzed by HRP has been previously observed (Danner et al., 1972). Similar activations were witnessed at concentrations of $50nM$ HRP and $0.2-0.75mM$ phenol (at both H_2O_2 concentrations). For computational reasons and to facilitate the determination of kinetic parameters, values of % remaining activity at 30 seconds for these samples only were used as the 100% (control) data point for subsequent calculations of % remaining activity vs. time and single-exponential decay analysis. Data obtained

at higher enzyme/phenol concentrations were better behaved and did not require this manipulation.

Semi-log plots of $\ln \%$ remaining activity vs. time of data collected during the first 60-90 seconds for all samples generated a family of lines possessing correlation coefficients of ≥ 0.993 and demonstrating a dependence of both rate and magnitude of inactivation on phenol concentration (Appendix I: Figures I1a, b; I2a, b; I3a, b; Figure 3-17). These plots are useful conventional indicators of reaction order but first-order inactivation rate constants, k_{obs} were not determined from them, but rather from subsequent single-exponential decay analysis (to follow). Plots for the most part, were reasonably well-behaved but at all enzyme concentrations, data evaluated beyond 90 seconds at the higher phenol concentrations began to curve, fitting poorly to a straight line. Table 3-17 is a summary of averaged total $\%$ activity remaining by 120s and 5min. for various concentrations of HRP, phenol and H_2O_2 . In general, solutions containing lower concentrations of enzyme exposed to low concentrations of phenol ($\leq 0.5mM$) were not inactivated to the extent, during the first 100 seconds (the faster portion of inactivation observed with these curves), of solutions containing higher enzyme concentrations at either H_2O_2 . However, as phenol concentrations increased, the higher concentration enzyme appeared to be better protected. No obvious dependence of activity loss during the initial

[Phenol] (mM)	[HRP] (nM)	[H ₂ O ₂] (mM)	Total % Remaining Activity	
			120s	5min.
0.2	25	0.5	81.3	65.5
"	"	1.0	94.8	43.3
"	50	0.5	62.7	34.0
"	"	1.0	67.0	42.0
"	100	0.5	66.0	50.0
"	"	1.0	60.7	37.8
0.5	25	0.5	36.5	9.34
"	"	1.0	38.3	9.50
"	50	0.5	22.4	6.62
"	"	1.0	26.9	8.67
"	100	0.5	25.8	10.1
"	"	1.0	16.8	4.96
0.75	25	0.5	24.2	9.52
"	"	1.0	19.3	5.90
"	50	0.5	13.8	3.50
"	"	1.0	15.7	3.54
"	100	0.5	17.6	7.41
"	"	1.0	10.6	2.60
1.0	25	0.5	17.4	9.69
"	"	1.0	20.9	3.99
"	50	0.5	10.7	2.20
"	"	1.0	10.3	1.99
"	100	0.5	14.5	11.5
"	"	1.0	7.90	1.61
2.0	25	0.5	6.41	9.85
"	"	1.0	7.80	2.32
"	50	0.5	3.45	1.14
"	"	1.0	4.11	5.13
"	100	0.5	19.7	22.9
"	"	1.0	2.60	0.36

Table 3-17 Summary of total % inactivation of various concentrations of HRP by enzyme-generated phenoxy radicals in the presence of a variety of phenol and H₂O₂ concentrations: T=25°C, pH 7.4.

portion or total inactivation at the end of 5 or 20 minutes was observed with respect to the two H_2O_2 concentrations examined. Inactivation was not observed in solutions containing HRP and phenol alone, indicating and concurring with Ma and Rokita's observation (1988) that inactivation requires phenol turnover by H_2O_2 -activated enzyme. A greater degree of inactivation was observed in solutions containing HRP/ H_2O_2 and phenol compared to solutions containing HRP and H_2O_2 alone (Figure 3-18) further substantiating the requirement for catalysis. It also illustrates that inactivation mediated by phenoxy radicals was more extensive than inactivation caused by excess H_2O_2 . Addition of H_2O_2 to solutions of HRP and phenol caused a yellow-brown colour to appear that became darker with time. Visible absorbance spectra of these solutions exhibited an absorbance maximum at 400nm (Figure 3-19) and the oxidation product of p,p'-biphenol, p-diphenoquinone, is apparently the major contributor ($\epsilon=34,700M^{-1}cm^{-1}$) (Pelizetti et al., 1974; Sawahata and Neal, 1982).

Appendix I contains summary tables showing H_2O_2 consumption observed by 5 minutes in the presence of various concentrations of phenol, H_2O_2 and HRP (Tables I1a, b; I2a, b and I3a, b). In general, H_2O_2 consumption was not very efficient at the higher H_2O_2 concentration (1.0mM), being generally less than one-half at the end of 5 minutes. More than half of the lower H_2O_2 concentration was consumed by this

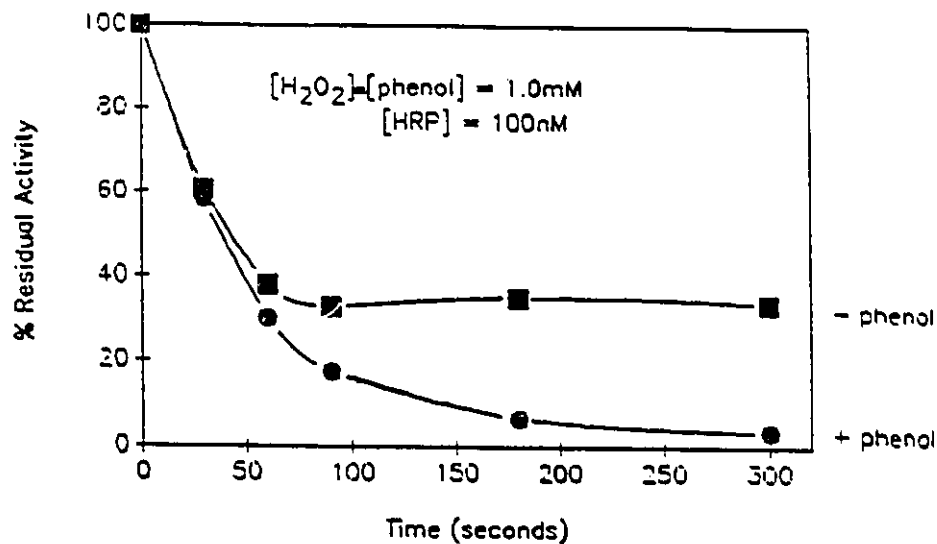


Figure 3-18 Comparison of time-dependent inactivation of 100nM HRP by H_2O_2 alone and by enzyme-generated phenoxy radicals ($T=25^\circ C$, $pH 7.4$).

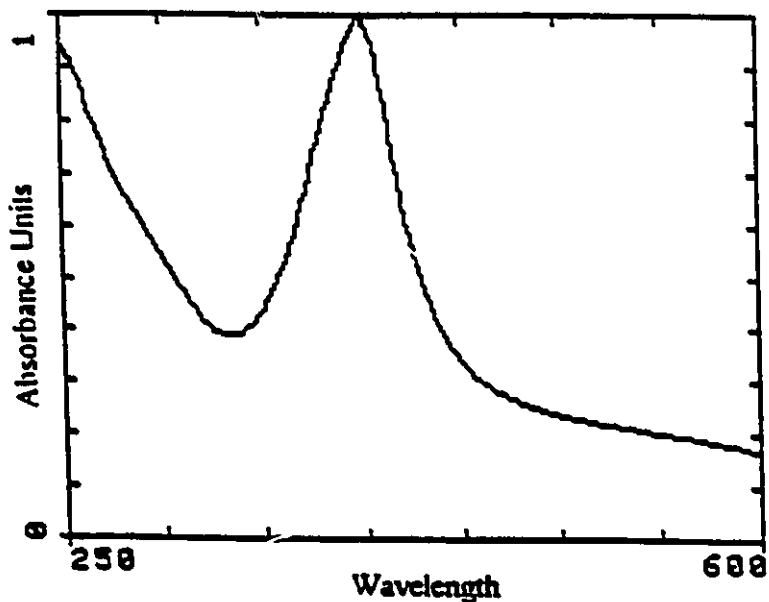


Figure 3-19 Visible spectrum of the product of HRP-catalyzed H_2O_2 oxidation of phenol (after 5 minutes incubation). $[HRP]=100nM$; $[phenol]=0.2mM$; $[H_2O_2]=0.5mM$; $T=25^\circ C$, $pH 7.4$.

time. At all enzyme and H_2O_2 concentrations, H_2O_2 consumption was approximately 200-300 μ M, increasing slightly with increasing phenol concentration, but not significantly, the exception being 25nM enzyme and 1.0mM H_2O_2 . Here it is possible that decreased H_2O_2 consumption was due to combined inactivation from both phenoxy radicals and excess H_2O_2 . This does not explain the erroneous result for 0.2mM phenol. Beyond this concentration, phenol could serve to protect the enzyme against inactivation, but not very well. However, % inactivation at the end of the experiment at all enzyme and H_2O_2 concentration combinations approached 100% with rising phenol concentration. Consumption of H_2O_2 by the end of 5 minutes at 50 and 100nM HRP had improved to over one-half of the original H_2O_2 present. Consumption efficiency increased little or only very slightly with rising phenol concentration. However, at 1.0mM H_2O_2 , consumption decreased to less than one-fifth for the 50nM enzyme and only one-third at HRP concentrations of 100nM. The final extent of inactivation, therefore, appears to depend not so much on H_2O_2 concentration as on phenol and enzyme concentration, particularly in terms of the enzyme's availability to both rapidly produce and be attacked by phenoxy radicals. Incomplete consumption of H_2O_2 could be explained if only a certain amount was needed to generate an adequate number of phenoxy radicals capable of performing non-enzymic oxidation on other phenol molecules and the enzyme itself. Non-enzymatically generated phenoxy

radicals could continue to inactivate the enzyme and react with phenol in the absence of further H_2O_2 consumption.

The shapes of the inactivation curves were similar to those obtained by Arnao et al. (1990a) during H_2O_2 -mediated inactivation of HRP (Figure 1-3). Successful evaluations were performed by them using a double-exponential decay equation identical to that used to inspect H_2O_2 -mediated HRP inactivation in this study. Double- and single-exponential decay analyses were performed as described previously in Section 3.1.1 by ENZFITTER™ using fractional values of % residual activity vs. time observed during the first five minutes (when inactivation was essentially complete) and estimates of A_1 , A_2 , k_1 and k_2 . The majority of the data sets behaved exceptionally well to single-exponential decay analyses suggesting this to be the better model for inactivation; major difficulties and errors were encountered with attempts to fit data to a double-exponential decay equation. Calculated values, fits to decay curves and first-order inactivation rate constants, k_{obs} , obtained from single-exponential decay analyses are presented in Appendix I. An example of a single-exponential decay curve fit to data obtained from experiments in which 25nM HRP was exposed to 1.0mM H_2O_2 and 2.0mM phenol is presented in Table 3-18 and Figure 3-20. Initial values (A) are also given along with the tables of observed and calculated data values. All values were approximately 1.00, with one or two exceptions,

	Time (seconds)	Residual	Calculated
1	0.00000E+00	1.00000E+00	1.01863E+00
2	3.00000E+01	6.22300E-01	5.63569E-01
3	6.00000E+01	2.84400E-01	3.11803E-01
4	9.00000E+01	1.45400E-01	1.72509E-01
5	1.20000E+02	7.83300E-02	9.54433E-02
6	1.50000E+02	5.96500E-02	5.28054E-02
7	1.80000E+02	3.40000E-02	2.92153E-02
8	2.40000E+02	2.81000E-02	8.94285E-03
9	3.00000E+02	2.32000E-02	2.73742E-03

Table 3-18 Example data set of observed and calculated fractional remaining activity vs. time used in single-exponential decay analysis: [HRP]=25nM; [H₂O₂]=1.0mM; [phenol]=2.0mM.

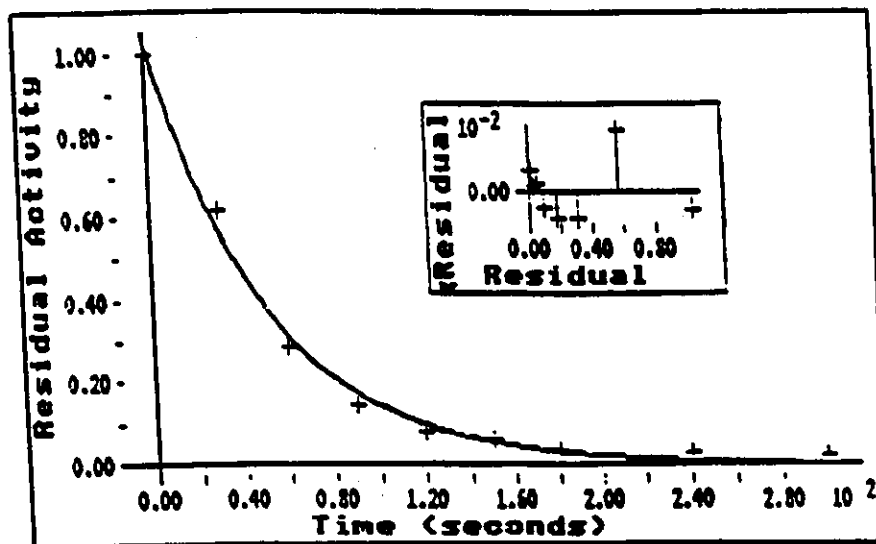


Figure 3-20 Plot of experimental inactivation data in Table 3-18 fit to a single-exponential decay curve. Inset: plot of % residual vs. % remaining for experimental values.

indicating that the inactivation process began as soon as activity lower than 100% was observed. For the manipulated data (see earlier), it also suggested that the highest % remaining activity values observed during activation (30 second readings) were reasonable estimates of 100% activity and closely represented where inactivation commenced. Standard errors associated with these calculated initial values were small: typically less than 3%.

Tables 3-19a, b, -20a, b and -21a, b give single-exponential decay determined k_{obs} values vs. phenol concentration. Figures 3-21a, b, -22a, b and 23a, b are plots of this data fit to a linear-least squares line. Values for k_{obs} exhibited phenol concentration dependence and to some extent, enzyme concentration dependence, which supports the hypothesis of the more enzyme present, the more radicals are generated to inactivate the enzyme and the easier it becomes for these radicals to find an enzyme molecule to inactivate. In all plots except 100nM HRP and 1.0mM H_2O_2 (all values fell on a straight line) the value for 2.0mM phenol is excluded. Inclusion of this value at the low enzyme concentration yielded what appeared to be saturation curves that behaved poorly upon attempts to linearize all data (see insets of Figures 3-21a, b; -22a, b and -23a, b - arbitrarily fit curves). This was not such a problem at enzyme concentrations of >25nM: in general, when the 2mM values were used, these curves became more linear, exhibiting correlation coefficients

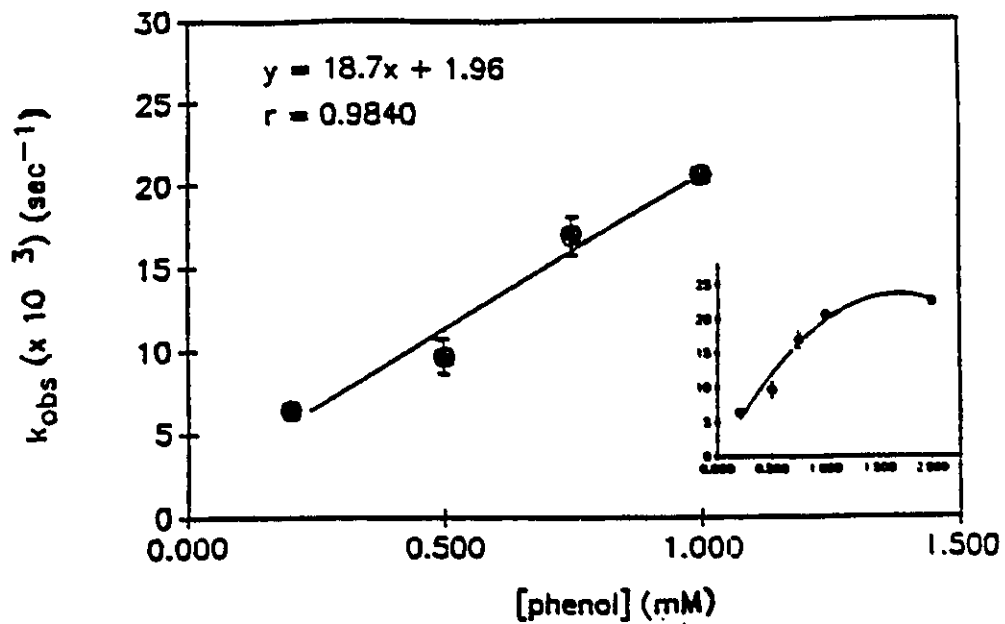
[Phenol] (mM)	k_{obs} ($\times 10^{-3}$) (sec ⁻¹) (single-exponential decay)
0.2	6.44 \pm 0.13
0.5	9.68 \pm 1.08
0.75	16.98 \pm 1.13
1.00	20.65 \pm 0.72
2.00	22.56 \pm 0.47

(a)

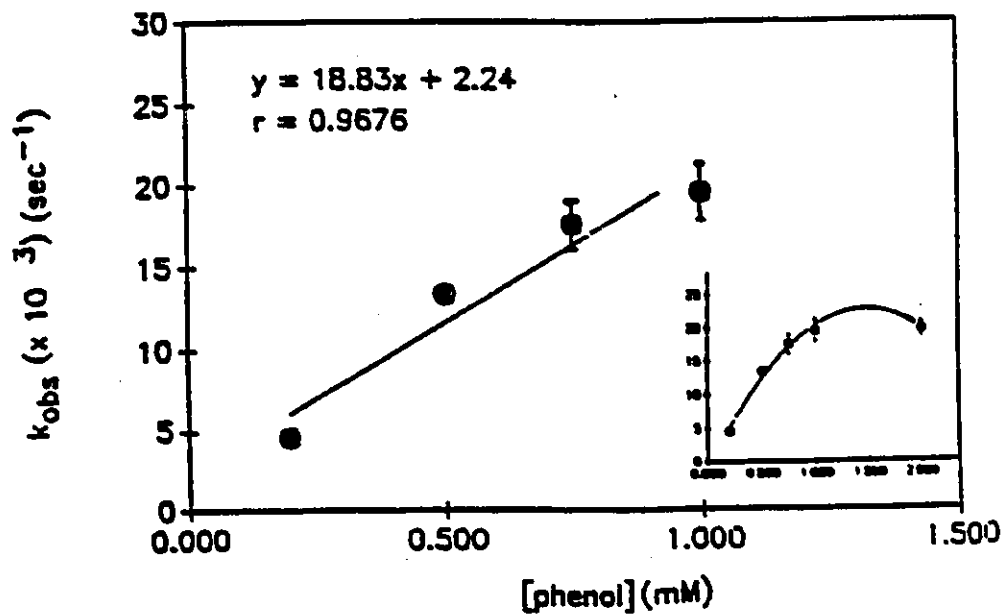
[Phenol] (mM)	k_{obs} ($\times 10^{-3}$) (sec ⁻¹) (single-exponential decay)
0.2	4.58 \pm 0.34
0.5	13.34 \pm 0.57
0.75	17.58 \pm 1.48
1.00	19.61 \pm 1.74
2.00	19.73 \pm 1.04

(b)

Tables 3-19a, b Values of k_{obs} calculated from single-exponential decay analysis for [HRP]=25nM and [H₂O₂]=0.5mM (a) and 1.0mM (b).



(a)



(b)

Figure 3-21a, b Plots of k_{obs} vs. phenol concentration data in Table 19 (a) and (b), respectively. Inset: values fit to a second-order (with respect to phenol) regression curve (same axes labels as primary plot).

[Phenol] (mM)	k_{obs} ($\times 10^3$) (sec ⁻¹) (single-exponential decay)
0.2	3.87 \pm 0.26
0.5	11.90 \pm 0.56
0.75	16.44 \pm 0.88
1.00	18.51 \pm 0.84
2.00	29.66 \pm 1.28

(a)

[Phenol] (mM)	k_{obs} ($\times 10^3$) (sec ⁻¹) (single-exponential decay)
0.2	4.51 \pm 0.64
0.5	10.35 \pm 0.87
0.75	15.95 \pm 0.62
1.00	19.15 \pm 1.05
2.00	31.04 \pm 0.69

(b)

Tables 3-20a, b Values of k_{obs} calculated from single-exponential decay analysis for [HRP]=50nM and [H₂O₂]=0.5mM (a) and 1.0mM (b).

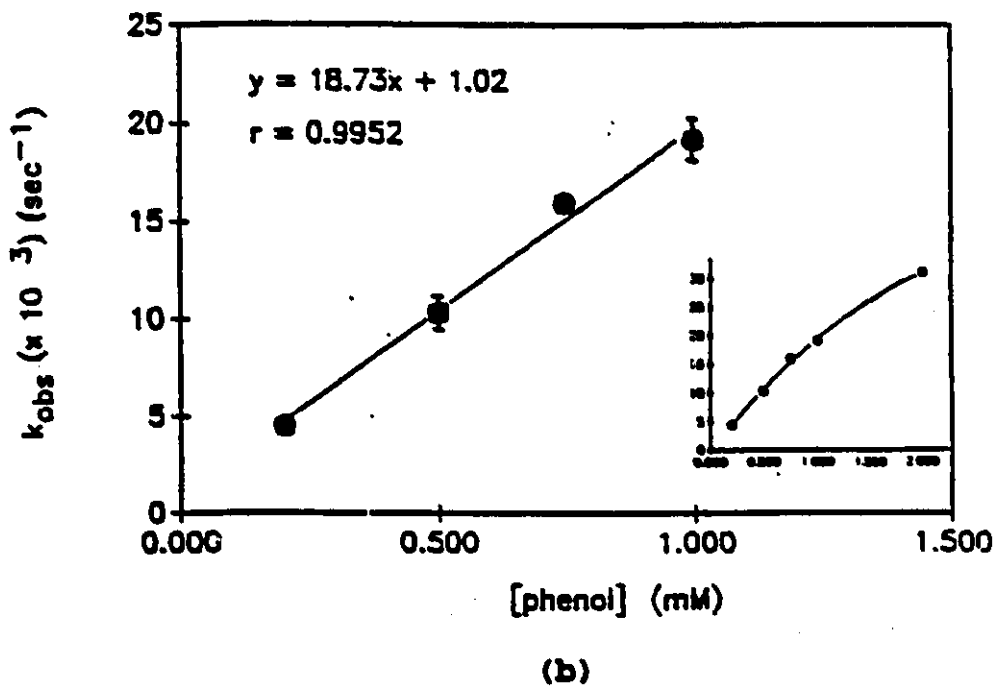
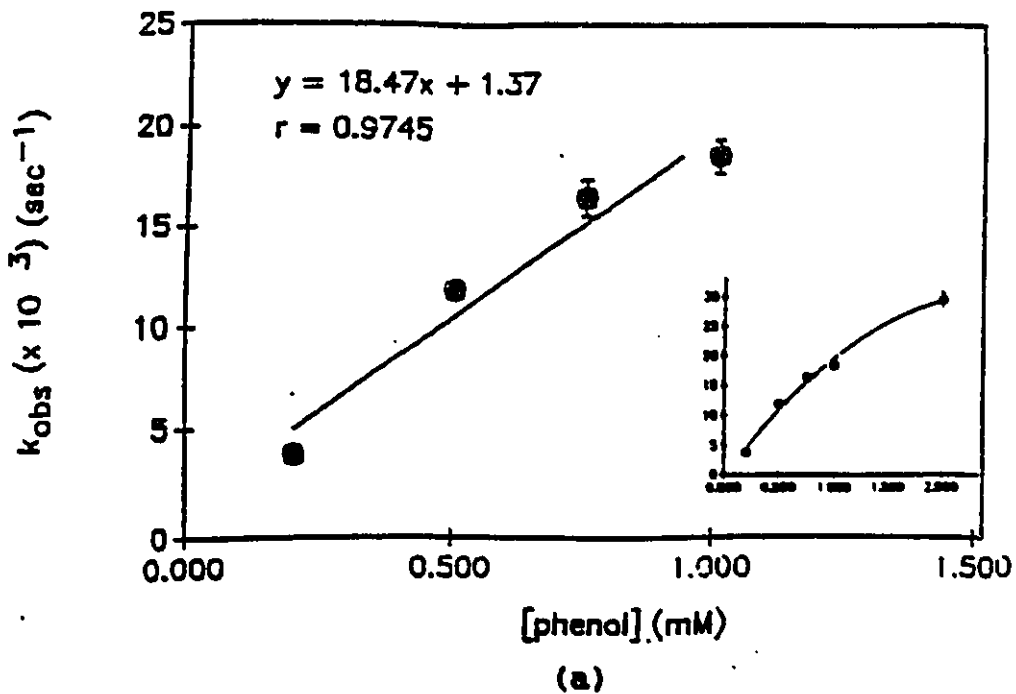


Figure 3-22a, b Plots of k_{obs} vs. phenol concentration data in Table 20 (a) and (b), respectively. Inset: values fit to a second-order (with respect to phenol) regression curve (same axes labels as primary plot).

[Phenol] (mM)	k_{obs} ($\times 10^3$) (sec^{-1}) (single-exponential decay)
0.2	2.65 ± 0.24
0.5	11.29 ± 1.03
0.75	$(5.79) \pm 0.53$
1.00	14.44 ± 2.08
2.00	19.12 ± 5.47

(a)

[Phenol] (mM)	k_{obs} ($\times 10^3$) (sec^{-1}) (single-exponential decay)
0.2	3.81 ± 0.24
0.5	14.90 ± 0.73
0.75	19.68 ± 0.96
1.00	26.02 ± 1.43
2.00	45.62 ± 2.59

(b)

Tables 3-21a, b Values of k_{obs} calculated from single-exponential decay analysis for [HRP]=100nM and [H₂O₂]=0.5mM (a) and 1.0mM (b).

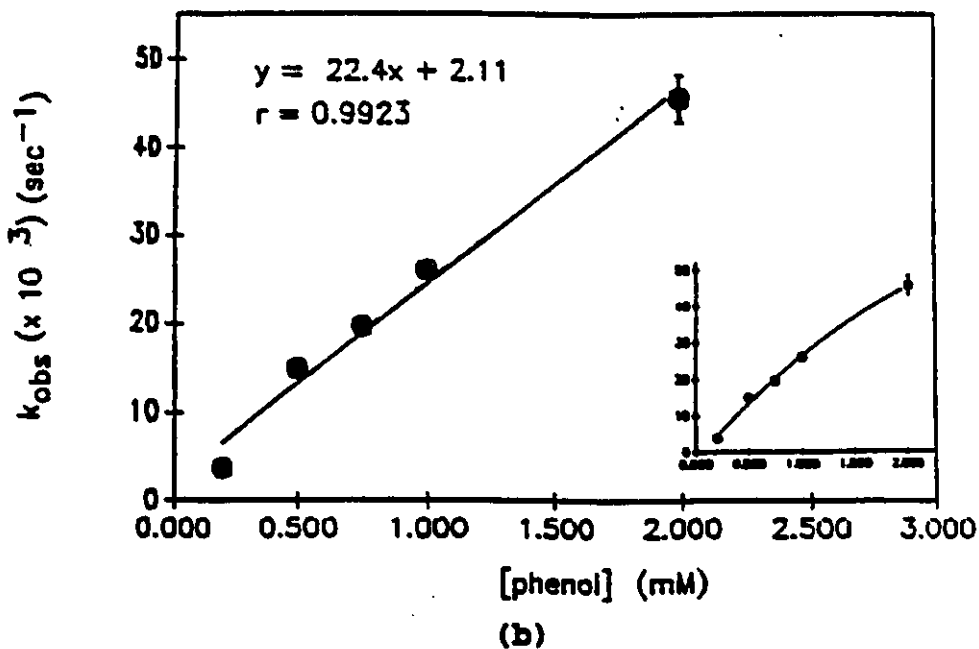
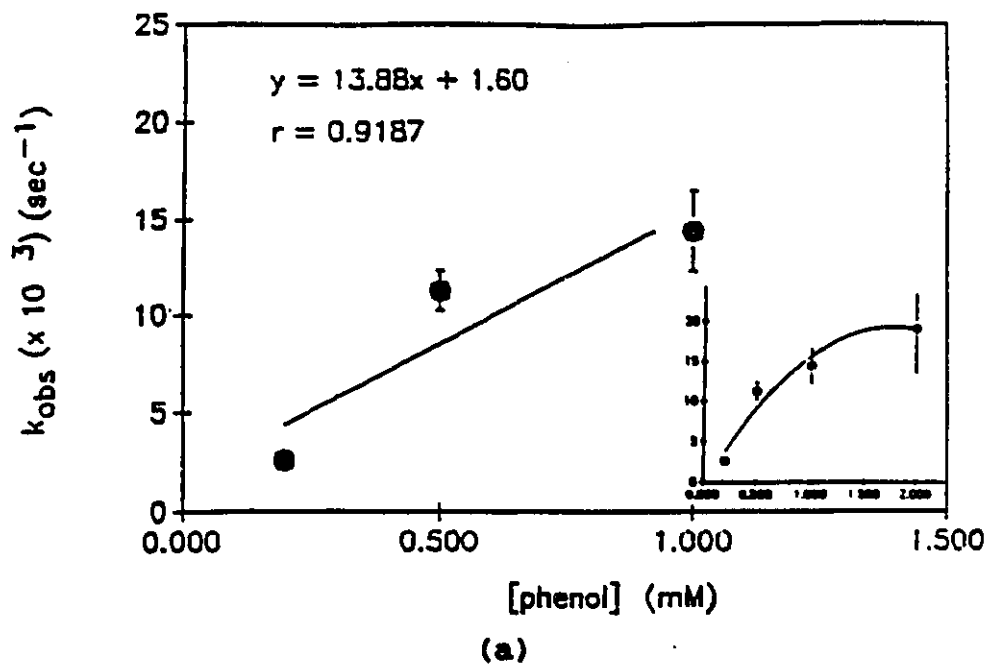


Figure 3-23a, b Plots of k_{obs} vs. phenol concentration data in Table 21 (a) and (b), respectively. Inset: values fit to a second-order (with respect to phenol) regression curve (same axes labels as primary plot).

of 0.97 to 0.993. Inactivation at 2.0mM phenol was very rapid: the first point observed at 30 seconds indicated the major portion of inactivation to have occurred prior to this time. Much like H_2O_2 -mediated enzyme inactivation, it was felt that phenoxy radical enzyme inactivation, especially at higher concentrations of both phenol and enzyme, was too rapid to be accurately monitored by available equipment. An insufficient number of data points were likely procured during the initial stages of inactivation to be analyzed precisely. This in turn, renders these k_{obs} values, at this high concentration of phenol, underestimates of the true inactivation rate, at least at the higher phenol concentrations. If this argument follows, then the apparent linear behaviour of the data in these plots points to inactivation being a pseudo-first order process with respect to phenol concentration or perhaps more accurately, phenoxy radical concentration. Once formed, the phenoxy radicals are capable of carrying out oxidations mimicing enzyme catalysis of phenol, making it appear as if the enzyme is non-saturable with respect to phenol concentration. However, support for inactivation being second-order rather than first-order is supplied from reports of second-order reactions of phenoxy radicals with a variety of molecules (Tripathi and Schuler, 1984; Ye and Schuler, 1989). Plots of k_{obs} vs. phenol concentration then behave according to the equation:

$$k_{\text{obs}} = k_{\text{app}} [\text{I}]$$

where [I] represents phenol concentration. The slopes of these equations yielded the second-order inactivation rate constant k_{app} . Table 3-22 lists the k_{app} values determined from each plot. A mean k_{app} was calculated from these values to be $(1.93 \pm 0.391) \times 10^{-2} \text{M}^{-1} \text{sec}^{-1}$. Close agreement among these values, indicated in the relatively small standard deviation (accountable by an insufficient number of data points gathered during the initial stages of inactivation); further supports phenoxy radical inactivation of HRP to be a second-order reaction.

Inactivation kinetics become more complex in the presence of donor substrates, which upon conversion into free radicals, may leave the active site and inactivate the enzyme again at the active site or at a protein moiety remote from the active site (Yamazaki et al., 1960). Treatment of inactivation as one of competitive/un- or non-competitive is precluded by the absence of a detectable Michaelis-Menten complex of the inhibitor and the enzyme (Dunford and Stillman, 1976) and the irreversibility of the process. However, despite these limitations, the inactivation observed closely resembles that examined by Ortiz de Montellano et al. (1988) during sodium azide mechanism-based inactivation of HRP. As with phenol, sodium azide had to be catalytically turned-over in the presence of H_2O_2 , producing the azidyl radical. This radical

[HRP] (nM)	[H ₂ O ₂] (mM)	k _{app} (x 10 ² M ⁻¹ sec ⁻¹)
25	0.5	1.87 ± 0.240
"	1.0	1.88 ± 0.347
50	0.5	1.85 ± 0.301
"	1.0	1.87 ± 0.131
100	0.5	1.39 ± 0.596
"	1.0	2.71 ± 0.270

Table 3-22 Values of k_{app}, the second-order inactivation rate constant, obtained from the slopes of plots of k_{app} vs. phenol concentration in Appendix I. From these values a mean k_{app} value was determined to be (1.93 ± 0.391) x 10⁻² M⁻¹sec⁻¹ at 25°C, pH 7.4.

remained at the active site once produced and completely inactivated the enzyme in a time-dependent manner producing a series of linear $\ln \%$ remaining activity curves that became less linear and more curved over smaller periods of time as substrate concentration rose. The inactivation reaction took place primarily at the prosthetic group of the heme rather than with the protein matrix. A similar sort of inactivation was observed by Ator et al. (1987) during exposure of HRP, in the presence of H_2O_2 , to phenyl- and alkylhydrazines. The site of attack of both the bigger and bulkier phenyl radical intermediate of phenylhydrazine and the smaller hydrazine-derived alkyl radicals was shown to be primarily at the exposed δ -meso carbon of the porphyrin with some secondary-inactivation resulting from attack at the 8-methyl group (Figure 1-1). Inactivation occurred at the level of Compound II and produced an intermediate bearing a visible spectrum similar to that of choleglobin, an intermediate found along the path to oxidative hemoglobin degradation that possesses a cleaved porphyrin prosthetic group. Inactivation by phenyl-, as opposed to alkylhydrazines, occurred too fast for kinetic parameters K_i and k_{inact} to be obtained: a similar difficulty was encountered in this study. Both groups demonstrated that catalytic turnover was essential to inactivation and that inactivation was a pseudo-first order process, dependent upon, contrary to our findings, H_2O_2 concentration. Along with the irreversibility of inactivation, these criteria prompted them

to describe inactivation as a mechanism-based process. Observance of identical criteria in this study permits this process to also be labelled as a mechanism-based inactivation. No such attempt was made to discuss the inactivation mechanism observed by Ma and Rokita (1988). However, it too was time- and phenol concentration-dependent, requiring substrate turnover.

The single-exponential decay equation used to obtain the first-order inactivation rate constants k_{obs} , served as a simple and reasonable model to analyze this process. Despite the difficulties encountered in obtaining reliable kinetic parameters when evaluating HRP using traditional kinetic techniques, the general trends, such as effects of enzyme, phenol and H_2O_2 concentration were unambiguous rendering more complex kinetic analyses unwarranted for the purposes of this study. However, for future investigations, with the proper equipment, it would be of interest to determine the exact order of inactivation with respect to phenol and H_2O_2 (if applicable). It might then be possible to determine more reliable kinetic parameters (K_I , k_{inact} and k_{obs} over a broader range of phenol concentrations). With these values, it might also be possible to determine if a partitioning between pathways, one catalytic and the other inactivating, perhaps at the level of Compound II, exists as suggested by Ator and Ortiz de Montellano in alkylhydrazine mechanism-based inactivation (1987). A partition ratio could then assist

researchers, particularly those interested in working under conditions in which HRP could potentially become inactivated, in determining the appropriate concentrations of substrates to use in order to prevent or minimize inactivation, prolonging enzyme lifetime and utility in a number of applications.

CHAPTER 4

SUMMARY AND CONCLUSIONS

The focus of this study was to characterize the time-dependent inactivation of HRP by H_2O_2 and enzyme-generated phenoxy radicals. Analytical methods used to detect and to evaluate inactivation were investigated and if needed, optimized, permitting both qualitative and quantitative evaluation of inactivation.

Isoelectric focusing of the BM. HRP Grad II preparation revealed the presence of only catalytically identical isoenzymes B and C. Absence of other possible contaminating isozymes rendered the subsequent kinetic investigations exclusive to the behaviour of these catalytically identical isoenzymes.

The K_m and k_{cat} , based on H_2O_2 , HDCBS and AAP substrates in the HDCBS/AAP colourimetric assay used to evaluate remaining activity during H_2O_2 time-dependent inactivation of HRP, were determined to be ($T=25^\circ C$, pH 7.4):

$$K_m \text{ (mM): } H_2O_2 - (41.01 \pm 1.15) \times 10^{-3}$$

$$HDCBS - 1.4 \pm 0.148$$

$$AAP - 3.94 \pm 0.847$$

$$k_{cat} \text{ (min.}^{-1}\text{): } H_2O_2 - 800$$

HDCBS - 1,200

AAP - 1,000

The assay recipe was not changed from its original format used by previous investigators working in this laboratory (Artiss et al., 1981; Harake, 1986) (see Appendix B).

K_m and k_{cat} based on H_2O_2 and phenol substrates in the AAP/phenol colourimetric assay used to evaluate remaining activity during phenoxy radical time-dependent inactivation of HRP, were determined to be (T=25°C, pH 7.4):

K_m (mM): H_2O_2 - 0.152 ± 0.050
Phenol - 1.37 ± 0.12

k_{cat} (min.⁻¹): H_2O_2 - 21,800
Phenol - 26,700

Optimal rate generating concentrations of components were determined to be 10.0mM phenol, and 0.4mM H_2O_2 . Inhibition was observed with increasing AAP concentrations. Therefore, its concentration was kept at 0.84mM, based on Suntory Enzyme company's recommendation for this same assay.

Time-dependent inactivation by H_2O_2 appeared to exhibit mechanism-based kinetics with respect to H_2O_2 concentration. Inactivation curves of % remaining activity vs. time exhibited a rapid phase, in which the magnitude and rate of

activity loss during the first 0-60 seconds for most samples were H_2O_2 concentration dependent. This phase was followed by a slow phase characterized by a gradual loss of enzyme activity that was neither time- nor H_2O_2 concentration-dependent. The presence of donor substrates, HDCBS and AAP, served to protect the enzyme from inactivation. A pseudo-first order inactivation rate constant, k_{obs} , was determined for each H_2O_2 concentration using double-exponential decay treatments of the rapid inactivation data. Plots of all k_{obs} values vs. H_2O_2 concentration were reasonably linear, pointing to a second-order dependence on both enzyme and H_2O_2 concentration. A k_{app} of $0.023\text{M}^{-1}\text{s}^{-1}$ was calculated from the slopes of primary k_{obs} vs. H_2O_2 concentration plots. However, inactivation was too rapid at concentrations $>1.0\text{mM}$ to follow and evaluate properly. How much of a role inactivation played at low H_2O_2 concentrations (ie. $100\mu\text{M}$) where substrate depletion was very likely responsible for the observed hyperbolic rather than biphasic curves, was questionable. Despite this, a qualitative maximum rate of inactivation, k_{inact} , was determined to be around 0.20sec^{-1} ($t_{1/2} = 3.5\text{sec}$) and an inhibitor binding constant, K_{iapp} , was approximately 4.4mM . In general, these double-reciprocal plots were ill-behaved suggesting there to be no stringent association between the enzyme and H_2O_2 prior to inactivation. The entire inactivation process was more complex than either double- or single-exponential decay, and

involved both a reversible inactivation pathway leading to Compound III, which likely accounted for the observed rapid inactivation, and a path leading to an irreversibly inactivated intermediate, Compound P₆₇₀. Formation of P₆₇₀ and an equilibrium situation of Compound III and other HRP intermediates probably accounted for the slow phase of inactivation. Formation of P₆₇₀ along the irreversible inactivation pathway appeared to be favored at H₂O₂ concentrations >0.75mM; likewise, Compound III formation appeared to be predominant at lower concentrations.

Enzyme-generated phenoxy radical inactivation was rapid, time-dependent and irreversible, requiring substrate turnover, and appeared to be second-order with respect to phenol concentration. Generally, at low phenol concentrations, low enzyme concentrations were not inactivated to the same extent as higher concentrations. The converse was observed at higher phenol concentrations. Rate and magnitude of inactivation were not obviously dependent on H₂O₂ concentration. Values of k_{obs} obtained using a single-exponential decay equation were likely under-estimates of the true values, at least at phenol concentrations of greater than 1.0 or 2.0mM; however, they were dependent on phenol concentration. A second-order inactivation rate constant k_{app} was determined at all HRP concentrations to be $(1.93 \pm 0.391) \times 10^{-2} M^{-1} s^{-1}$ (T=25°C, pH 7.4). Based on the irreversibility of inactivation and the requirement for

phenol turnover, inactivation appears to be mechanism-based. The final event leading to inactivation is likely the same in both H_2O_2 and phenoxy radical inactivations (oxidative cleavage of the porphyrin ring). However, the mechanisms leading to this final stage of inactivation are different.

REFERENCES

- Aguda, B.D. and Larter, R. (1991) *J. Am. Chem. Soc.* 113, 7913-7916.
- Aibara, S., Koboyashi, T., and Morita, Y. (1981) *J. Biochem.* 90, 489-496.
- Adediran, S.A. and Lambeir, A.M. (1989) *Eur. J. Biochem.* 186, 571-578.
- Arnao, M.B., Acosta, M., del Rio, J.A., Varón, R. and Garcia-Canovas, F. (1990a) *Biochim. Biophys. Acta* 1041, 43-47.
- Arnao, M.B., Acosta, M., del Rio, J.A. and Garcia-Canovas, F. (1990b) *Biochim. Biophys. Acta* 1038, 85-89.
- Artiss, J.D., Draisey, T.F., Thibert, R.J. and Taylor, K.E. (1979) *Microchem. J.* 24, 239-258.
- Artiss, J.D., Thibert, R.J., McIntosh, J.M. and Zak, B. (1981) *Microchem. J.* 26, 487-505.
- Ator, M.A., David, S.K. and Ortiz de Montellano, P.R. (1987) *J. Biol. Chem.* 262, 14,954-14,960.
- Ator, M.A. and Ortiz de Montellano, P.R. (1987) *J. Biol. Chem.* 262, 1542-1551.
- Baek, H.K. and van Wart, H.E. (1989) *Biochemistry* 28, 5714-5719.
- Baek, H.K. and van Wart, H.E. (1992) *J. Amer. Chem. Soc.* 114, 718-725.
- Bagger, S. and Williams, R.J.P. (1971) *Acta Chem. Scan.* 25, 976-982.
- Barham, D. and Trinder, P. (1972). *Analyst* 97, 142-145.
- Boss, S. (1986) Ph.D. Thesis. Department of Chemistry and Biochemistry, University of Windsor, Windsor, Ontario, Canada.
- Brewster, M.E., Doerge, D.R., Huang, M.J., Kamiuki, J.J., Pop, E. and Bodor, N. (1991) *Tetrahedron* 47, 7525-7536.

- Brill, A.S. (1977) Molecular Biology, Biochemistry and Biophysics Vol. 26 "Transition Metals in Biochemistry" Ch. 4, 83-116. (Kleinzeller, A. and Springer, G.F. eds.) Springer-Verlag, NY.
- Brown, S.B., Jones, P. and Suggett, A. (1968) Faraday Soc. Trans. 64, 986-993.
- Chance, B. (1949) Arch. Biochem. Biophys. 21, 416-430.
- Childs, R.E. and Bardsley, W.G. (1975) Biochem. J. 145, 93-103
- Cleland, W.W. (1963) Biochim. Biophys. Acta 67, 104-137.
- Conyers, S.M. and Kidwell, D.A. (1991) Anal. Biochem. 192, 207-211.
- Danner, D.J., Brignac, P.J., Arceneux, D. and Patel, V. (1973) Arch. Biochem. Biophys. 156, 759-763.
- Davies, D.M., Jones, P. and Mantle, D. (1976) Biochem. J. 157, 247-253.
- Dawson, J.H. (1984) Science 240, 433-439.
- Dec, J. and Bollag, J.M. (1990) Arch. Environ. Contam. Toxicol. 19, 543-558.
- Dolman, D., Newell, G.A., Thurlow, M.D. and Dunford, H.B. (1975) Can. J. Biochem. 53, 495-501.
- Dunford, H.B. and Stillman, J.S. (1976) Coord. Chem. Rev. 19, 187-251.
- Emerson, E. (1943) J. Org. Chem. 3, 153.
- Everse, J., Everse, K.E. and Grisham, M.B. (eds.) (1990) "Peroxidases in Chemistry and Biology", Vol. II. CRC Press, Ann Arbor, MI.
- Fersht, A. (1977) Enzyme Structure and Mechanism (second edition) W.H. Freeman and Co., N.Y.
- Gallati, V.H. (1977) J. Clin Chem. Clin. Biochem. 15, 699-703.
- Gentry, R.D. (1978) Introduction to Calculus for the Biological and Health Sciences. Addison-Wesley Pub. Co., Don Mills, Ont.
- Gonzalez-Vergara, E., Meyer, M. and Goff, H.M. (1985)

Biochemistry 24, 6561-6567.

Griffin, B.W. (1977) FEBS Letters 74, 139-143.

Griffin, B.W. and Ting, P.L. (1978) Biochemistry 17, 2206-2211.

Harake, B. (1991) PhD. Thesis. Department of Chemistry and Biochemistry, University of Windsor, Windsor, Ontario, Canada.

Harake, B. (1988) MSc. Thesis. Department of Chemistry and Biochemistry, University of Windsor, Windsor, Ontario, Canada.

Hayaishi, Y. and Yamazaki, I. (1979) J. Biol. Chem. 254, 9101-9106.

Job, D. and Dunford, H.B. (1976) Eur. J. Biochem. 66, 607-614.

Kasinsky, H.E. and Hackett, D.P. (1968) Phytochemistry 7, 1147-1150.

Kay, E., Shannon, L.M. and Lew, J.Y. (1967) J. Biol. Chem. 242, 2470-2473.

Keilin, D. and Hartree, E.F. (1951) Biochem. J. 49, 88-104.

Klibanov, A.M., Alberti, B.W., Morris, E.D. and Felskin, L.M. (1980) J. Appl. Biochem. 2, 414-421.

Klibanov, A.M. and Morris, E.D. (1981) Enz. Microbiol. Technol. 3, 119-122.

Klibanov, A.M., Tu, T.M. and Scott, K.P. (1983) Science 221, 259-261.

Lindsay, R.H., Gaitan, E., Jolley, R.L., Cocksey, R.C. and Hill, J. (1986) Am. Chem. Soc. Abs. 191, envr. 20.

Ma, X. and Rokita, S.E. (1988) Biochem. Biophys. Res. Commun. 157, 160-165.

Maloney, S.W., Marem, J., Malleveille, J. and Fiesinger, F. (1986) Environ. Sci. Technol. 20, 249-253.

Marklund, S. (1973) Arch. of Biochem. and Biophys. 154, 614-622.

Nakajima, R. and Yamazaki, I. (1980) J. Biol. Chem. 255, 2067-2077.

Nakajima, R. and Yamazaki, I. (1987) J. Biol. Chem. 262,

2576-2581.

Neilson, B.L. and Brown, L.R. (1984) Anal. Biochem. 141, 311-315.

Nicell, J. (1991) PhD. Thesis. Dept. of Civil and Environmental Engineering, University of Windsor, Windsor, Ontario, Canada.

Noble, R.W. and Gibson, Q.H. (1970) J. Biol. Chem. 245, 2409-2413.

Ngo, T.T. and Lenhoff, H. (1980) Anal. Biochem. 105, 389-397.

Oberg L.G., Glas, B., Swanson, S.E., Rappe, C. and Paul, K.G. (1990) Arch. Environ. Contam. Toxicol. 19, 930-938.

Ortiz de Montellano, P.R., David, S.K., Ator, M.A., and Tew, D. (1988) Biochem. 27, 5470-5476.

Ortiz de Montellano, P.R. and Grab, L.A. (1987) Biochemistry 26, 5310-5314.

Ortiz de Montellano, P.R. (1987) Accts. Chem. Res. 20, 289-294.

Peake, M.J., Sontrop, M.E. and Fraser, C.G. (1978) Clin. Chem. 24, 2026-2031.

Pelizetti, E., Mentosli, E., Baiocchi, C. and Carlotti, M.E. (1974) Atti Acad. Sci., Torino 108, 729-738.

Porstmann, B., Porstmann, T. and Nugel, E. (1981) J. Clin. Chem. Clin. Biochem. 19, 435-439.

Poulos, T.L. (1987) Adv. Inorg. Biochem. 7, 1-36.

Putz, G.R., Barret, D.A. and Witte, D.L. (1976) Amer. J. Med. Tech. 42, 13-18.

Purcell, G.V., Behenna, D.B. and Walsh, P.R. (1978) Clin. Chem. 24, 1015.

Ryu, K. and Dordick, J.S. (1992) Biochemistry 31, 2588-2598.

Sakurada, J., Takahashi, S. and Hosoya, T. (1986) J. Biol. Chem. 261, 9657-9662.

Saunders, B.C., Holmes-Siedle, A.G. and Stark, B.P. (1964) "Peroxidase". Butterworths and Co. (Canada) Ltd., Toronto.

- Sawahata, T. and Neal, R.A. (1982) Biochem. Biophys. Res. Comm. 109, 988-994.
- Segel, I.H. (1976) Enzyme Kinetics. Wiley and Sons, Inc. NY.
- Sharpe, P. (1972) Clin. Chem. 40, 115-120.
- Sharpe, P., Riley, C., Cook, J.G.H. and Pink, P.J.F. (1972) Clin. Chem. 36, 93-98.
- Schuler, R.H. Neta, P., Zemel, H. and Fessenden, R.W. (1976) J. Am. Chem. Soc. 98, 3825.
- Shiga, T. and Imaizumi, K. (1973) Arch. Biochem. Biophys. 154, 540-547.
- Smith, A.M., Morrison, W.L. and Milham, P.J. (1982) Biochem. 21, 4414-4419.
- Trinder, P. (1969) Ann. Clin. Biochem. 6, 24.
- Tripathi, G.N.R. and Schuler, R.H. (1982) Chem. Phys. Lett. 88, 253-255.
- Tripathi, G.N.R. and Schuler, R.H. (1984) J. Chem. Phys. 81, 113-121.
- Walsh, C. (1979) Enzymatic Reaction Mechanisms. W.H Freeman and Co. San Francisco.
- Yamazaki, I., Mason, H.S. and Piette, L. (1960) J. of Biol. Chem. 235, 2444-2449.
- Yamazaki, I. and Yokota, K. (1973) Molecular and Cellular Biochem. 2, 39-52.
- Ye, Mingyu and Schuler, R.H. (1989) J. Phys. Chem. 93, 1898-1902.

APPENDIX A

CALCULATION OF HRP CONCENTRATION FROM SORET (404nm) ABSORBANCE

The Soret band is an intense absorbance maximum ($\epsilon \approx 10^5$) observed during uv./visible spectrophotometric examination of hemoproteins containing a Protoporphyrin IX prosthetic group (Figure A-1). It appears toward the far uv. (400nm) and it is characteristic of macrocyclic conjugation due to allowed $\pi-\pi^*$ electron transitions in a location remote from the iron ion (Saunders et. al., 1964; Brill, 1977; Smith, 1975). In a heterogeneous solution of proteins, the absorbance at this wavelength can be used as a direct indication of heme protein concentration, as long as the extinction coefficient is known. This circumvents using the absorption maximum, characteristic to all proteins, located in the uv. around 276 nm, which is the result of electron density associated with aromatic amino acid residues such as tyrosine and phenylalanine. To determine the concentration of HRP stock solutions, the following calculation was performed ($\epsilon_{404} = 102,000 \text{ M}^{-1}/\text{cm}$; Everse et. al., 1990)

Absorbance 404nm \div 102,000 M^l/cm = molar concentration
(mol/L)

To determine the concentration in mg/mL, the molar concentration was multiplied by the molecular weight of HRP (40,000 g/mole):

molar concentration HRP (mol/L) \times 40,000 g/mole = g HRP/L

Concentration in mg/mL:

g/L \times 1000 mg/g \times 1 L/1000mL = mg HRP/mL

The above calculations are based on the assumption that HRP is the only hemoprotein present in the sample.

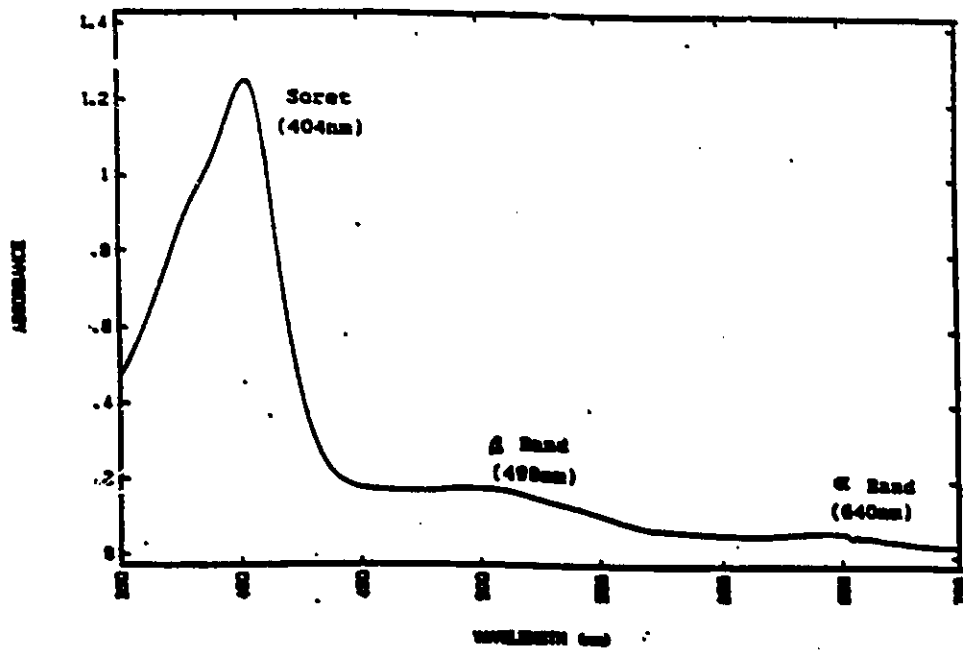


Figure A1 Visible spectrum of native HRP

APPENDIX B

HDCBS/AAP ACTIVITY ASSAY AND CALCULATION OF SPECIFIC ACTIVITY

B1. Activity Assay:

In a typical catalytic cycle, HRP is oxidized and consequently activated by a molecule of H_2O_2 . In this activated state, HRP can readily oxidize a variety of electron donors. 4-aminoantipyrine (AAP) is an example of a donor substrate which has been shown to be oxidized by HRP intermediates to cationic electrophiles (Griffin, 1977; Griffin and Ting, 1978; Porstman et. al., 1981). Once generated, these electrophiles can react with electron-rich aromatic compounds to produce a chromogen (Griffin, 1977; Griffin and Ting, 1978). The rate of production of the electrophilic species from the electron donor is dependent on the donor itself and HRP, but is independent of the aromatic compound. Consequently, enzyme turnover of substrates into final dye product is dependent only on the concentration and structure of the electron donor.

AAP is an excellent electron donor substrate of HRP and has been used with phenol as the aromatic partner for activity determinations (Conyers et. al., 1991; Gallati, 1977; Griffin, 1977; Porstmann et. al., 1981). HDCBS has been found by other workers in this laboratory (Artiss et. al., 1979; 1981) to

work effectively as the aromatic compound. Non-enzymatic coupling occurs with the AAP cation radical through displacement of the chlorine atom para to the hydroxyl group (Emerson, 1943; Artiss et. al., 1981), yielding a stable and soluble product, which is probably a quinonimine (Abs. maximum 510nm) by analogy to the one proposed to be generated in the reaction of AAP with phenol (Figure B1-1) (Emerson, 1943; Gallati, 1977). The initial velocity of this HRP catalyzed reaction is linear (at saturating concentrations of all substrates and low enzyme concentrations) and readily measured over a period of 30 to 60 seconds.

Using the nomenclature of Cleland (1963), HRP has been characterized as exhibiting a Ter Bi Ping Pong (Porstmann et. al., 1981; Childs and Bardsley, 1975) (Figure B1-2) or a Peroxidase Ping Pong (Everse et. al., 1990) reaction mechanism in which H_2O_2 is the first substrate to be reduced, producing H_2O which is subsequently released from the active site. Griffin (1977) has suggested that Cpds. I and II of HRP are able to oxidize AAP in a 2 electron transfer reaction generating an aminoantipyrene cation free-radical (Figure B1-3). This free-radical reacts with a molecule of HDCBS while another AAP molecule enters the active site to be similarly oxidized. Griffin and Ting (1978) suggested that the aminoantipyrene cation radical may undergo further enzymatic oxidation to yield an iminium cation, which is then hydrolyzed into an amine and formaldehyde, but that other

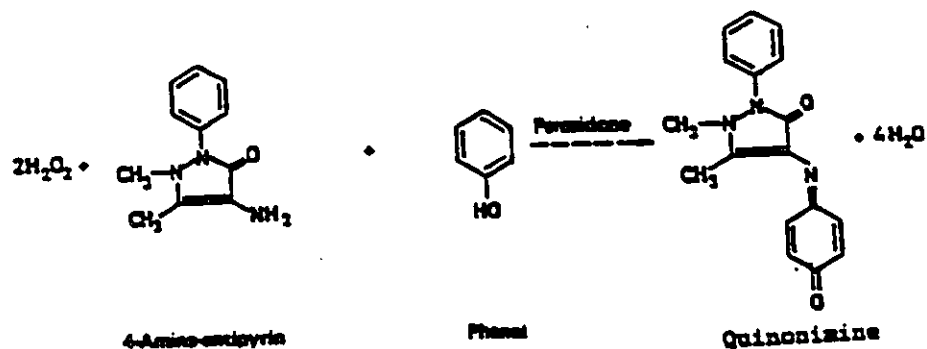


Figure B1-1 Reaction scheme of AAP and Phenol in the presence of HRP and H_2O_2 (Gallati, 1977).

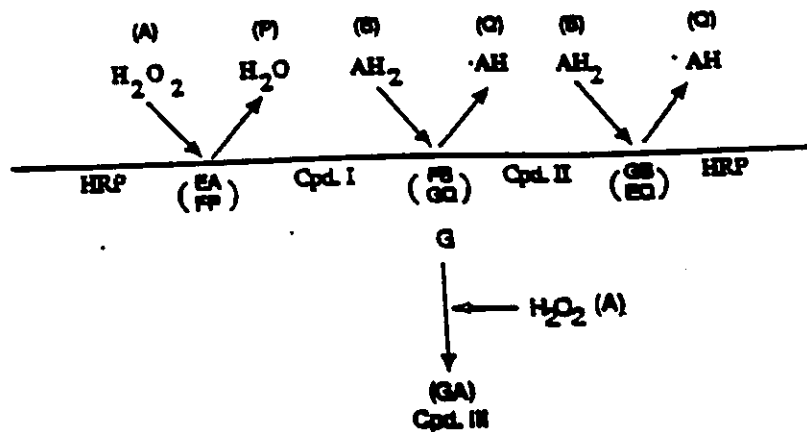


Figure B1-2 Peroxidase ping-pong mechanism (Everse et al., 1990; Childs and Bardsley, 1975).

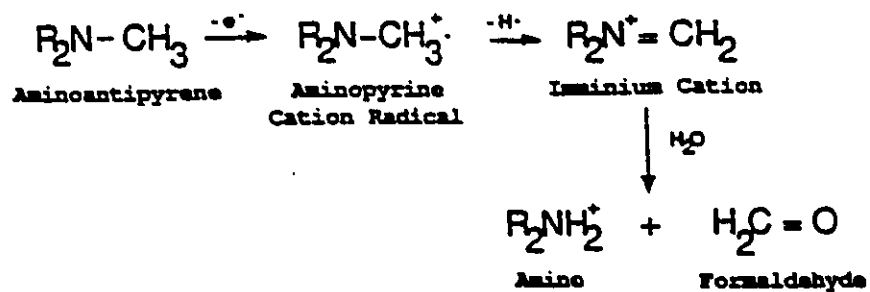


Figure B1-3 Reaction of AAP with oxidised HRP with Compounds I and II (Griffin and Ting, 1978).

routes of oxidation were likely to be more prevalent. However, in contrast to Griffin and Ting's reaction scheme, Gallati (1977) suggests that the Trinder reagent, AAP, is not recognized as a substrate by the enzyme in the coupled reaction with phenol. Rather, he reports that phenol is enzymatically oxidized to a quinone, which then undergoes nucleophilic attack by the nitrogen atom of the amino group on the AAP molecule to form a Schiff base, producing the quinonimine product. A variety of phenolic derivatives can also undergo enzymatic oxidation as the donor substrate (Saunders et al., 1964) and the question arose as to which substrate, AAP or phenol/phenolic derivative, was the first to react with the enzyme. However, unpublished work performed in this laboratory (Baynton, 1988), in which solutions containing H_2O_2 /AAP and H_2O_2 /HDCBS were passed through Whatman filter paper, to which HRP had been chemically immobilised, into solutions containing non-enzymatically exposed HDCBS and AAP, respectively, suggested that the reaction scheme proposed by Griffin and Ting is the chromogen forming reaction and that HDCBS is not a direct substrate for the enzyme, despite its phenolic nature. Solutions containing the H_2O_2 /AAP couple, passed through the enzyme-containing filters into a solution of HDCBS produced the typical pink colour observed in the activity assay (λ max = 510 nm). No colour formation was observed when the solution containing the H_2O_2 /HDCBS substrate pair was passed through an enzyme-immobilised disk into the

solution containing AAP.

The AAP/HDCBS chromogenic system has proven to be most effective in determining HRP activity and sensitivity correlates well to literature values obtained employing similar as well as other popular, well-studied chromogenic systems (Purcell et al., 1978; Putz et al., 1976; Peake et al., 1978; Conyers and Kidwell, 1991).

Assay Recipe: To a 1.5mL semi-micro cuvette measure the following:

500 μ L 18.0 mM (4.8 mg/mL) HDCBS

250 μ L 9.6 mM (1.95mg/mL) AAP

50-100 μ L 0.1 M NaPP, pH 7.4

50-100 μ L HRP sample

Initiate the reaction by the addition of 100 μ L of 1.0mM H₂O₂ (prepared from a 10-fold dilution of a 10.0mM H₂O₂: 56 μ L of 60% (v/v) H₂O₂ stock solution made up to 100mL in distilled water). Monitor the reaction at 510nm for 30 to 60 seconds (Figure B1-4).

Reaction Blank: all of above components with 100 μ L water in place of H₂O₂.

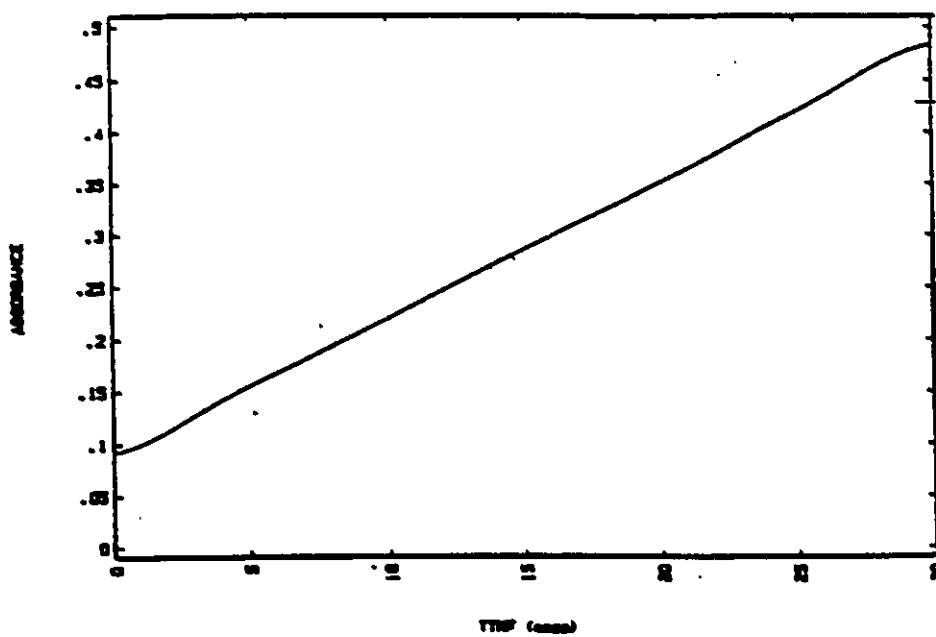


Figure B1-4 Increase in absorbance at 510nm vs. time (HDCBS/AAP activity assay).

B2. Specific Activity Calculation (U/mg):

The initial rate of the reaction is determined from the average slope over a range of data ($\Delta\text{Abs. } 510\text{nm/min.}$). Using this value, the specific activity (the number of μmoles substrate consumed/product produced per mg of enzyme) is calculated using an extinction coefficient of $25,000 \text{ M}^{-1}/\text{cm}$ (based on H_2O_2) as follows:

$$\text{slope } (\Delta\text{Abs. } 510\text{nm/min.}) \div 25,000 \text{ M}^{-1}/\text{cm} = \text{M/minute}$$

Reaction volume = 1.0mL. Therefore:

$$\text{M/minute} \times 0.001 \text{ L} \times 10^{-6} \mu\text{moles/mole} = \mu\text{moles/minute or}$$

U

$$\text{U} \div \text{mg HRP (based on heme absorbance)} = \text{U/mg}$$

APPENDIX C
PHENOL/AAP ACTIVITY ASSAY REAGENT

This chromogenic system has been investigated by other researchers for its usefulness in the determination of HRP activity (Porstmann et al, 1981; Gallati, 1977; see Appendix B for proposed reaction scheme). Generally, it is less sensitive (lower abs. 510 values vs. time and extinction coefficient: $6,000\text{M}^{-1}/\text{cm}$) than other popular chromogenic systems used to determine HRP activity. But for our purposes, it was ideal. The saturating phenol concentrations present in the reagent countered any possible interferences by phenol arriving in the samples taken from incubation mixtures. As observed with the HDCBS/AAP activity assay, linear plots of abs. 510nm vs. time are obtained for the first 30 to 60 seconds of the reaction under conditions of saturating substrate and limiting enzyme concentrations. The slope (rate: Abs. 510nm/min.) is calculated over a range of averaged data points, and values obtained for incubation samples could be directly compared to rates obtained for control samples containing enzyme alone.

To prepare the reagent, measure into a 25-30mL graduated cylinder:

3.4 mg AAP (0.171 mg/mL; [final] = 0.84mM)
18.82 mg phenol (crystals) (0.904 mg/mL; [final] =
10.0mM)
800 μ L 10.0 mM H₂O₂ (0.034% (v/v); [final] = 0.4mM or
0.0014%)
1.6 mL NaPP, pH 7.4

Make up to 20mL with distilled water. Measure into a 1.5 mL semi-micro cuvette enough reagent so that HRP arriving from the sample has a [final] (in a 1.0mL reaction volume) of approximately 1-50 nM (1-50 pmoles) (ie. 800 μ L reagent + 200 μ L sample containing 100nM HRP). Follow the colour development at 510nm.

Blank: above volume of reagent + volume of NaPP, pH 7.4 equal to the sample volume.

An extinction coefficient was determined for this activity assay (based on H₂O₂) to be 6,000M⁻¹/cm (Figure C1; see Methods section 2.2.4.2).

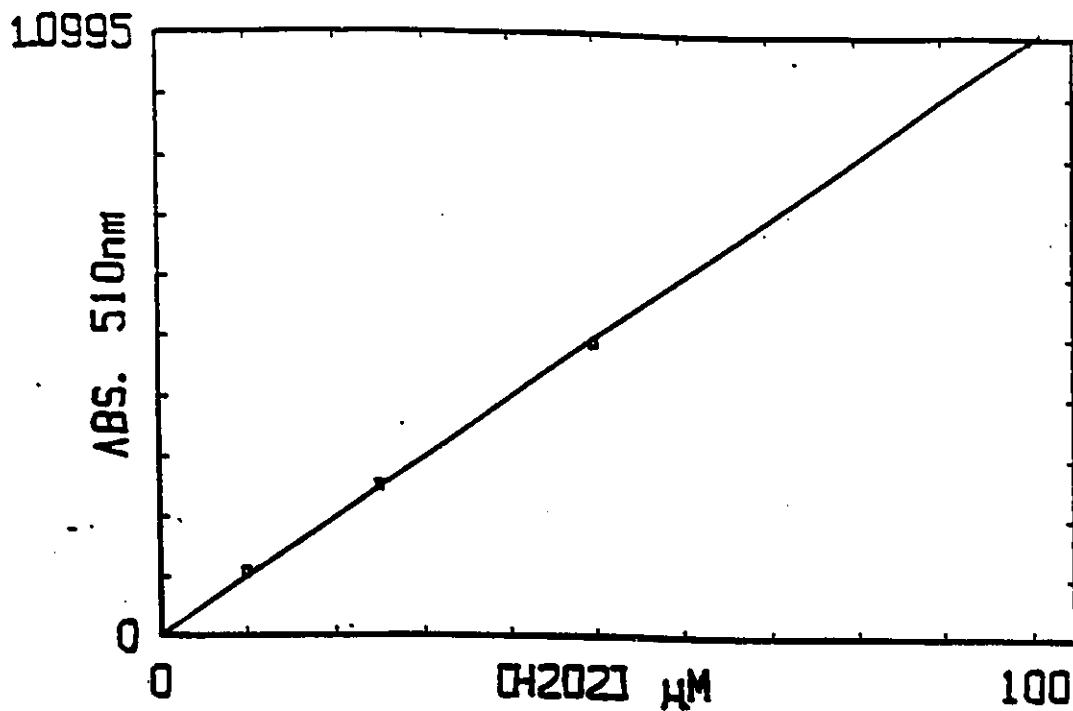


Figure C1 Standard curve of absorbance at 510nm vs. hydrogen peroxide concentration: determination of extinction coefficient.

APPENDIX D

CALCULATION OF PHENOL CONCENTRATION FROM UV. SPECTRUM

Molar Concentration:

$$\frac{\text{Abs. } 272\text{nm}}{1,300 \text{ M}^{-1}/\text{cm}} \times 1000\text{mmole/mole} = \text{mM [phenol]}$$

(* determined from workers in this laboratory)

Concentration in mg/mL:

$$\text{M [phenol]} \times \text{MW. phenol (94.11 g/mol)}$$

(Figure D1: u.v. absorbance spectrum of phenol solution)

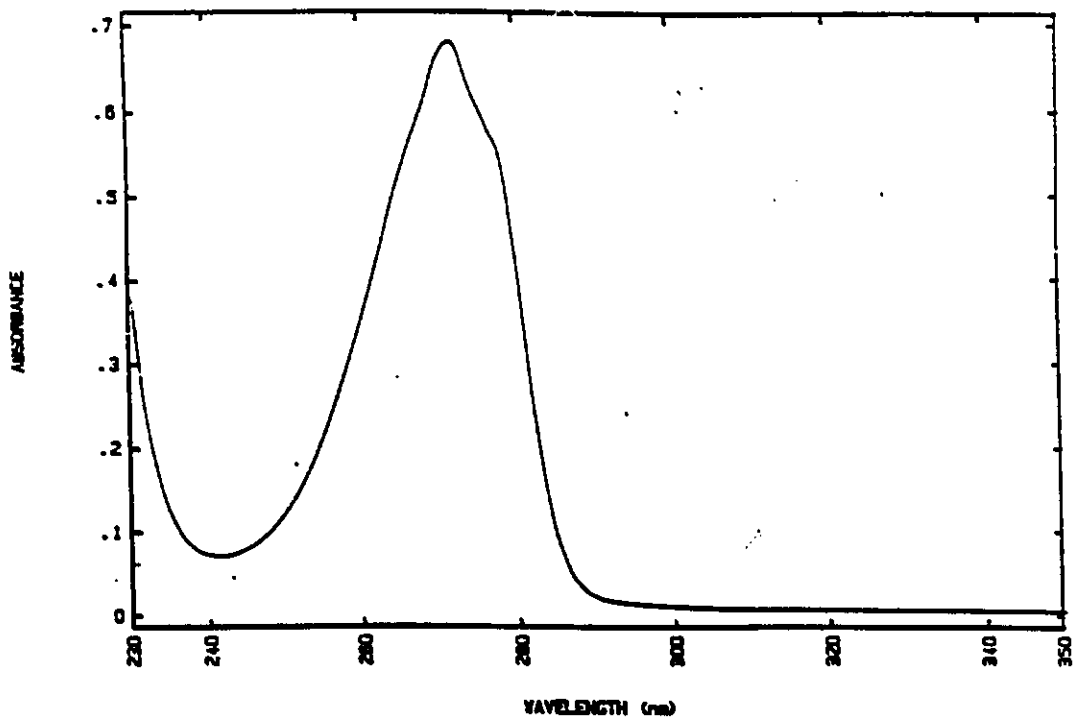


Figure D1 UV. absorption spectrum of 0.5mM solution of phenol (in 0.1M phosphate

APPENDIX E

HYDROGEN PEROXIDE ASSAY AND CONCENTRATION DETERMINATION

E1. Colourimetric Reagent Recipe:

This reagent will detect H_2O_2 concentrations ranging from $100\mu M$ to $1.0mM$. To a $50mL$ graduated cylinder, measure:

20.25 mg AAP ($4.1mg/mL$; [final] = $2.0mM$)

1.39 mL $0.375M$ phenol stock ($0.941mg/mL$; [final] = $10mM$)

1.09 mL $2.3\mu L$ BM. HRP ($0.092 mg/mL$; [final] = $50nM$)

Make up to $50mL$ with NaPP, pH 7.4. Measure $800\mu L$ of reagent into $1.5mL$ semi-micro cuvette. To this, add $200\mu L$ sample.

Standard H_2O_2 Sample: $800\mu L$ reagent + $200\mu L$ of stock H_2O_2 representing the final concentration of H_2O_2 present in the sample at $t = 0$ seconds.

Blank: $800\mu L$ reagent + $200\mu L$ water.

E2. Calculation of H₂O₂ Concentration:

$$\frac{\text{Abs. 510nm sample}}{\text{Abs. 510nm H}_2\text{O}_2 \text{ standard}} \times [\text{H}_2\text{O}_2] \text{ standard} = [\text{sample}]$$

APPENDIX F

SAMPLE CALCULATIONS OF SPECIFIC ACTIVITY AND k_{cat}

(HRP concentrations are based on the heme absorption at 404nm, as shown in Appendix A).

1. Specific Activity:

$$\frac{\text{A.U./min.}}{25,000 \text{ M}^{-1}} \times \text{volume of activity assay} = \text{moles/min.}$$

$$\text{moles/min.} \times 1 \times 10^{-6} \text{ } \mu\text{moles/mole} = \mu\text{moles/min.} = \text{U}$$

Amount of HRP in sample: mg based on heme concentration:

$$\text{Specific Activity} = \text{U/mg HRP in sample}$$

$$\text{eg. } \frac{0.7411 \text{ min}^{-1}}{25,000 \text{ M}^{-1}} \times 0.001 \text{ L} = 2.9 \times 10^{-8} \text{ moles/min.}$$

$$2.9 \times 10^{-8} \text{ moles/min.} \times (1 \times 10^{-6} \text{ } \mu\text{moles/mole}) = 29 \text{ U}$$

$$\text{Specific Activity: } \frac{29 \text{ U}}{0.2 \text{ mg}} = \underline{145 \text{ U/mg HRP}}$$

2. k_{cat} :

$\text{U}/\mu\text{moles HRP}$ (based on heme concentration) = amount of substrate molecule turned over/min.

$$\text{eg. } \frac{29 \text{ U}}{5 \times 10^{-3} \text{ } \mu\text{moles}} = \underline{5,800 \text{ min}^{-1}}$$

APPENDIX G

‡ remaining activity vs. time data from H₂O₂-mediated time-dependent inactivation of HRP, fit to curves representing double-exponential decay described by the equation:

$$y = A_1 \exp -k_1 t + A_2 \exp -k_2 t$$

and tables of data evaluated using single-exponential decay equations used to evaluate the fast and slow inactivation phases individually. Data analyses were performed by the enzyme kinetics program Enzfitter™. Tables of experimental values and values calculated by Enzfitter™ are presented along with plots illustrating the fit of the data to the calculated double exponential decay equation. Tables of determined A₁, A₂, -k₁ and -k₂ of values are also given.

<u>Time (sec.)</u>	<u>% Remaining (Observed)</u>	<u>Calculated</u>
0	100	99.73
5	96.0	97.28
10	96.5	95.04
20	91.0	91.11
30	87.2	87.81
50	83.0	82.70
300	69.0	69.02
600	66.0	65.99

Table G1 Observed and calculated % remaining activity data vs. time used for double-exponential decay evaluation (100 μ M H₂O₂).

Data evaluated for rapid phase:

<u>Time (sec.)</u>	<u>% Remaining (Observed)</u>	<u>Calculated</u>
0	100	99.00
5	96.0	97.15
10	96.5	95.34
20	91.0	91.81
30	87.2	88.41
50	83.0	81.99

Data evaluated for slow phase:

<u>Time (sec.)</u>	<u>% Remaining (Observed)</u>	<u>Calculated</u>
50	83.0	76.71
300	69.0	74.34
600	66.0	71.59
900	71.0	68.94
1200	69.0	66.40

Table G2 Observed and calculated % remaining activity data vs. time used for single-exponential decay evaluation (100 μ M H₂O₂).

Exponential Decay Process	Initial Value (A1)	Initial Value (A2)	k_1 Fast Phase ($\times 10^{-2}$)	k_2 Slow Phase ($\times 10^{-4}$)
double	27.80 ± 2.607	71.93 ± 2.600	1.892 ± 0.267	1.437 ± 0.758
single	99.00 ± 0.832	77.19 ± 5.010	0.377 ± 0.036	1.256 ± 0.985

Table G3 Values of A_1 , A_2 , $-k_1$ and $-k_2$ and their standard error determined for double- and single-exponential decay processes ($100\mu\text{M H}_2\text{O}_2$).

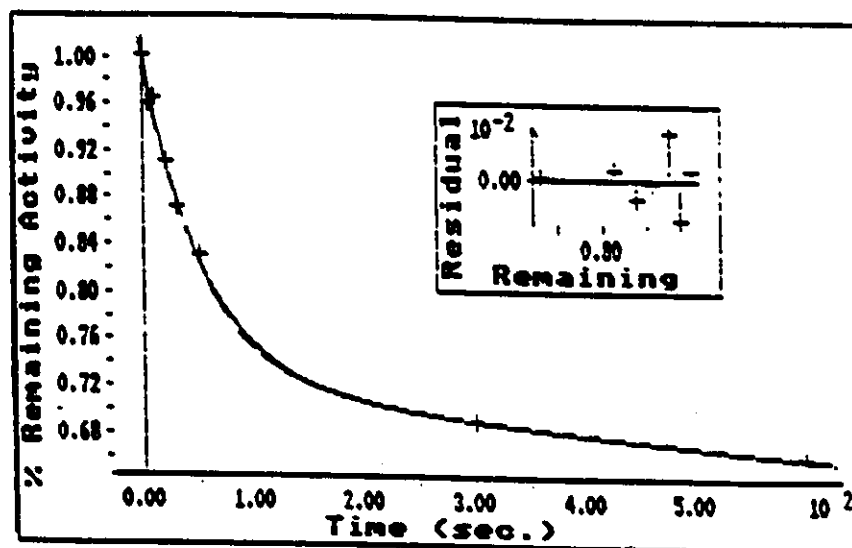


Figure G1 Plot of observed data fit to calculated double-exponential decay curve ($100\mu\text{M H}_2\text{O}_2$). (Inset: plot of % residual vs. % remaining for observed values).

<u>Time (sec.)</u>	<u>% Remaining (Observed)</u>	<u>Calculated</u>
0	100	100.8
5	93.1	95.71
10	89.5	91.08
20	89.7	83.00
30	78.9	76.30
50	66.4	66.13
300	45.6	43.56
600	42.2	42.89

Table G4 Observed and calculated % remaining activity data vs. time used for double-exponential decay evaluation ($500\mu\text{M H}_2\text{O}_2$).

Data evaluated for rapid phase:

<u>Time (sec.)</u>	<u>% Remaining (Observed)</u>	<u>Calculated</u>
0	100	98.98
5	93.1	95.28
10	89.5	91.72
20	89.7	84.99
30	79.8	78.76
50	66.0	67.63

Data evaluated for slow phase:

<u>Time (sec.)</u>	<u>% Remaining (Observed)</u>	<u>Calculated</u>
300	45.6	46.09
600	42.2	41.92
900	39.3	38.13
1200	33.7	34.67

Table G5 Observed and calculated % remaining activity data vs. time used for single-exponential decay evaluation ($500\mu\text{M H}_2\text{O}_2$).

Exponential Decay Process	Initial Value (A1)	Initial Value (A2)	k_1 Fast Phase ($\times 10^{-2}$)	k_2 Slow Phase ($\times 10^{-4}$)
double	56.99 ± 10.445	43.81 ± 10.504	1.869 ± 0.508	0.355 ± 5.103
single	98.97 ± 1.960	50.68 ± 1.650	0.762 ± 0.092	3.163 ± 0.431

Table G6 Values of A1, A2, $-k_1$, and $-k_2$, and their standard error determined for double- and single-exponential decay processes ($500\mu\text{M H}_2\text{O}_2$).

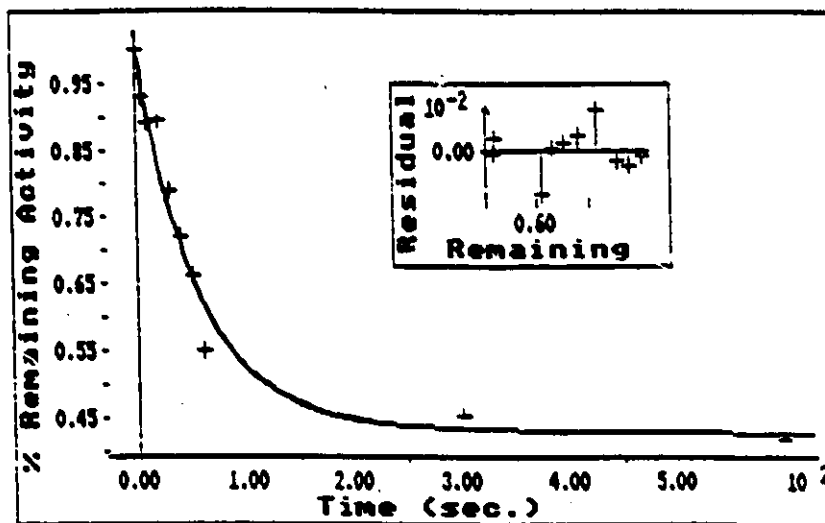


Figure G2 Plot of observed data fit to calculated double-exponential decay curve ($500\mu\text{M H}_2\text{O}_2$). (Inset: plot of % residual vs. % remaining for observed values).

<u>Time (sec.)</u>	<u>% Remaining (Observed)</u>	<u>Calculated</u>
0	100	95.62
5	77.9	84.55
10	75.3	75.35
20	62.3	61.39
30	53.6	51.76
50	40.9	40.53
300	29.7	29.64
600	28.7	28.69

Table G7 Observed and calculated % remaining activity data vs. time used for double-exponential decay evaluation (750 μ M H₂O₂).

Data evaluated for rapid phase:

<u>Time (sec.)</u>	<u>% Remaining (Observed)</u>	<u>Calculated</u>
0	100	93.08
5	77.9	84.70
10	75.3	77.07
20	62.3	63.82
30	53.6	52.84
40	46.6	43.76

Data evaluated for slow phase:

<u>Time (sec.)</u>	<u>% Remaining (Observed)</u>	<u>Calculated</u>
50	40.2	35.75
300	29.7	33.93
600	29.0	31.86
900	30.0	29.92
1200	30.7	28.10

Table G8 Observed and calculated % remaining activity data vs. time used for single-exponential decay evaluation (750 μ M H₂O₂).

Exponential Decay Process	Initial Value (A1)	Initial Value (A2)	k_1 Fast Phase ($\times 10^{-2}$)	k_2 Slow Phase ($\times 10^{-4}$)
double	64.99 ± 5.597	30.62 ± 5.780	3.730 ± 0.747	1.090 ± 4.319
single	93.07 ± 3.789	36.12 ± 3.528	1.887 ± 0.252	2.093 ± 1.448

Table G9 Values of A_1 , A_2 , $-k_1$, and $-k_2$ and their standard error determined for double- and single-exponential decay processes ($750\mu\text{M H}_2\text{O}_2$).

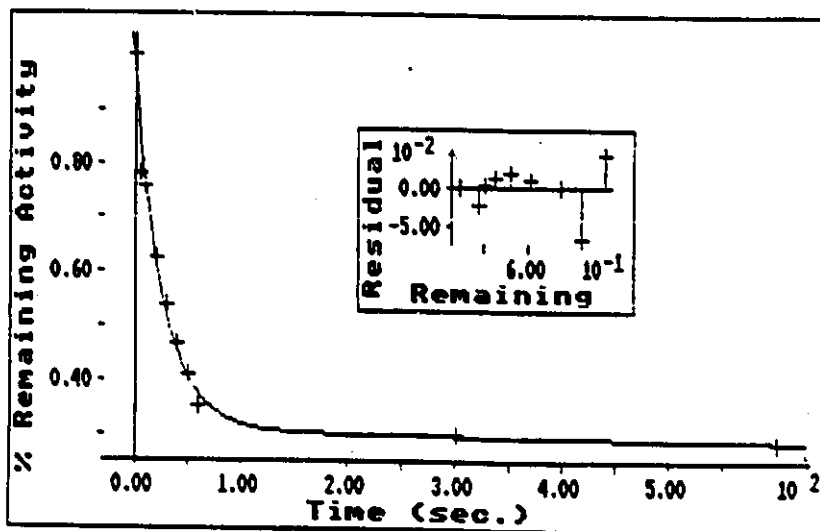


Figure G3 Plot of observed data fit to calculated double-exponential decay curve ($750\mu\text{M H}_2\text{O}_2$). (Inset: plot of % residual vs. % remaining for observed values).

<u>Time (sec.)</u>	<u>% Remaining (Observed)</u>	<u>Calculated</u>
0	100	98.24
5	83.6	85.21
10	73.3	74.83
20	60.0	59.96
30	51.2	50.54
50	40.1	40.78
300	34.2	35.10
600	36.7	36.39

Table G10 Observed and calculated % remaining activity data vs. time used for double-exponential decay evaluation (1.0mM H₂O₂).

Data evaluated for rapid phase:

<u>Time (sec.)</u>	<u>% Remaining (Observed)</u>	<u>Calculated</u>
0	100	93.85
5	83.6	85.35
10	73.3	77.63
20	60.0	64.21
30	51.2	53.11
40	47.2	43.93
50	40.1	36.34

Data evaluated for slow phase:

<u>Time (sec.)</u>	<u>% Remaining (Observed)</u>	<u>Calculated</u>
50	40.1	37.19
60	37.6	37.20
300	34.2	37.59
600	36.7	38.08
900	38.9	38.58
1200	40.2	39.08

Table G11 Observed and calculated % remaining activity data vs. time used for single-exponential decay evaluation (1.0mM H₂O₂).

Exponential Decay Process	Initial Value (A1)	Initial Value (A2)	k_1 Fast Phase ($\times 10^{-2}$)	k_2 Slow Phase ($\times 10^{-4}$)
double	64.31 ± 2.225	33.93 ± 2.197	4.536 ± 0.407	-1.126 ± 1.504
single	93.85 ± 3.243	37.11 ± 1.546	1.897 ± 0.184	-4.324 ± 6.079

Table G12 Values of A1, A2, $-k_1$, and $-k_2$, and their standard error determined for double- and single-exponential decay processes (1.0mM H_2O_2).

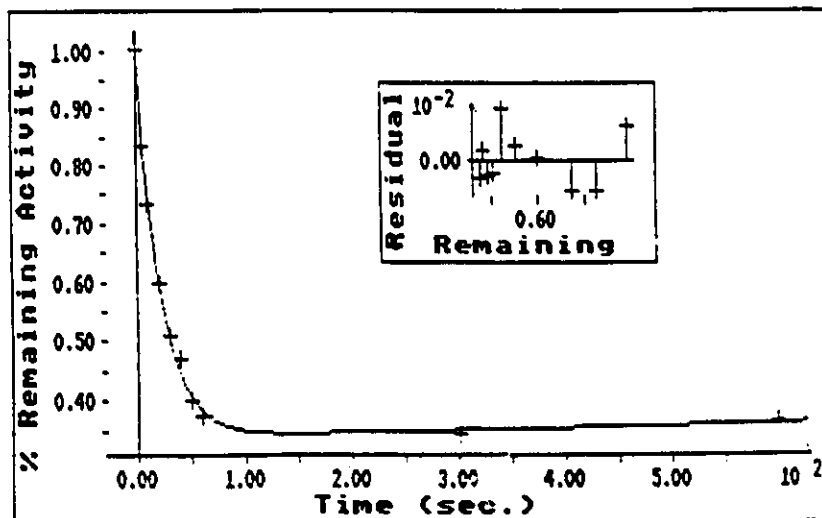


Figure G4 Plot of observed data fit to calculated double-exponential decay curve (1.0mM H_2O_2). (Inset: plot of % residual vs. % remaining for observed values).

<u>Time (sec.)</u>	<u>% Remaining (Observed)</u>	<u>Calculated</u>
0	100	96.31
5	66.8	73.12
10	56.4	57.02
20	40.7	37.80
30	31.0	28.35
50	23.0	21.32
300	14.3	15.56
600	13.9	12.76

Table G13 Observed and calculated % remaining activity data vs. time used for double-exponential decay evaluation (5.0mM H₂O₂).

Data evaluated for rapid phase:

<u>Time (sec.)</u>	<u>% Remaining (Observed)</u>	<u>Calculated</u>
0	100	89.57
5	66.8	74.93
10	56.4	62.69
20	40.7	43.87
30	31.0	30.70
40	25.2	21.49
50	23.0	15.04

Data evaluated for slow phase:

<u>Time (sec.)</u>	<u>% Remaining (Observed)</u>	<u>Calculated</u>
50	23.0	18.43
60	15.2	18.35
300	14.3	16.44
600	13.9	14.33
900	13.7	12.50

Table G14 Observed and calculated % remaining activity data vs. time used for single-exponential decay evaluation (5.0mM H₂O₂).

Exponential Decay Process	Initial Value (A1)	Initial Value (A2)	k_1 Fast Phase ($\times 10^{-2}$)	k_2 Slow Phase ($\times 10^{-4}$)
double	76.36 ± 4.614	19.95 ± 3.684	7.186 ± 1.148	7.441 ± 6.477
single	89.57 ± 5.995	18.61 ± 2.568	3.569 ± 0.516	4.575 ± 3.263

Table G15 Values of A1, A2, $-k_1$, and $-k_2$, and their standard error determined for double- and single-exponential decay processes (5.0mM H_2O_2).

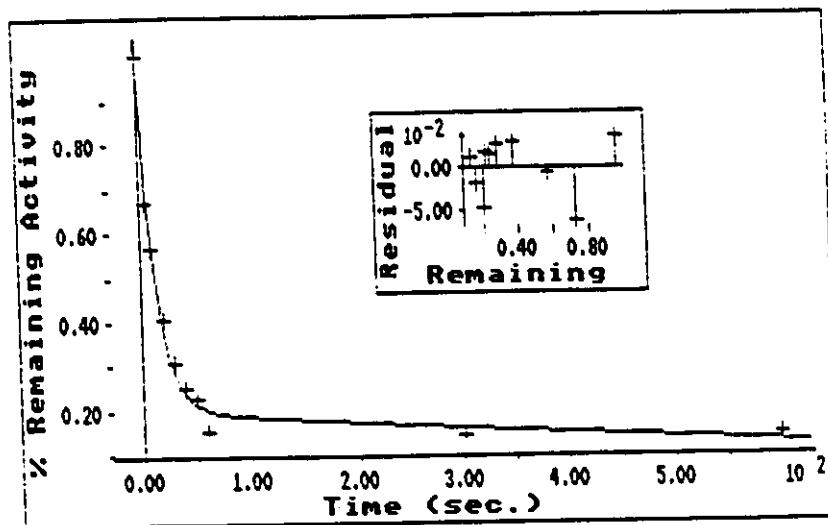


Figure G5 Plot of observed data fit to calculated double-exponential decay curve (5.0mM H_2O_2). (Inset: plot of % residual vs. % remaining for observed values).

<u>Time (sec.)</u>	<u>% Remaining (Observed)</u>	<u>Calculated</u>
0	100	100
5	23.7	23.67
10	20.2	20.58
20	18.0	19.30
30	20.7	18.18
60	14.3	15.18

Table G16 Observed and calculated % remaining activity data vs. time used for double-exponential decay evaluation (10.0mM H₂O₂).

Data evaluated for rapid phase:

<u>Time (sec.)</u>	<u>% Remaining (Observed)</u>	<u>Calculated</u>
0	100	98.92
5	23.7	30.52
10	20.1	9.413

Data evaluated for slow phase:

<u>Time (sec.)</u>	<u>% Remaining (Observed)</u>	<u>Calculated</u>
10	20.1	17.08
20	18.0	18.35
30	13.8	16.65
60	14.3	16.54
300	15.4	14.19
600	11.5	11.71

Table G17 Observed and calculated % remaining activity data vs. time used for single-exponential decay evaluation (10.0mM H₂O₂).

Exponential Decay Process	Initial Value (A1)	Initial Value (A2)	k_1 Fast Phase ($\times 10^{-2}$)	k_2 Slow Phase ($\times 10^{-4}$)
double	78.24 ± 3.192	21.76 ± 2.395	68.42 ± 22.86	59.94 ± 34.57
single	98.92 ± 12.71	17.19 ± 1.362	23.52 ± 7.245	6.404 ± 3.660

Table G18 Values of A1, A2, $-k_1$ and $-k_2$ and their standard error determined for double- and single-exponential decay processes (10.0mM H_2O_2).

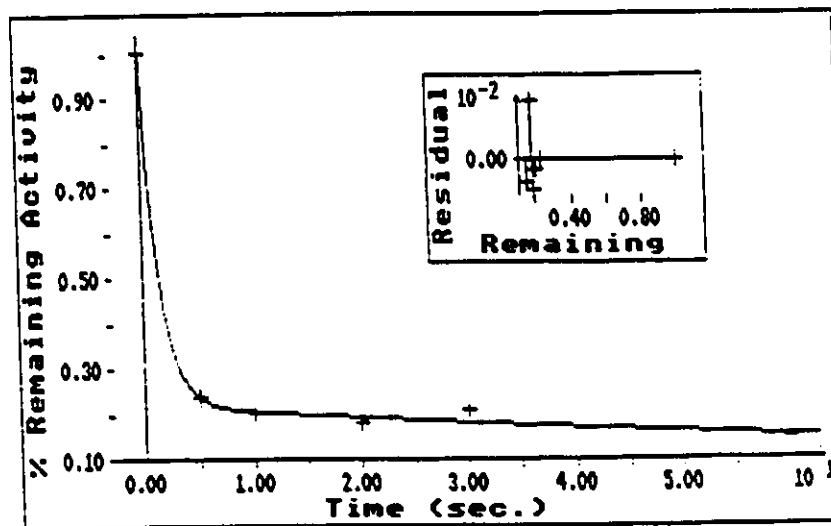


Figure G6 Plot of observed data fit to calculated double-exponential decay curve (10.0mM H_2O_2). (Inset: plot of % residual vs. % remaining for observed values).

<u>Time (sec.)</u>	<u>% Remaining (Observed)</u>	<u>Calculated</u>
0	100	100
5	7.50	7.503
10	7.46	7.092
30	5.90	6.559
60	6.13	5.835

Table G19 Observed and calculated % remaining activity data vs. time used for double-exponential decay evaluation (50.0mM H₂O₂).

Data evaluated for rapid phase:

<u>Time (sec.)</u>	<u>% Remaining (Observed)</u>	<u>Calculated</u>
0	100	99.95
5	7.50	8.657
10	7.46	7.498

Data evaluated for slow phase:

<u>Time (sec.)</u>	<u>% Remaining (Observed)</u>	<u>Calculated</u>
10	7.46	6.874
30	5.90	6.836
50	7.10	6.779
300	6.23	6.214
600	5.60	5.597

Table G20 Observed and calculated % remaining activity data vs. time used for single-exponential decay evaluation (50.0mM H₂O₂).

Exponential Decay Process	Initial Value (A1)	Initial Value (A2)	k_1 Fast Phase ($\times 10^{-2}$)	k_2 Slow Phase ($\times 10^{-4}$)
double	92.63 ± 1.259	7.373 ± 0.9631	116.60 ± 81.93	39.60 ± 36.07
single	99.95 ± 6.809	6.898 ± 0.3993	489.26 ± 156.31	3.483 ± 2.168

Table G21 Values of A1, A2, $-k_1$ and $-k_2$ and their standard error determined for double- and single-exponential decay processes (50.0mM H₂O₂).

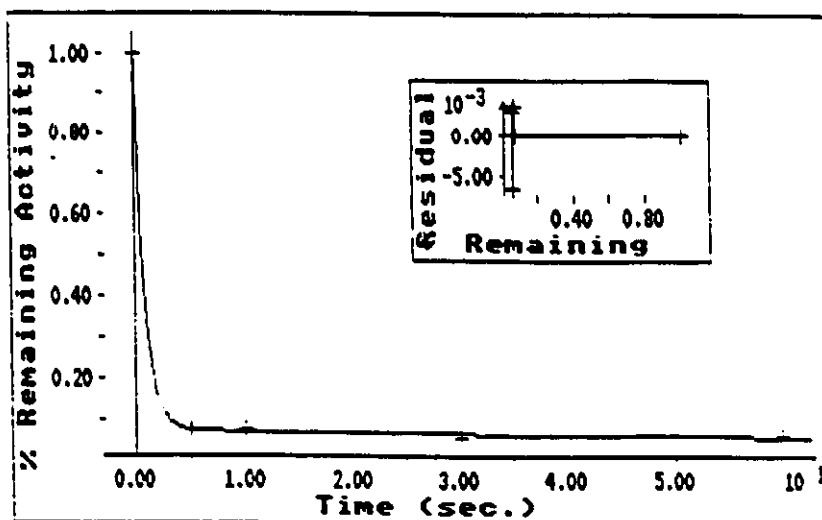


Figure G7 Plot of observed data fit to calculated double-exponential decay curve (50.0mM H₂O₂). (Inset: plot of % residual vs. % remaining for observed values).

APPENDIX H

Tables and figures of changes that occur to the visible absorption spectra of solutions of native HRP when various concentrations of H_2O_2 are added. Changes occurring in the Soret and far red regions were monitored using HRP concentrations of $10\mu M$ and $30\mu M$, respectively, at $25^\circ C$, pH 7.4. Arrows indicate development (\uparrow) or decay (\downarrow) of an absorbance maximum at a particular wavelength, determined by the spectrometer to be a significant peak.

Time (sec.)	Peaks observed (nm)	Absorbance Values
0	404	0.731
5	400	0.370
10	402	0.374
20	402	0.375
30	404	0.378
40	406	0.381
50	406	0.383
60	408	0.388

Table H1 Absorbance changes occurring in the Soret upon exposure to 100 μ M H₂O₂ for one minute ([HRP]=7.5 μ M).

Time (sec.)	Peaks Observed (nm)	Absorbance Values
0	494	0.515
	640	0.187
5	656	0.165
	564	0.317
	650	0.264
10	656	0.261
	560	0.321
	650	0.257
20	656	0.255
	558	0.323
	650	0.251
30	656	0.250
	558	0.323
	656	0.246
40	534	0.314
	558	0.325
	656	0.242
50	532	0.317
	558	0.327
	650	0.243
60	656	0.240
	532	0.318
	558	0.327
	648	0.241
	656	0.238

Table H2 Absorbance changes occurring in the far red region upon exposure of 33 μ M HRP to 100 μ M H₂O₂ for one minute.

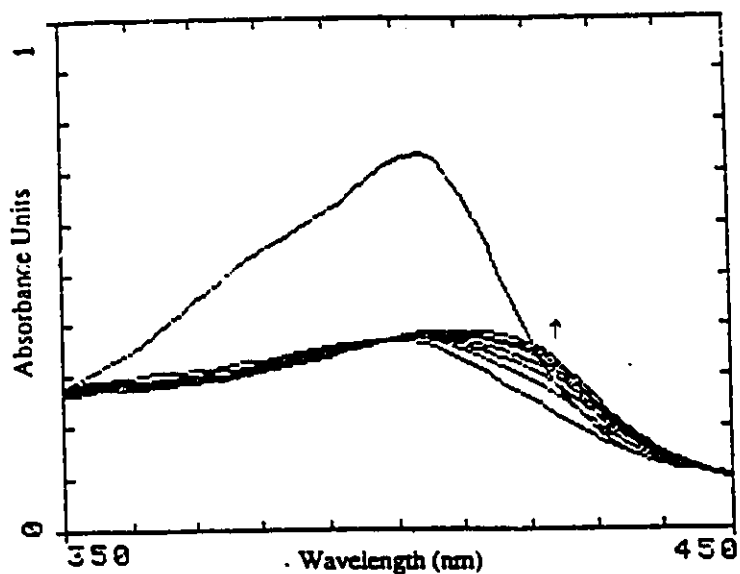


Figure H1 Development of an absorbance maximum at 406nm upon exposure of 7.3 μ M HRP to 100 μ M H₂O₂ over a period of sixty seconds (see Table I-1 for absorbance values).

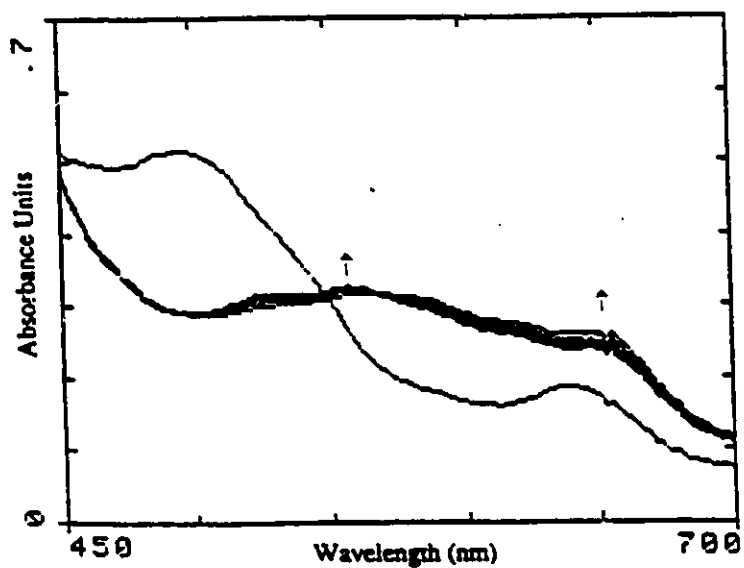


Figure H2 Development of absorbance maxima at 558 and 656nm upon exposure of 33 μ M HRP to 100 μ M H₂O₂ over a period of sixty seconds (see Table I-2 for absorbance values).

Time (sec.)	Peaks observed (nm)	Absorbance Values
0	404	0.732
5	400	0.369
10	406	0.374
20	412	0.388
30	414	0.412
40	416	0.420
50	416	0.435
60	416	0.441

Table H3 Absorbance changes occurring in the Soret upon exposure to 1.0mM H₂O₂ for one minute ([HRP]=7.5μM).

Time (sec.)	Peaks Observed (nm)	Absorbance Values
0	494	0.515
	640	0.187
	656	0.163
5	562	0.320
	650	0.260
	656	0.256
10	558	0.325
	648	0.246
	656	0.244
20	558	0.328
	648	0.239
	656	0.236
30	554	0.329
	656	0.234
40	556	0.331
	656	0.242
50	554	0.332
	656	0.229
60	656	0.240
	554	0.333
	656	0.227

Table H4 Absorbance changes occurring in the far red region upon exposure of 33μM HRP to 1.0mM H₂O₂ for one minute.

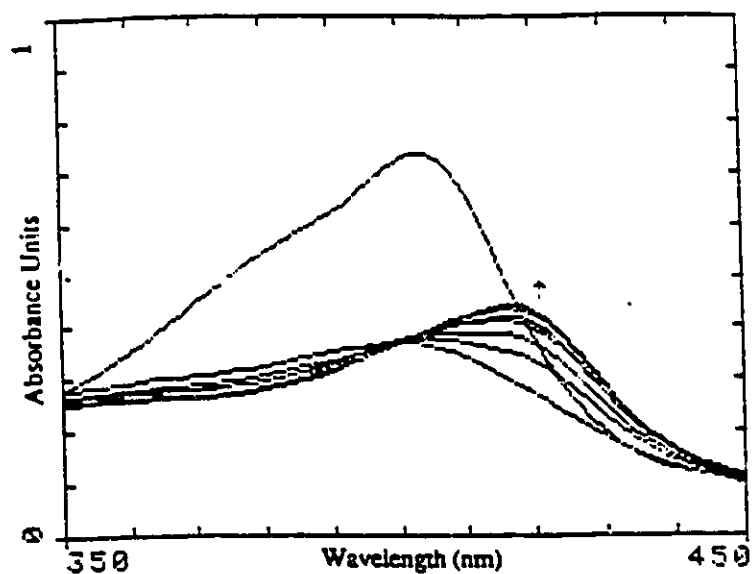


Figure H3 Development of an absorbance maximum at 406nm upon exposure of 7.3 μ M HRP to 1.0mM H₂O₂ over a period of sixty seconds (see Table I-3 for absorbance values).

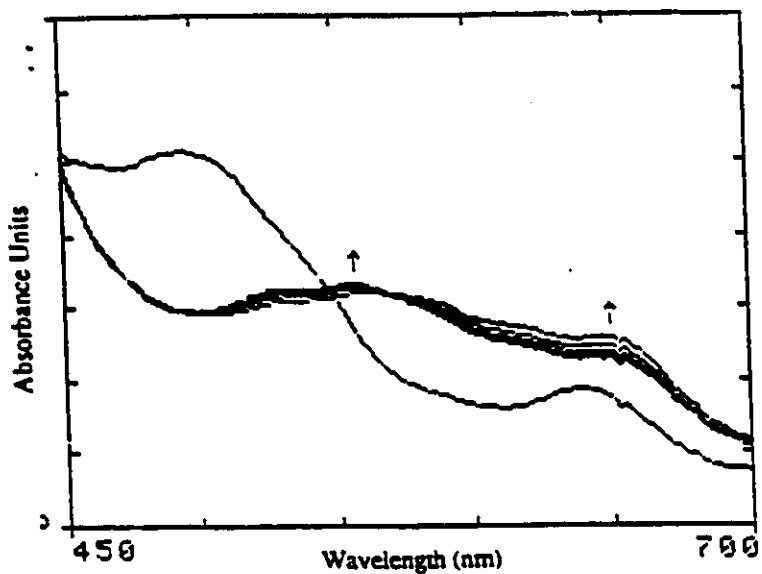


Figure H4 Development of absorbance maxima at 556 and 656nm upon exposure of 33 μ M HRP to 1.0mM H₂O₂ over a period of sixty seconds (see Table I-4 for absorbance values).

Time (sec.)	Peaks observed (nm)	Absorbance Values
0	404	0.709
5	416	0.402
10	418	0.515
20	418	0.547
30	418	0.559
40	418	0.562
50	418	0.562
60	418	0.560

Table H5 Absorbance changes occurring in the Soret upon exposure to 10.0mM H₂O₂ for one minute ([HRP]=7.5μM).

Time (sec.)	Peaks Observed (nm)	Absorbance Values
0	494	0.511
	640	0.185
	656	0.160
5	544	0.347
	656	0.221
10	542	0.368
	576	0.330
20	656	0.172
	542	0.383
	576	0.340
30	656	0.164
	542	0.394
40	578	0.347
	542	0.401
	578	0.353
50	654	0.171
	676	0.161
	554	0.408
	578	0.359
60	654	0.180
	676	0.173
	554	0.413
	654	0.190
	668	0.190
	676	0.184

Table H6 Absorbance changes occurring in the far red region upon exposure of 33μM HRP to 10.0mM H₂O₂ for one minute.

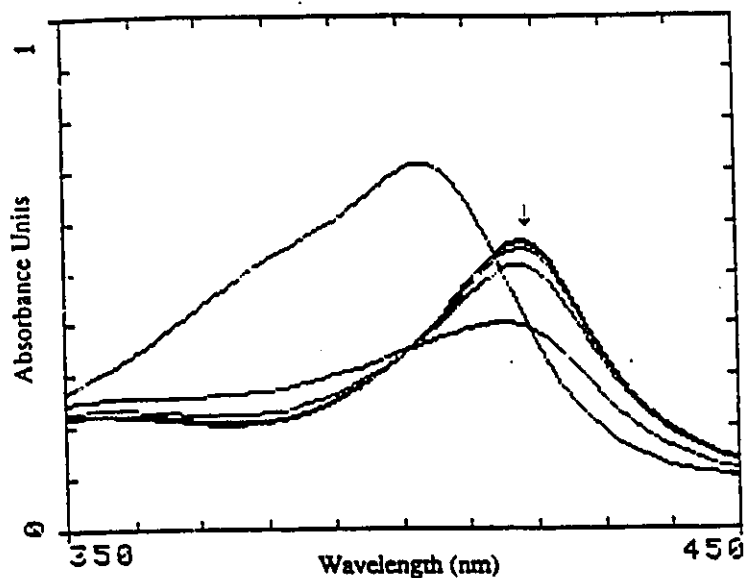


Figure H5 Decay of absorbance maximum at 418nm upon exposure of 7.3 μ M HRP to 10.0mM H₂O₂ over a period of sixty seconds (see Table I-5 for absorbance values).

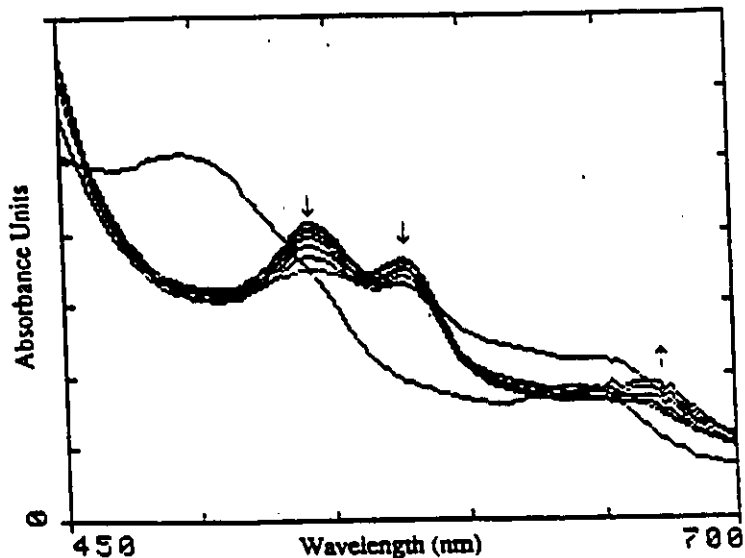


Figure H6 Decay of absorbance maxima at 554 and 578nm, and development of a maximum at 676nm upon exposure of 33 μ M HRP to 10.0mM H₂O₂ over a period of sixty seconds (see Table I-6 for absorbance values).

Time (sec.)	Peaks observed (nm)	Absorbance Values
0	404	0.682
5	418	0.539
10	418	0.600
20	418	0.602
30	418	0.603
40	418	0.594
50	418	0.591
60	418	0.585

Table H7 Absorbance changes occurring in the Soret upon exposure to 25.0mM H₂O₂ for one minute ([HRP]=6.6μM).

Time (sec.)	Peaks Observed (nm)	Absorbance Values
0	494	0.552
	640	0.218
	656	0.196
5	542	0.430
	576	0.387
10	542	0.458
	576	0.398
20	662	0.172
	542	0.467
	576	0.403
30	668	0.181
	554	0.473
	578	0.409
40	656	0.189
	670	0.199
	542	0.475
50	578	0.411
	670	0.213
	542	0.479
60	578	0.417
	670	0.227
	544	0.476
	578	0.413
	670	0.234

Table H8 Absorbance changes occurring in the far red region upon exposure of 33μM HRP to 25.0mM H₂O₂ for one minute.

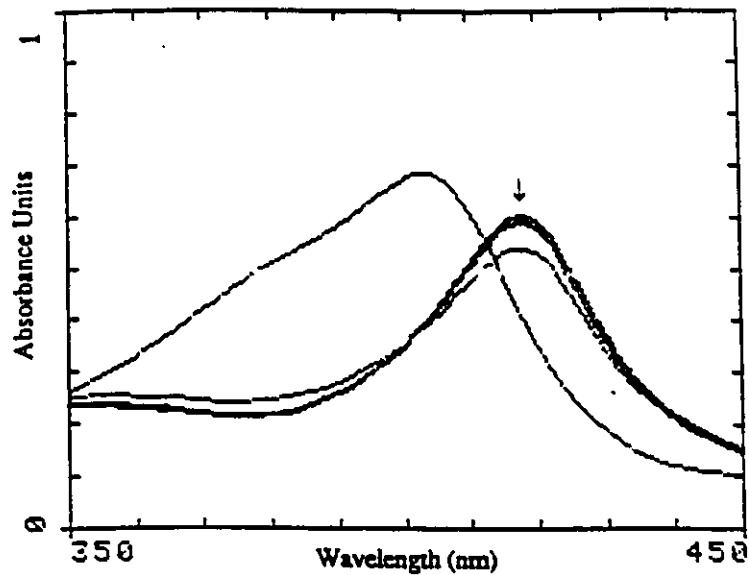


Figure H7 Decay of absorbance maximum at 418nm upon exposure of 6.6 μ M HRP to 25.0mM H₂O₂ over a period of sixty seconds (see Table I-7 for absorbance values).

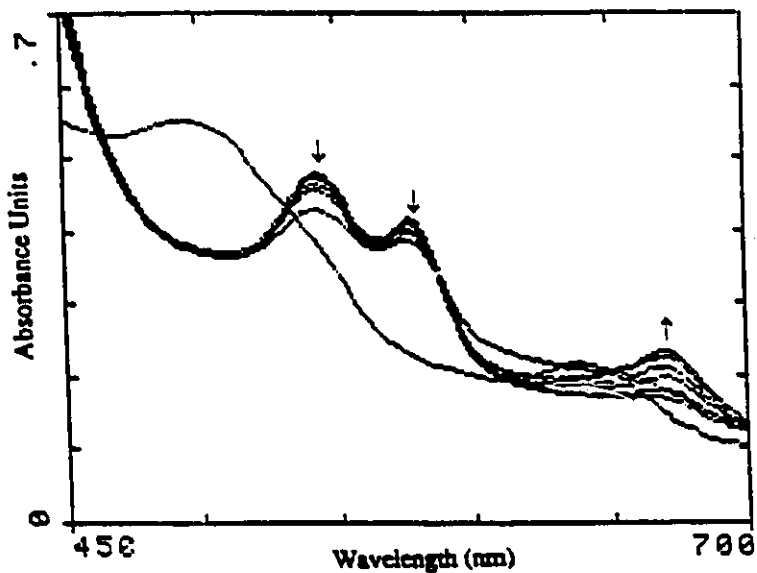


Figure H8 Decay of absorbance maxima at 554 and 578nm, and development of a maximum at 670nm upon exposure of 33 μ M HRP to 25.0mM H₂O₂ over a period of sixty seconds (see Table I-8 for absorbance values).

Time (sec.)	Peaks observed (nm)	Absorbance Values
0	404	0.694
5	418	0.560
10	418	0.590
20	418	0.589
30	418	0.587
40	418	0.586
50	418	0.588
60	418	0.578

Table H9 Absorbance changes occurring in the Soret upon exposure to 50.0mM H₂O₂ for one minute ([HRP]=6.6μM).

Time (sec.)	Peaks Observed (nm)	Absorbance Values
0	494	0.522
	640	0.191
5	544	0.421
	578	0.365
	676	0.141
10	542	0.429
	578	0.366
	670	0.134
20	544	0.453
	578	0.371
	670	0.152
30	554	0.439
	578	0.375
	672	0.168
40	542	0.440
	578	0.377
	670	0.180
50	544	0.443
	578	0.381
	670	0.193
60	544	0.444
	578	0.381
	672	0.201

Table H10 Absorbance changes occurring in the far red region upon exposure of 33μM HRP to 50.0mM H₂O₂ for one minute.

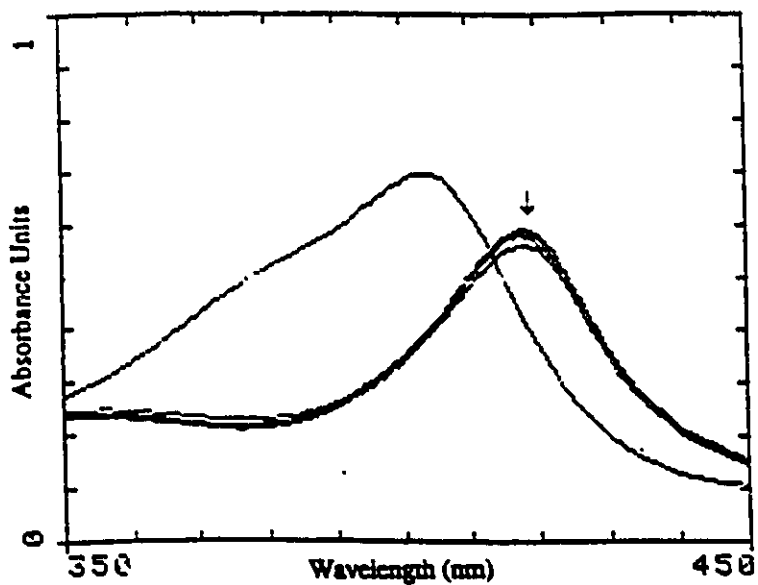


Figure H9 Decay of absorbance maximum at 418nm upon exposure of 6.6 μ M HRP to 50.0mM H₂O₂ over a period of sixty seconds (see Table I-9 for absorbance values).

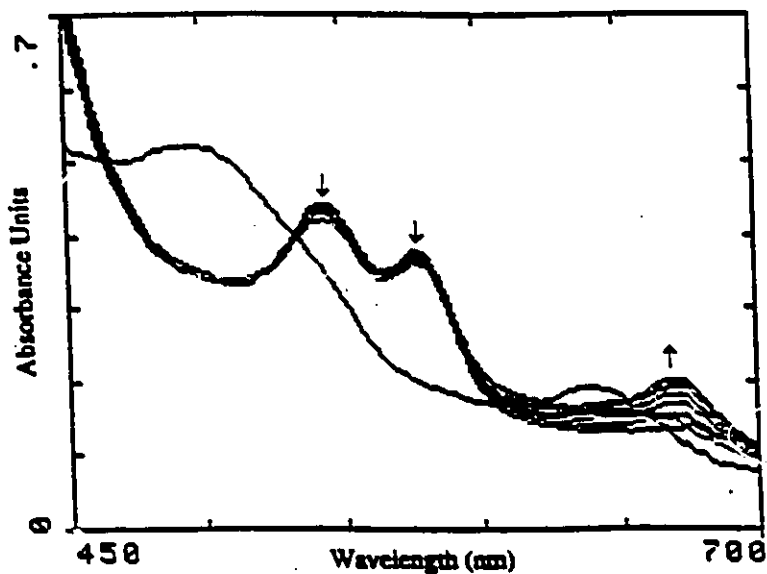


Figure H10 Decay of absorbance maxima at 544 and 578nm, and development of a maximum at 670nm upon exposure of 33 μ M HRP to 50.0mM H₂O₂ over a period of sixty seconds (see Table I-10 for absorbance values).

APPENDIX I

Summary tables and plots of observed and calculated values (from ENFITTER™ using single-exponential decay analyses) of fractional residual activity vs. time, and tables of H₂O₂ consumption by 5 minutes at various concentrations of HRP and phenol (T=25°C, pH 7.4).

[Phenol] (mM)	Total % Inactivation by 5 minutes	Total [H ₂ O ₂] (μM) consumed by 5 minutes
0.20	66.1	308
0.50	93.4	328
0.75	96.5	353
1.00	97.8	344
2.00	98.9	328

(a)

[Phenol] (mM)	Total % Inactivation by 5 minutes	Total [H ₂ O ₂] (μM) consumed by 5 minutes
0.20	58.0	233
0.50	91.3	71
0.75	96.5	92
1.00	98.0	156
2.00	100.0	216

(b)

Tables Ia, b Summary of the total % inactivation and the total H₂O₂ consumed during 5 minutes for solutions containing 25nM HRP incubated with (a) 0.5mM H₂O₂ and (b) 1.0mM H₂O₂, and various concentrations of phenol (T=25°C, pH 7.4)

[Phenol] (mM)	Total % Inactivation by 5 minutes	Total [H ₂ O ₂] (μM) consumed by 5 minutes
0.20	65.6	123
0.50	93.4	170
0.75	95.2	190
1.00	96.9	154
2.00	98.5	181

(a)

[Phenol] (mM)	Total % Inactivation by 5 minutes	Total [H ₂ O ₂] (μM) consumed by 5 minutes
0.20	56.7	111
0.50	90.5	460
0.75	94.1	143
1.00	96.0	302
2.00	97.7	244

(b)

Tables I2a, b Summary of the total % inactivation and the total H₂O₂ consumed during 5 minutes for solutions containing 50nM HRP incubated with (a) 0.5mM H₂O₂ and (b) 1.0mM H₂O₂, and various concentrations of phenol (T=25°C, pH 7.4)

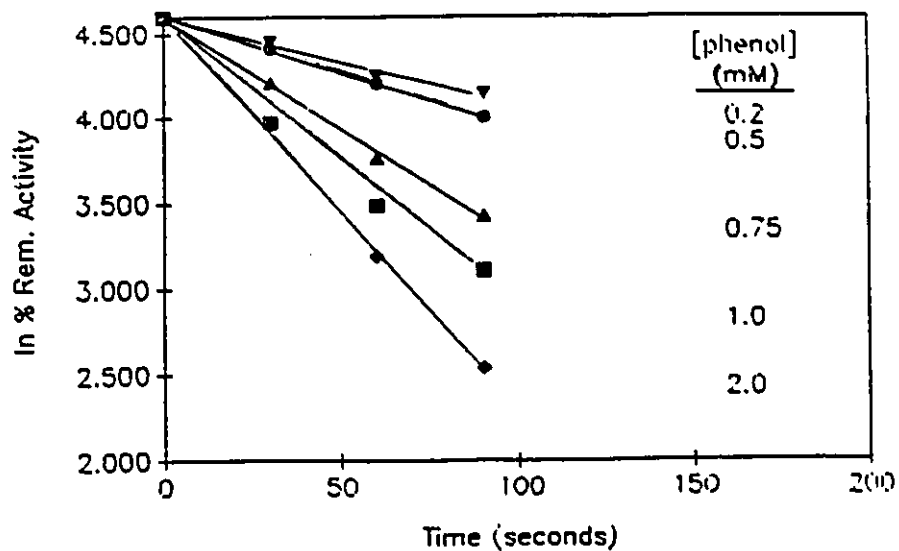
<u>[Phenol] (mM)</u>	<u>Total % Inactivation by 5 minutes</u>	<u>Total [H₂O₂] (μM) consumed by 5 minutes</u>
0.20	50.0	234
0.50	89.9	329
0.75	92.5	317
1.00	88.5	381
2.00	84.5	468

(a)

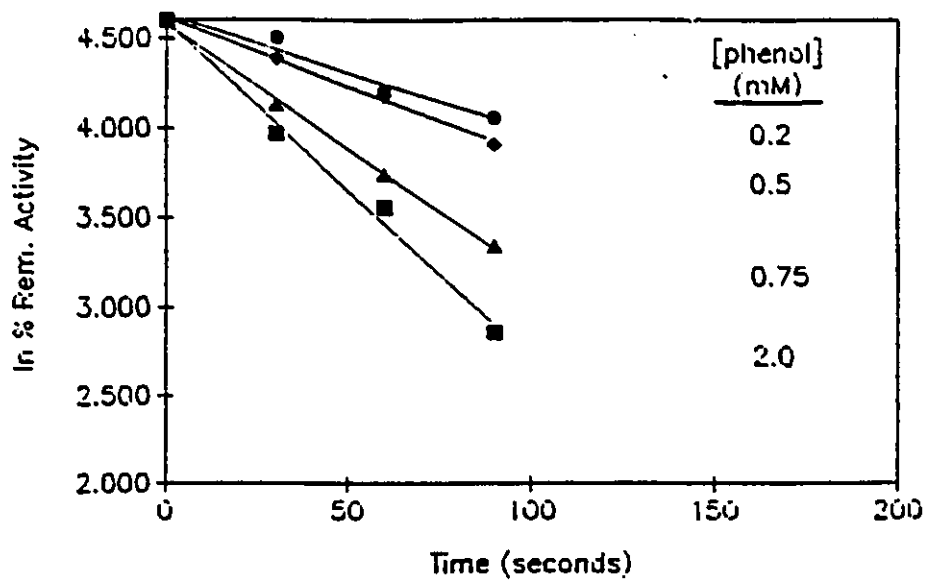
<u>[Phenol] (mM)</u>	<u>Total % Inactivation by 5 minutes</u>	<u>Total [H₂O₂] (μM) consumed by 5 minutes</u>
0.20	62.2	151
0.50	95.0	314
0.75	97.4	321
1.00	98.4	330
2.00	99.6	308

(b)

Tables I3a, b Summary of the total % inactivation and the total H₂O₂ consumed during 5 minutes for solutions containing 100nM HRP incubated with (a) 0.5mM H₂O₂ and (b) 1.0mM H₂O₂, and various concentrations of phenol (T=25°C, pH 7.4)

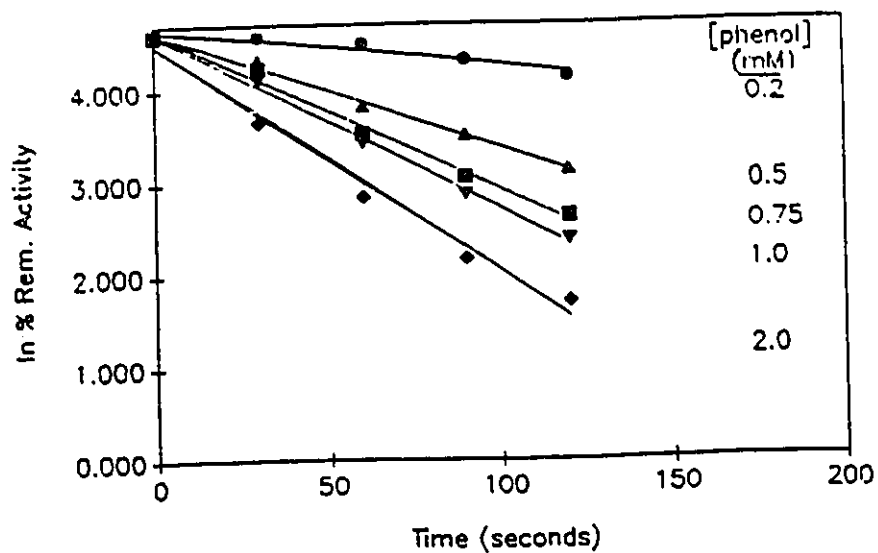


(a)

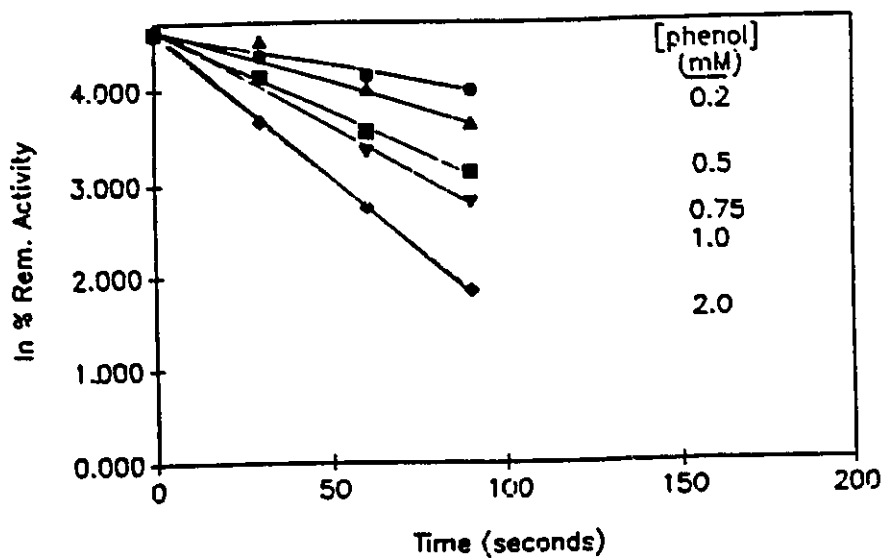


(b)

Figures 11a, b Time-dependent inactivation of 25nM HRP by enzyme-generated phenoxy radicals during the first 100 seconds. (a) $[H_2O_2]=0.5mM$; (b) $[H_2O_2]=1.0mM$; $T=25^\circ C$, pH 7.4.

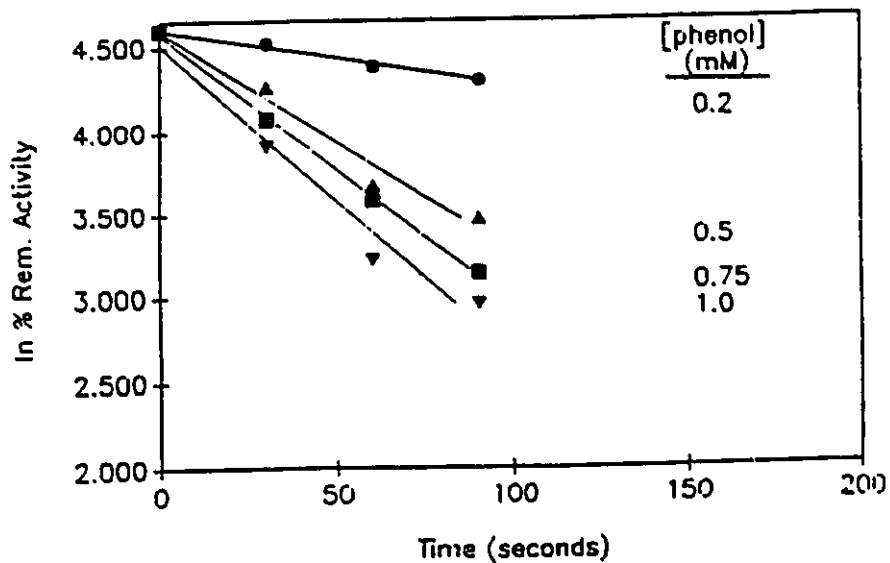


(a)

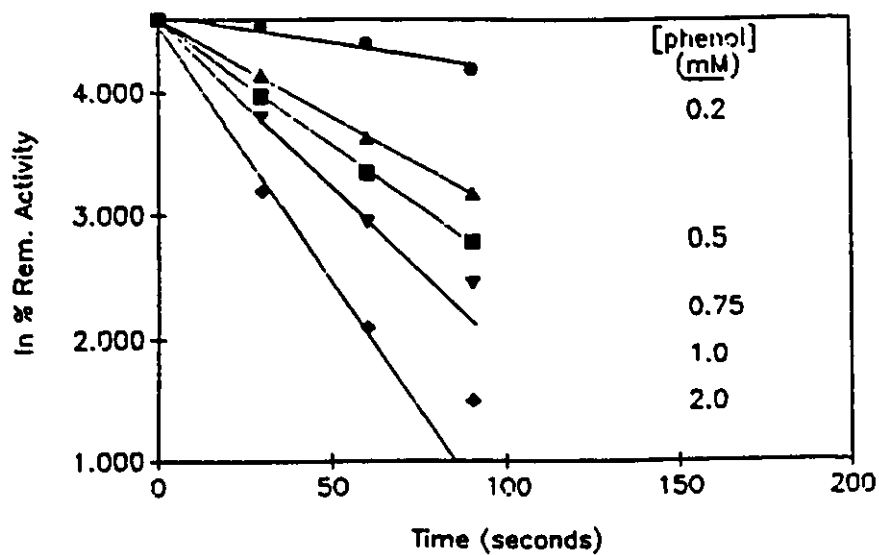


(b)

Figures I2a, b Time-dependent inactivation of 50nM HRP by enzyme-generated phenoxyl radicals during the first 100 seconds. (a) $[H_2O_2]=0.5mM$; (b) $[H_2O_2]=1.0mM$; $T=25^\circ C$, pH 7.4.



(a)



(b)

Figures I3a, b Time-dependent inactivation of 100nM HRP by enzyme-generated phenoxyl radicals during the first 100 seconds. (a) $[H_2O_2] = 0.5mM$; (b) $[H_2O_2] = 1.0mM$; $T = 25^\circ C$, pH 7.4.

	Time (seconds)	Residual	Calculated
1	0.00000E+00	1.00000E+00	9.93206E-01
2	3.00000E+01	8.19000E-01	8.18612E-01
3	6.00000E+01	6.67300E-01	6.74710E-01
4	9.00000E+01	5.45500E-01	5.56104E-01
5	1.20000E+02	4.68100E-01	4.58348E-01
6	1.50000E+02	3.64000E-01	3.77776E-01
7	1.80000E+02	3.13000E-01	3.11367E-01
8	2.40000E+02	2.30700E-01	2.11520E-01

Table I4 Observed and calculated fractional remaining activity data vs. time used for single-exponential decay analysis: [HRP] = 25nM; [H₂O₂]=0.5mM; [phenol]=0.2mM. Initial value (A) = 99.32 ± 0.00955.

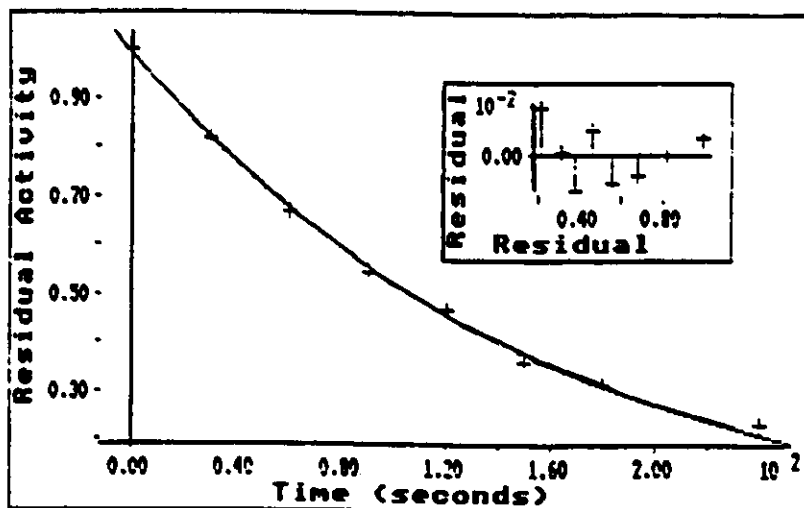


Figure I4 Plot of observed data in Table I4 fit to calculated single-exponential decay curve. Inset: plot of % residual vs. % remaining for experimental values.

	Time (seconds)	Residual	Calculated
1	0.00000E+00	1.00000E+00	1.10556E+00
2	3.00000E+01	9.91000E-01	8.27043E-01
3	6.00000E+01	6.64000E-01	6.18691E-01
4	9.00000E+01	4.27100E-01	4.62827E-01
5	1.20000E+02	3.05000E-01	3.46230E-01
6	1.50000E+02	2.19400E-01	2.59006E-01
7	1.80000E+02	1.65500E-01	1.93756E-01
8	2.40000E+02	1.02100E-01	1.08429E-01
9	3.00000E+02	6.51000E-02	6.06788E-02

Table 15 Observed and calculated fractional remaining activity data vs. time used for single-exponential decay analysis: [HRP] = 25nM; [H₂O₂]=0.5mM; [phenol]=0.5mM. Initial value (A) = 110.56 ± 0.0685.

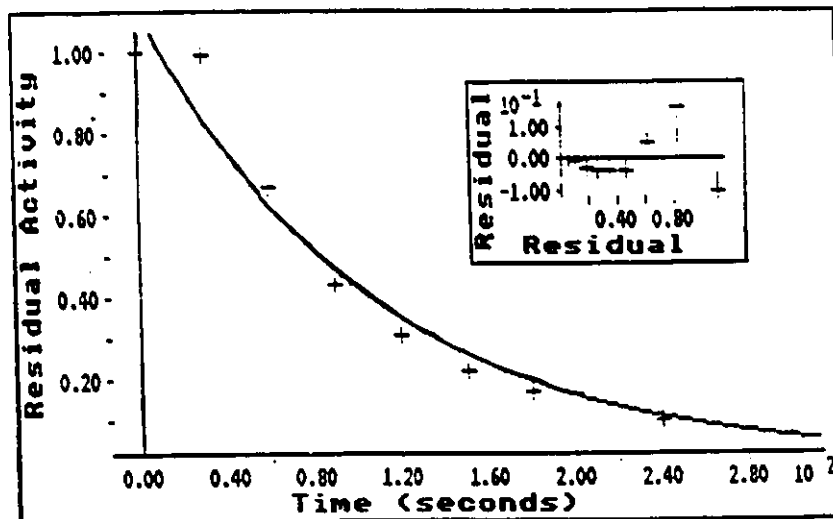


Figure 15 Plot of observed data in Table 15 fit to calculated single-exponential decay curve. Inset: plot of % residual vs. % remaining for experimental values.

	Time (seconds)	Residual	Calculated
1	0.00000E+00	1.00000E+00	9.68740E-01
2	3.00000E+01	5.27400E-01	5.83679E-01
3	6.00000E+01	3.26300E-01	3.51675E-01
4	9.00000E+01	2.25500E-01	2.11889E-01
5	1.20000E+02	1.58900E-01	1.27666E-01
6	1.50000E+02	1.18300E-01	7.69205E-02
7	1.80000E+02	6.71000E-02	4.63457E-02
8	2.40000E+02	4.47000E-02	1.68245E-02

Table I6 Observed and calculated fractional remaining activity data vs. time used for single-exponential decay analysis: [HRP] = 25nM; [H₂O₂]=0.5mM; [phenol]=0.75mM. Initial value (A) = 96.87 ± 0.0359.

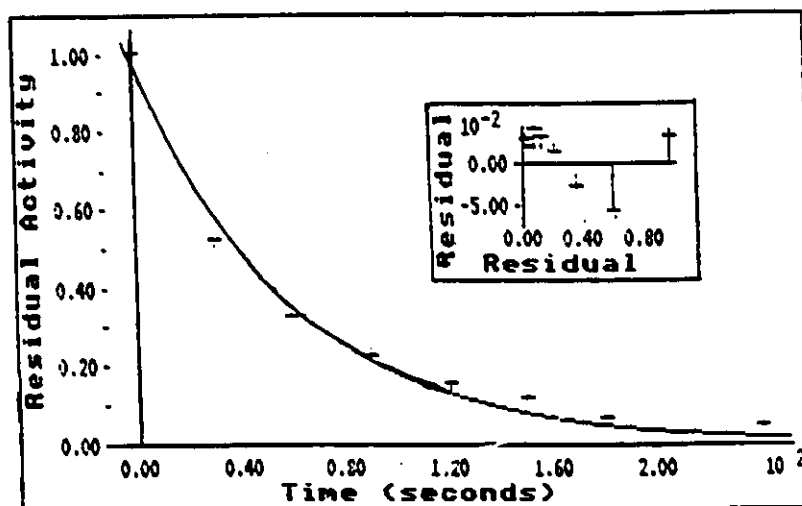


Figure I6 Plot of observed data in Table I6 fit to calculated single-exponential decay curve. Inset: plot of % residual vs. % remaining for experimental values.

	Time (seconds)	Residual	Calculated
1	0.00000E+00	1.00000E+00	9.95964E-01
2	3.00000E+01	5.33200E-01	5.35976E-01
3	6.00000E+01	2.61000E-01	2.88434E-01
4	9.00000E+01	1.86000E-01	1.55220E-01
5	1.20000E+02	8.70000E-02	8.35313E-02
6	1.50000E+02	4.71000E-02	4.49522E-02
7	1.80000E+02	3.31000E-02	2.41909E-02

Table I7 Observed and calculated fractional remaining activity data vs. time used for single-exponential decay analysis:
 [HRP] = 25nM; [H₂O₂] = 0.5mM; [phenol] = 1.0mM.
 Initial value (A) = 99.60 ± 0.0183.

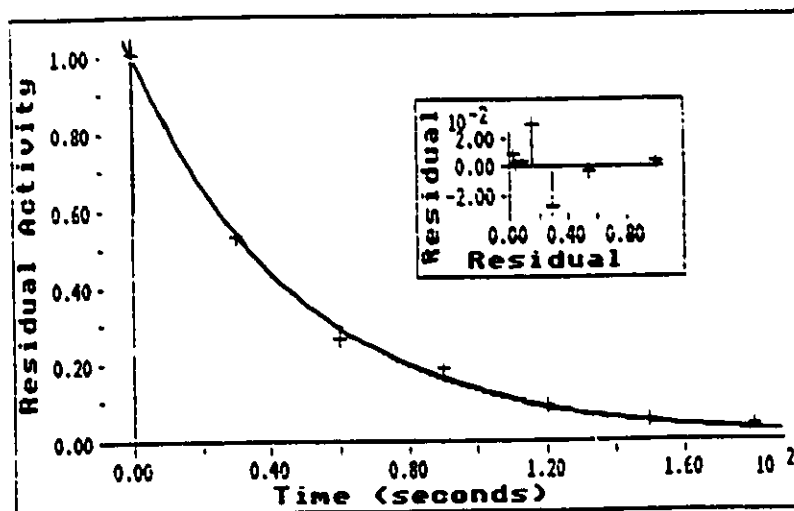


Figure I7 Plot of observed data in Table I7 fit to calculated single-exponential decay curve. Inset: plot of % residual vs. % remaining for experimental values

	Time (seconds)	Residual	Calculated
1	0.00000E+00	1.00000E+00	1.00240E+00
2	3.00000E+01	5.21000E-01	5.09386E-01
3	6.00000E+01	2.46300E-01	2.58853E-01
4	9.00000E+01	1.26800E-01	1.31541E-01
5	1.20000E+02	6.41000E-02	6.68449E-02
6	1.50000E+02	4.10000E-02	3.39684E-02
7	1.80000E+02	3.10000E-02	1.72616E-02
8	2.40000E+02	1.60000E-02	4.45755E-03
9	3.00000E+02	1.49000E-02	1.15109E-03

Table 18 Observed and calculated fractional remaining activity data vs. time used for single-exponential decay analysis:
 [HRP] = 25nM; [H₂O₂] = 0.5mM; [phenol] = 2.0mM.
 Initial value (A) = 100.24 ± 0.0109.

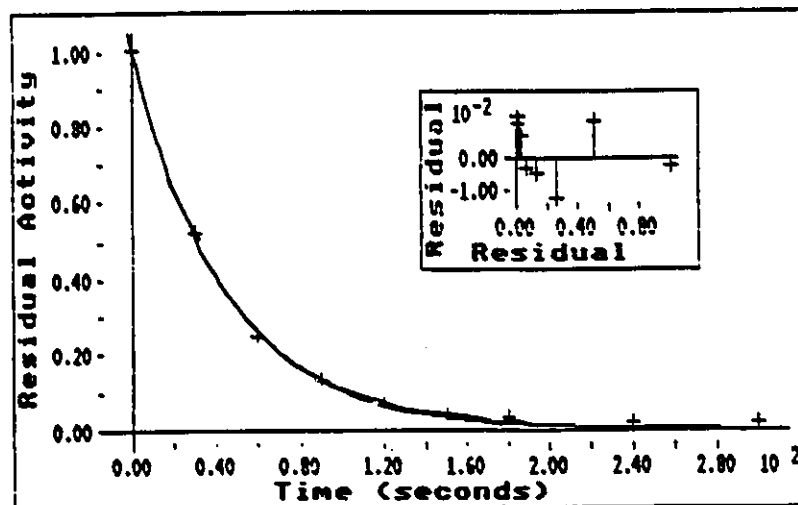


Figure 18 Plot of observed data in Table 18 fit to calculated single-exponential decay curve. Inset: plot of % residual vs. % remaining for experimental values

	Time (seconds)	Residual	Calculated
1	0.00000E+00	1.00000E+00	9.78780E-01
2	3.00000E+01	9.02400E-01	8.53238E-01
3	6.00000E+01	6.74600E-01	7.43799E-01
4	9.00000E+01	5.79900E-01	6.48397E-01
5	1.20000E+02	5.79900E-01	5.65231E-01
6	1.50000E+02	5.16200E-01	4.92732E-01
7	1.80000E+02	4.43600E-01	4.29533E-01
8	2.40000E+02	3.35800E-01	3.26412E-01
9	3.00000E+02	2.65000E-01	2.48049E-01

Table 19 Observed and calculated fractional remaining activity data vs. time used for single-exponential decay analysis: [HRP] = 25nM; [H₂O₂] = 1.0mM; [phenol] = 0.2mM. Initial value (A) = 97.88 ± 0.032.

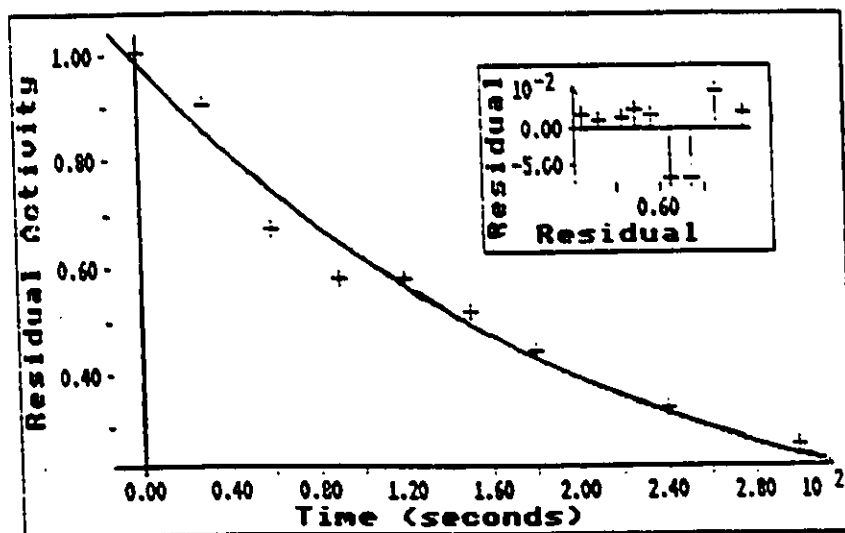


Figure 19 Plot of observed data in Table 19 fit to calculated single-exponential decay curve. Inset: plot of % residual vs. % remaining for experimental values

	Time (seconds)	Residual	Calculated
1	0.00000E+00	1.00000E+00	9.75895E-01
2	3.00000E+01	6.21600E-01	6.53970E-01
3	6.00000E+01	4.19800E-01	4.38241E-01
4	9.00000E+01	2.83700E-01	2.93676E-01
5	1.20000E+02	2.09700E-01	1.96799E-01
6	1.50000E+02	1.58800E-01	1.31880E-01
7	1.80000E+02	1.03600E-01	8.83757E-02
8	2.40000E+02	7.04000E-02	3.96865E-02

Table I10 Observed and calculated fractional remaining activity data vs. time used for single-exponential decay analysis: [HRP] = 25nM; [H₂O₂]=1.0mM; [phenol]=0.5mM. Initial value (A) = 97.59 ± 0.024.

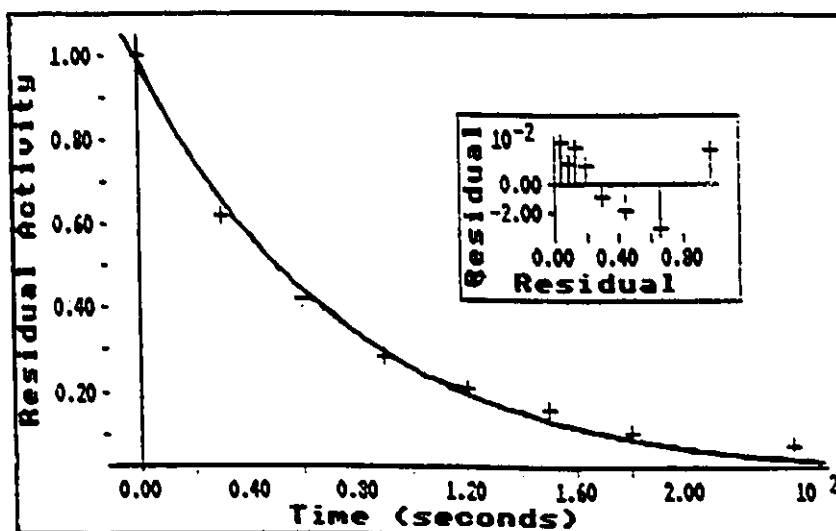


Figure I10 Plot of observed data in Table I10 fit to calculated single-exponential decay curve. Inset: plot of % residual vs. % remaining for experimental values.

	Time (seconds)	Residual	Calculated
1	0.00000E+00	1.00000E+00	9.77821E-01
2	3.00000E+01	5.31400E-01	5.77028E-01
3	6.00000E+01	3.51500E-01	3.40514E-01
4	9.00000E+01	1.74100E-01	2.00943E-01
5	1.50000E+02	1.29700E-01	6.99760E-02
6	1.80000E+02	7.90000E-02	4.12940E-02
7	2.40000E+02	5.31000E-02	1.43801E-02

Table I11 Observed and calculated fractional remaining activity data vs. time used for single-exponential decay analysis: [HRP] = 25nM; [H₂O₂]=1.0mM; [phenol]=0.75mM. Initial value (A) = 97.78 ± 0.0421.

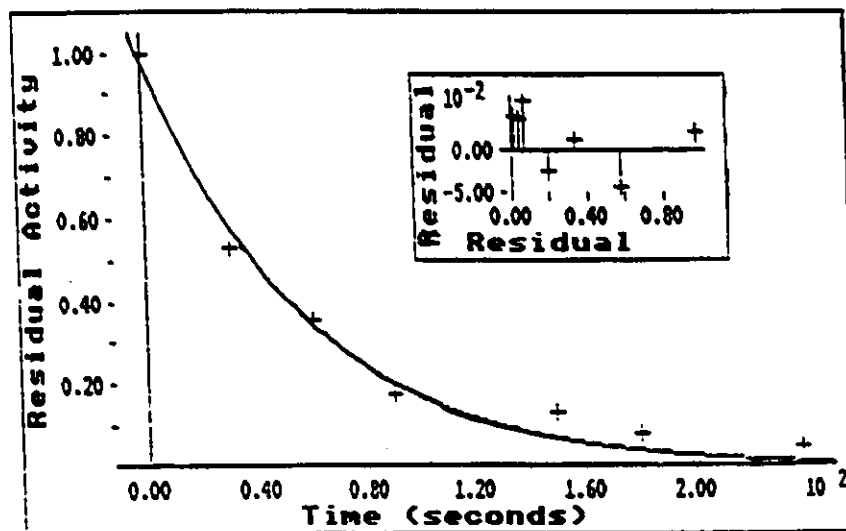


Figure I11 Plot of observed data in Table I11 fit to calculated single-exponential decay curve. Inset: plot of % residual vs. % remaining for experimental values.

	Time (seconds)	Residual	Calculated
1	0.00000E+00	1.00000E+00	9.63984E-01
2	3.00000E+01	4.48600E-01	5.35321E-01
3	6.00000E+01	2.96500E-01	2.97275E-01
4	9.00000E+01	1.99000E-01	1.65083E-01
5	1.20000E+02	1.33000E-01	9.16741E-02
6	1.50000E+02	8.00000E-02	5.09086E-02
7	1.80000E+02	5.68000E-02	2.82706E-02
8	2.40000E+02	3.80000E-02	8.71814E-03

Table I12 Observed and calculated fractional remaining activity data vs. time used for single-exponential decay analysis: [HRP] = 25nM; [H₂O₂]=1.0mM; [phenol]=1.0mM. Initial value (A) = 96.40 ± 0.046.

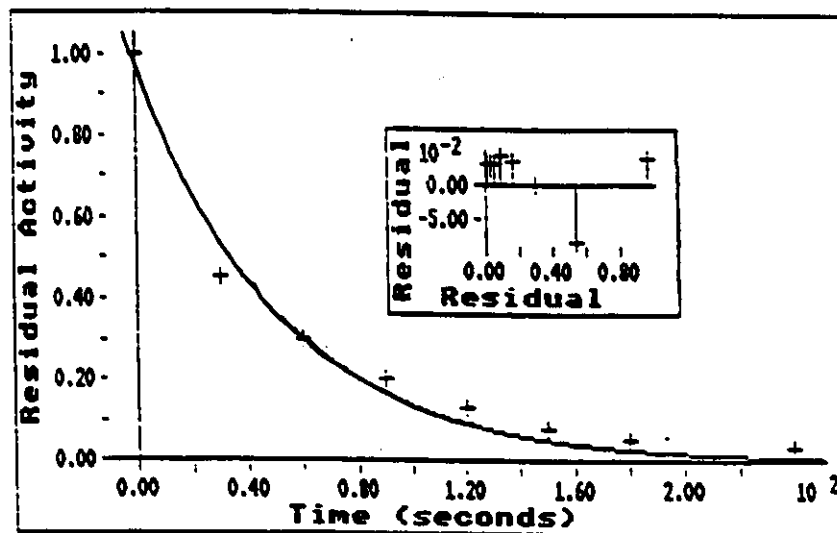


Figure I12 Plot of observed data in Table I12 fit to calculated single-exponential decay curve. Inset: plot of % residual vs. % remaining for experimental values.

	Time (seconds)	Residual	Calculated
1	0.00000E+00	1.00000E+00	1.01863E+00
2	3.00000E+01	6.22300E-01	5.63569E-01
3	6.00000E+01	2.84400E-01	3.11803E-01
4	9.00000E+01	1.45400E-01	1.72509E-01
5	1.20000E+02	7.83300E-02	9.54433E-02
6	1.50000E+02	5.96500E-02	5.28054E-02
7	1.80000E+02	3.40000E-02	2.92153E-02
8	2.40000E+02	2.81000E-02	8.94285E-03
9	3.00000E+02	2.32000E-02	2.73742E-03

Table I13 Observed and calculated fractional remaining activity data vs. time used for single-exponential decay analysis:
 [HRP] = 25nM; [H₂O₂] = 1.0mM; [phenol] = 2.0mM.
 Initial value (A) = 101.86 ± 0.0289.

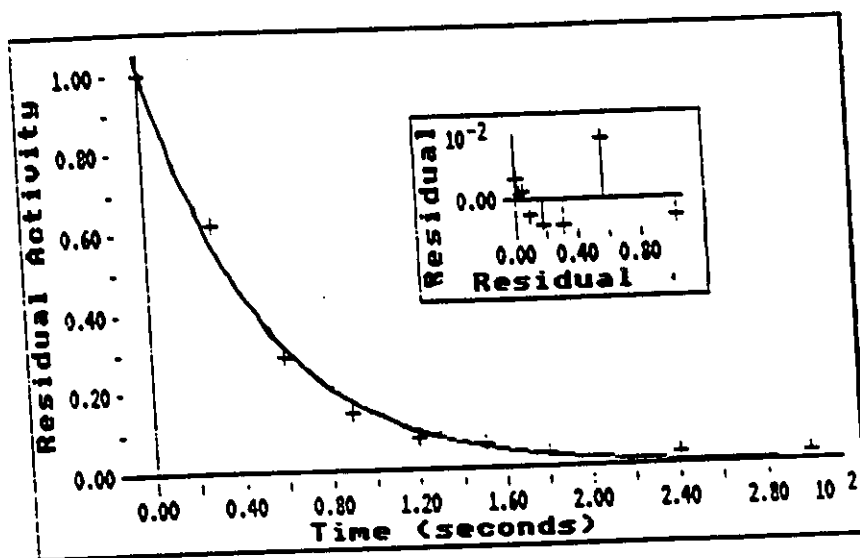


Figure I13 Plot of observed data in Table I13 fit to calculated single-exponential decay curve. Inset: plot of % residual vs. % remaining for experimental values.

	Time (seconds)	Residual	Calculated
1	0.00000E+00	1.00000E+00	1.03155E+00
2	6.00000E+01	8.88000E-01	8.17937E-01
3	9.00000E+01	7.46000E-01	7.28342E-01
4	1.20000E+02	6.27000E-01	6.48560E-01
5	1.50000E+02	5.40000E-01	5.77518E-01
6	1.80000E+02	4.98000E-01	5.14257E-01
7	2.40000E+02	4.11000E-01	4.07765E-01
8	3.00000E+02	3.39000E-01	3.23326E-01

Table I14 Observed and calculated fractional remaining activity data vs. time used for single-exponential decay analysis: [HRP] = 50nM; [H₂O₂]=0.5mM; [phenol]=0.2mM. Initial value (A) = 103.32 ± 0.0311.

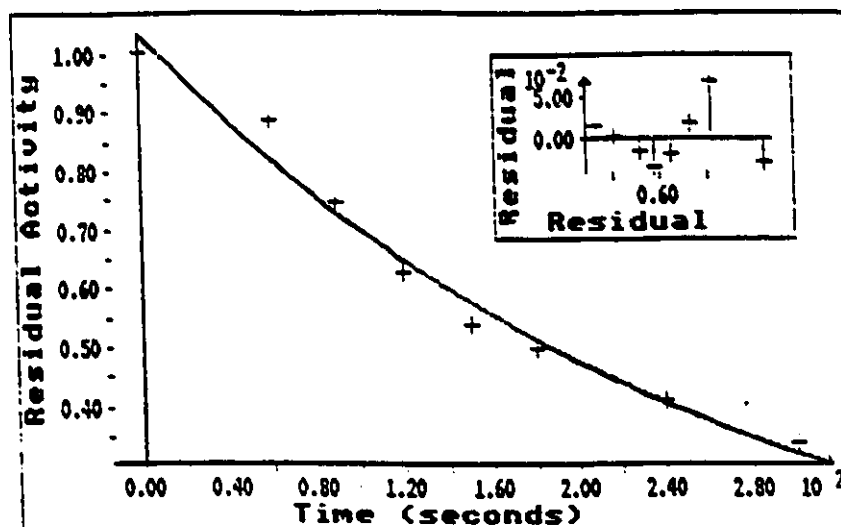


Figure I14 Plot of observed data in Table I14 fit to calculated single-exponential decay curve. Inset: plot of % residual vs. % remaining for experimental values.

	Time (seconds)	Residual	Calculated
1	0.00000E+00	1.00000E+00	1.00906E+00
2	3.00000E+01	7.50000E-01	7.06130E-01
3	6.00000E+01	4.66000E-01	4.94145E-01
4	9.00000E+01	3.17000E-01	3.45799E-01
5	1.20000E+02	2.24000E-01	2.41988E-01
6	1.50000E+02	1.79900E-01	1.69342E-01
7	1.80000E+02	1.34000E-01	1.18504E-01
8	2.40000E+02	8.70000E-02	5.80328E-02
9	3.00000E+02	6.62000E-02	2.84193E-02

Table I15 Observed and calculated fractional remaining activity data vs. time used for single-exponential decay analysis:
 [HRP] = 50nM; [H₂O₂] = 0.5mM; [phenol] = 0.5mM.
 Initial value (A) = 100.91 ± 0.027.

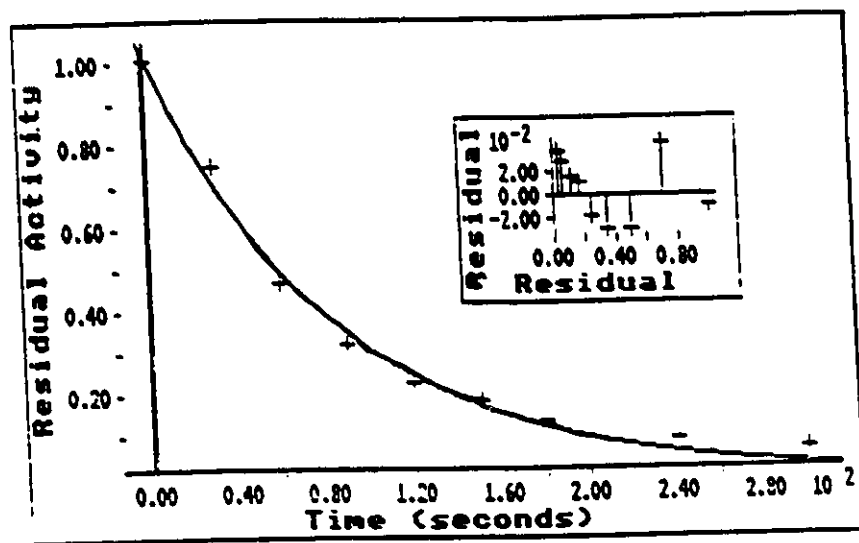


Figure I15 Plot of observed data in Table I15 fit to calculated single-exponential decay curve. Inset: plot of % residual vs. % remaining for experimental values

	Time (seconds)	Residual	Calculated
1	0.00000E+00	1.00000E+00	1.01107E+00
2	3.00000E+01	6.86000E-01	6.17396E-01
3	6.00000E+01	3.38000E-01	3.77004E-01
4	9.00000E+01	2.09300E-01	2.30212E-01
5	1.20000E+02	1.38000E-01	1.40576E-01
6	1.50000E+02	8.80000E-02	8.58406E-02
7	1.80000E+02	7.60000E-02	5.24173E-02
8	2.40000E+02	4.85000E-02	1.95452E-02
9	3.00000E+02	3.50000E-02	7.28792E-03

Table I16 Observed and calculated fractional remaining activity data vs. time used for single-exponential decay analysis: [HRP] = 50nM; [H₂O₂]=0.5mM; [phenol]=0.75mM. Initial value (A) = 101.11 ± 0.030.

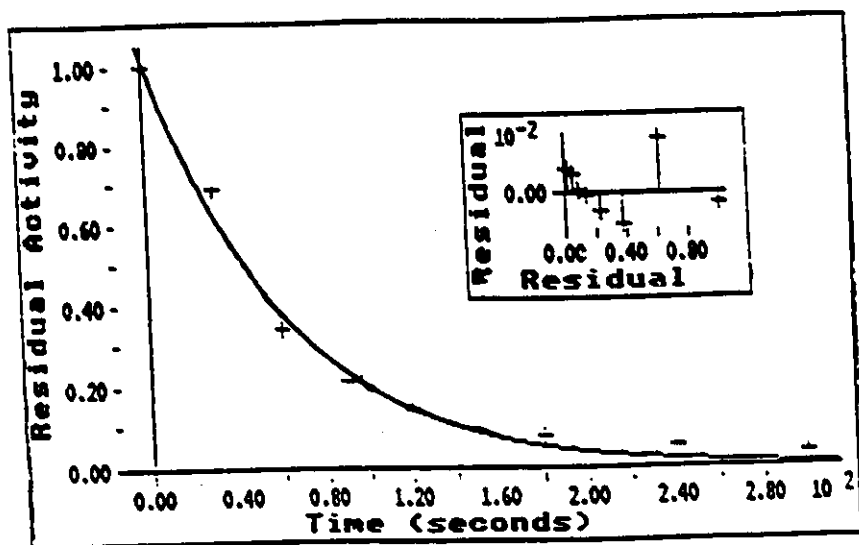


Figure I16 Plot of observed data in Table I16 fit to calculated single-exponential decay curve. Inset: plot of % residual vs. % remaining for experimental values

	Time (seconds)	Residual	Calculated
1	0.00000E+00	1.00000E+00	1.00673E+00
2	3.00000E+01	6.09000E-01	5.77743E-01
3	6.00000E+01	3.02300E-01	3.31556E-01
4	9.00000E+01	1.73000E-01	1.90274E-01
5	1.20000E+02	1.07000E-01	1.09195E-01
6	1.50000E+02	7.74000E-02	6.26648E-02
7	1.80000E+02	4.86000E-02	3.59622E-02
8	2.40000E+02	4.85000E-02	1.18438E-02
9	3.00000E+02	3.50000E-02	3.90063E-03

Table I17 Observed and calculated fractional remaining activity data vs. time used for single-exponential decay analysis: [HRP] = 50nM; [H₂O₂]=0.5mM; [phenol]=1.0mM. Initial value (A) = 100.67 ± 0.025.

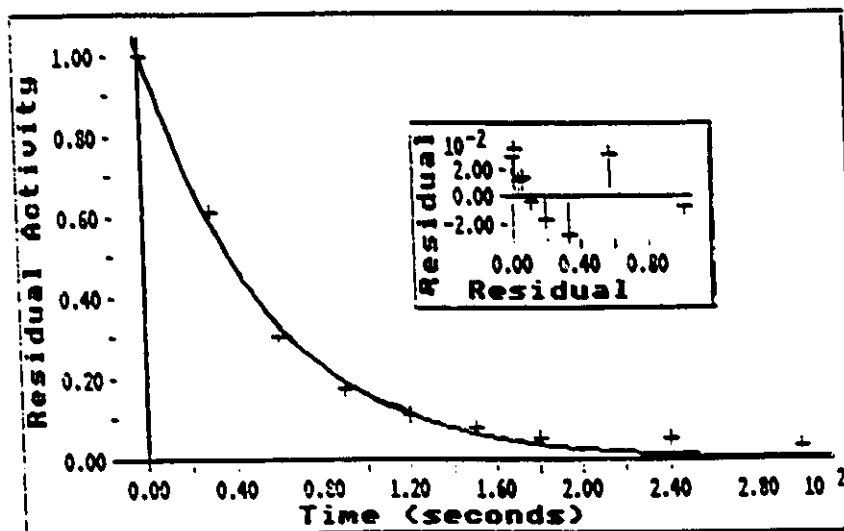


Figure I17 Plot of observed data in Table I17 fit to calculated single-exponential decay curve. Inset: plot of % residual vs. % remaining for experimental values

	Time (seconds)	Residual	Calculated
1	0.00000E+00	1.00000E+00	9.93294E-01
2	3.00000E+01	3.85000E-01	4.07977E-01
3	6.00000E+01	1.69300E-01	1.67569E-01
4	9.00000E+01	8.80000E-02	6.88260E-02
5	1.20000E+02	5.45000E-02	2.82690E-02
6	1.50000E+02	3.77000E-02	1.16110E-02
7	1.80000E+02	1.54000E-02	4.76900E-03
8	2.40000E+02	1.14000E-02	8.04534E-04

Table I18 Observed and calculated fractional remaining activity data vs. time used for single-exponential decay analysis:
 [HRP] = 50nM; [H₂O₂] = 0.5mM; [phenol] = 2.0mM.
 Initial value (A) = 99.33 ± 0.020.

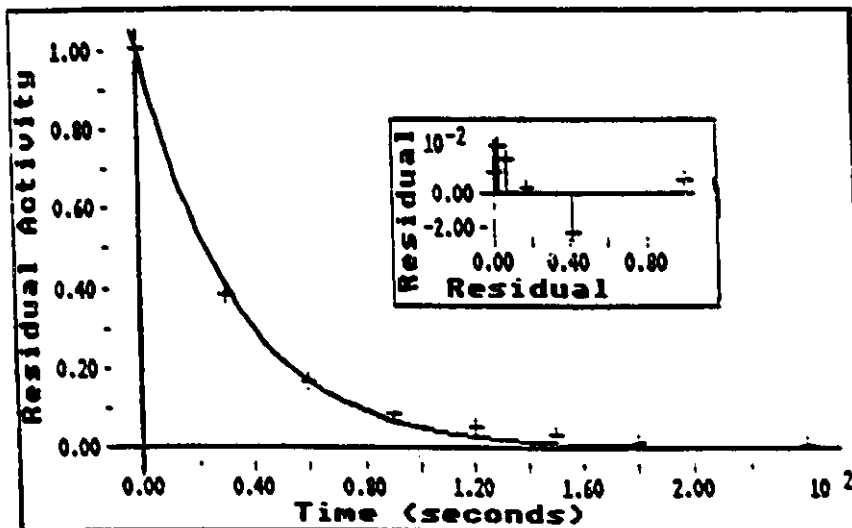


Figure I18 Plot of observed data in Table I18 fit to calculated single-exponential decay curve. Inset: plot of % residual vs. % remaining for experimental values

	Time (seconds)	Residual	Calculated
1	0.00000E+00	1.00000E+00	9.07122E-01
2	3.00000E+01	7.75900E-01	7.92383E-01
3	6.00000E+01	6.33800E-01	6.92157E-01
4	9.00000E+01	5.47600E-01	6.04608E-01
5	1.20000E+02	5.02300E-01	5.28133E-01
6	1.50000E+02	4.18900E-01	4.61331E-01
7	2.40000E+02	3.43990E-01	3.07482E-01
8	3.00000E+02	3.43990E-01	2.34617E-01

Table I19 Observed and calculated fractional remaining activity data vs. time used for single-exponential decay analysis: [HRP] = 50nM; [H₂O₂]=1.0mM; [phenol]=0.2mM. Initial value (A) = 90.71 ± 0.053.

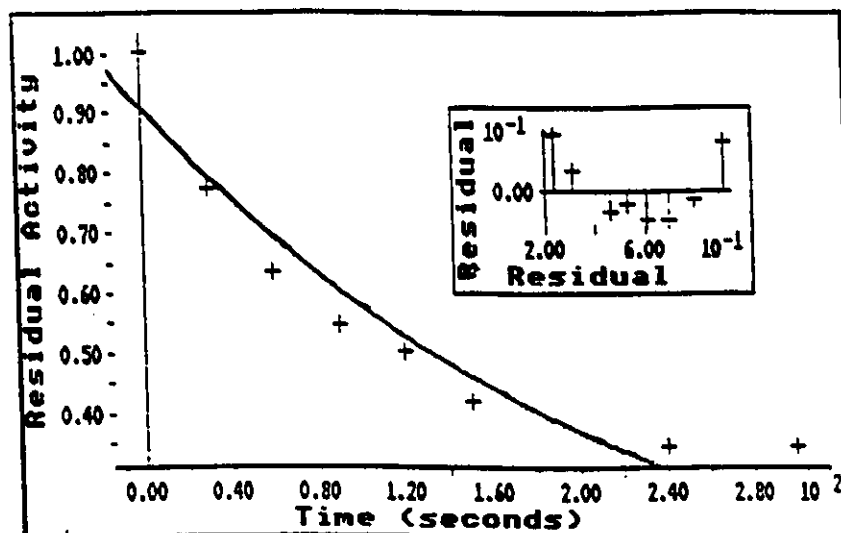


Figure I19 Plot of observed data in Table I19 fit to calculated single-exponential decay curve. Inset: plot of % residual vs. % remaining for experimental values

	Time (seconds)	Residual	Calculated
1	0.00000E+00	1.00000E+00	1.05518E+00
2	3.00000E+01	8.98000E-01	7.73501E-01
3	6.00000E+01	5.44000E-01	5.67017E-01
4	9.00000E+01	3.82100E-01	4.15653E-01
5	1.20000E+02	2.69000E-01	3.04695E-01
6	1.50000E+02	2.06500E-01	2.23357E-01
7	1.80000E+02	1.57500E-01	1.63733E-01
8	2.40000E+02	1.18200E-01	8.79843E-02
9	3.00000E+02	8.67000E-02	4.72797E-02

Table I20 Observed and calculated fractional remaining activity data vs. time used for single-exponential decay analysis:
 [HRP] = 50nM; [H₂O₂] = 1.0mM; [phenol] = 0.5mM.
 Initial value (A) = 105.51 ± 0.050.

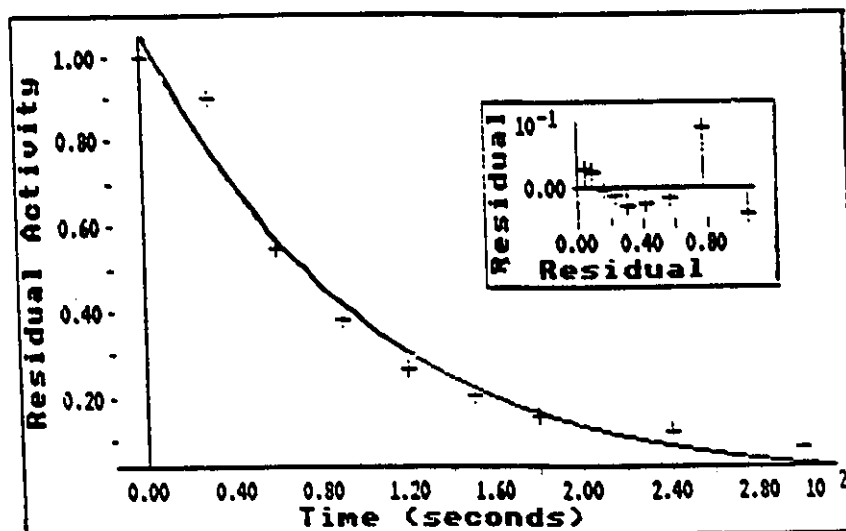


Figure I20 Plot of observed data in Table I20 fit to calculated single-exponential decay curve. Inset: plot of % residual vs. % remaining for experimental values

	Time (seconds)	Residual	Calculated
1	0.00000E+00	1.00000E+00	9.94234E-01
2	3.00000E+01	6.23000E-01	6.16185E-01
3	6.00000E+01	3.49000E-01	3.81887E-01
4	9.00000E+01	2.26000E-01	2.36678E-01
5	1.20000E+02	1.56700E-01	1.46683E-01
6	1.50000E+02	1.08000E-01	9.09082E-02
7	1.80000E+02	7.92000E-02	5.63412E-02
8	2.40000E+02	5.02000E-02	2.16407E-02
9	3.00000E+02	3.54000E-02	8.31223E-03

Table I21 Observed and calculated fractional remaining activity data vs. time used for single-exponential decay analysis: [HRP] = 50nM; [H₂O₂]=1.0mM; [phenol]=0.75mM. Initial value (A) = 99.42 ± 0.021.

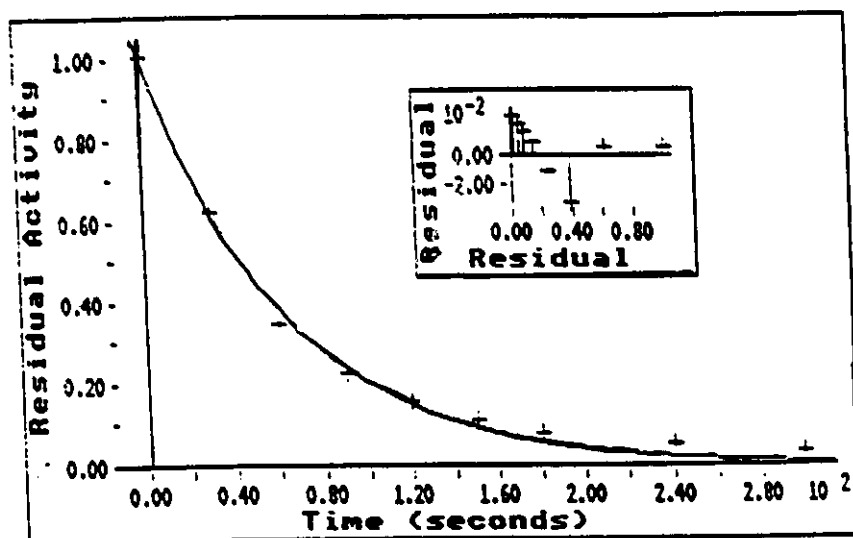


Figure I21 Plot of observed data in Table I21 fit to calculated single-exponential decay curve. Inset: plot of % residual vs. % remaining for experimental values

	Time (seconds)	Residual	Calculated
1	0.00000E+00	1.00000E+00	1.01431E+00
2	3.00000E+01	6.22800E-01	5.71002E-01
3	6.00000E+01	2.82000E-01	3.21443E-01
4	9.00000E+01	1.63000E-01	1.80955E-01
5	1.20000E+02	1.02900E-01	1.01868E-01
6	1.80000E+02	4.86000E-02	3.22829E-02
7	2.40000E+02	2.76300E-02	1.02307E-02
8	3.00000E+02	1.99000E-02	3.24220E-03

Table I22 Observed and calculated fractional remaining activity data vs. time used for single-exponential decay analysis:
 [HRP] = 50nM; [H₂O₂]=1.0mM; [phenol]=1.0mM.
 Initial value (A) = 101.43 ± 0.029.

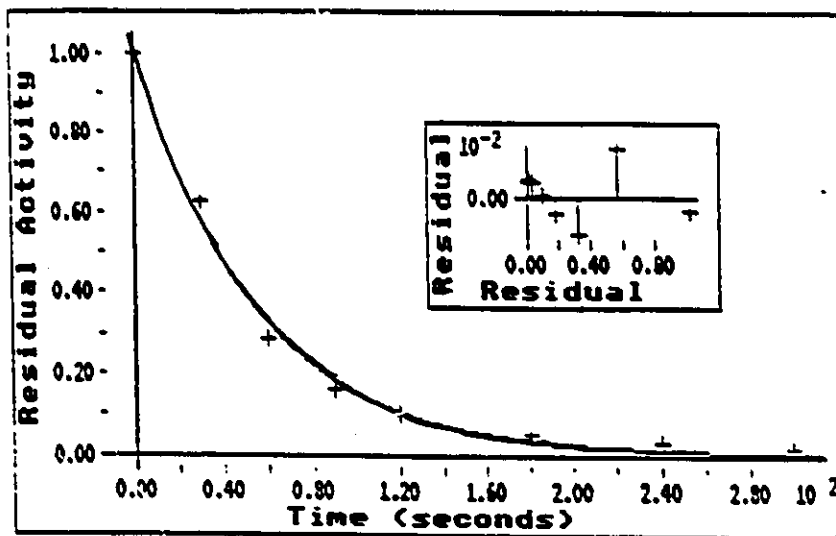


Figure I22 Plot of observed data in Table I22 fit to calculated single-exponential decay curve. Inset: plot of % residual vs. % remaining for experimental values

	Time (seconds)	Residual	Calculated
1	0.00000E+00	1.00000E+00	9.98347E-01
2	3.00000E+01	3.88000E-01	3.93395E-01
3	6.00000E+01	1.54300E-01	1.55016E-01
4	9.00000E+01	6.29800E-02	6.10834E-02
5	1.20000E+02	4.11000E-02	2.40697E-02
6	1.80000E+02	1.83000E-02	3.73737E-03
7	2.40000E+02	4.33000E-03	5.80310E-04

Table I23 Observed and calculated fractional remaining activity data vs. time used for single-exponential decay analysis: [HRP] = 50nM; [H₂O₂]=1.0mM; [phenol]=2.0mM. Initial value (A) = 99.83 ± 0.010.

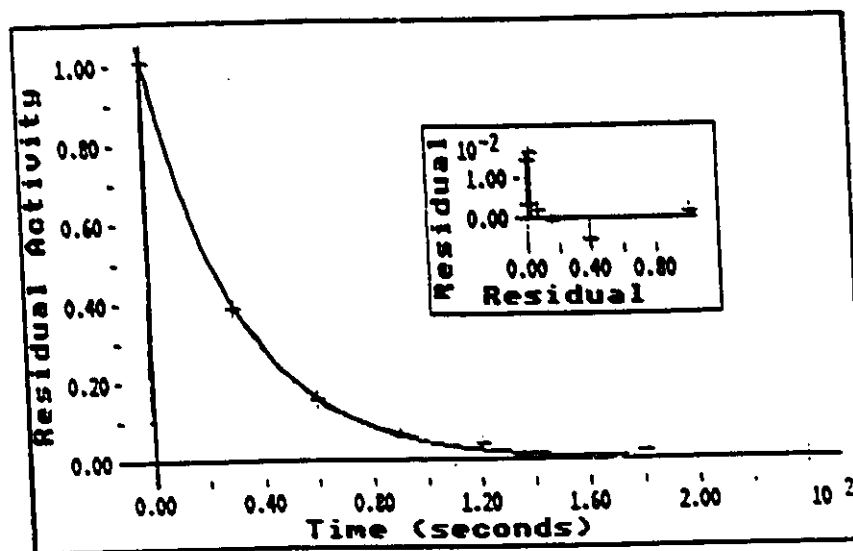


Figure I23 Plot of observed data in Table I23 fit to calculated single-exponential decay curve. Inset: plot of % residual vs. % remaining for experimental values

	Time (seconds)	Residual	Calculated
1	0.00000E+00	1.00000E+00	9.62719E-01
2	3.00000E+01	9.18000E-01	8.89198E-01
3	6.00000E+01	8.00500E-01	8.21292E-01
4	9.00000E+01	7.31000E-01	7.58571E-01
5	1.20000E+02	6.59900E-01	7.00640E-01
6	1.50000E+02	6.25400E-01	6.47133E-01
7	1.80000E+02	5.58700E-01	5.97713E-01
8	2.40000E+02	5.37980E-01	5.09906E-01
9	3.00000E+02	4.99600E-01	4.34999E-01

Table I24 Observed and calculated fractional remaining activity data vs. time used for single-exponential decay analysis: [HRP] = 100nM; [H₂O₂] = 0.5mM; [phenol] = 0.2mM. Initial value (A) = 96.27 ± 0.028.

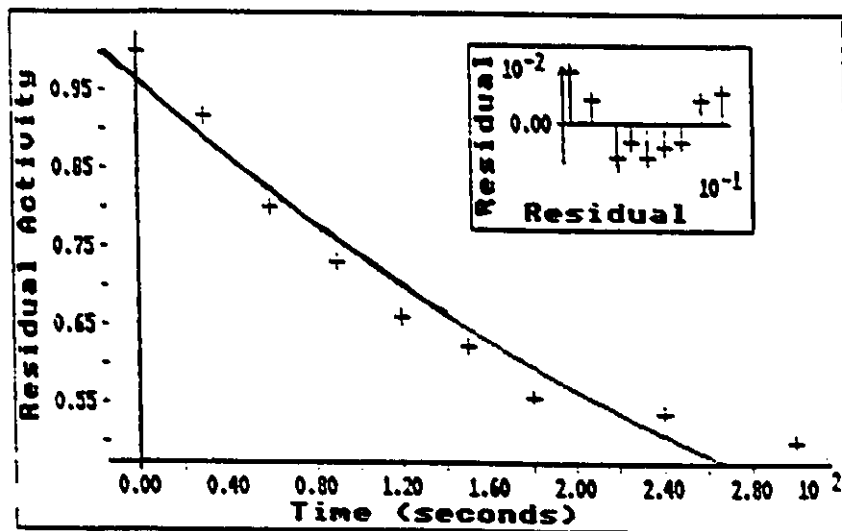


Figure I24 Plot of observed data in Table I24 fit to calculated single-exponential decay curve. Inset: plot of % residual vs. % remaining for experimental values

	Time (seconds)	Residual	Calculated
1	0.00000E+00	1.00000E+00	9.69996E-01
2	3.00000E+01	7.09100E-01	6.91327E-01
3	6.00000E+01	3.93000E-01	4.92716E-01
4	9.00000E+01	3.22000E-01	3.51164E-01
5	1.20000E+02	2.58000E-01	2.50279E-01
6	1.50000E+02	2.03900E-01	1.78376E-01
7	1.80000E+02	1.67300E-01	1.27131E-01
8	2.40000E+02	1.29000E-01	6.45769E-02
9	3.00000E+02	1.00800E-01	3.28023E-02

Table I25 Observed and calculated fractional remaining activity data vs. time used for single-exponential decay analysis: [HRP] = 100nM; [H₂O₂] = 0.5mM; [phenol] = 0.5mM. Initial value (A) = 97.0 ± 0.050.

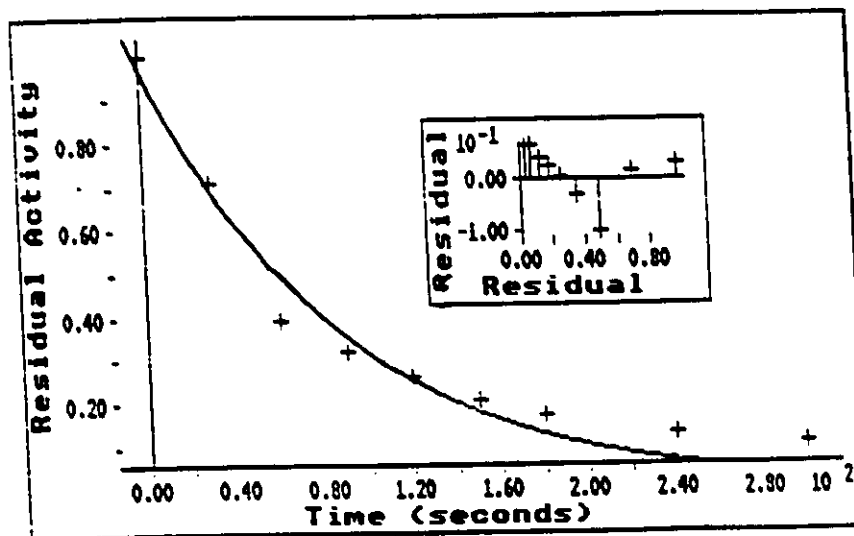


Figure I25 Plot of observed data in Table I25 fit to calculated single-exponential decay curve. Inset: plot of % residual vs. % remaining for experimental values

	Time (seconds)	Residual	Calculated
1	0.00000E+00	1.00000E+00	9.40152E-01
2	3.00000E+01	7.95900E-01	7.90211E-01
3	6.00000E+01	6.10500E-01	6.64184E-01
4	9.00000E+01	5.06500E-01	5.58256E-01
5	1.20000E+02	4.22600E-01	4.69222E-01
6	1.50000E+02	3.81300E-01	3.94388E-01
7	1.80000E+02	3.42200E-01	3.31489E-01
8	2.40000E+02	2.92400E-01	2.34185E-01
9	3.00000E+02	2.47900E-01	1.65444E-01

Table I26 Observed and calculated fractional remaining activity data vs. time used for single-exponential decay analysis: [HRP] = 100nM; [H₂O₂] = 0.5mM; [phenol] = 0.75mM. Initial value (A) = 94.02 ± 0.043.

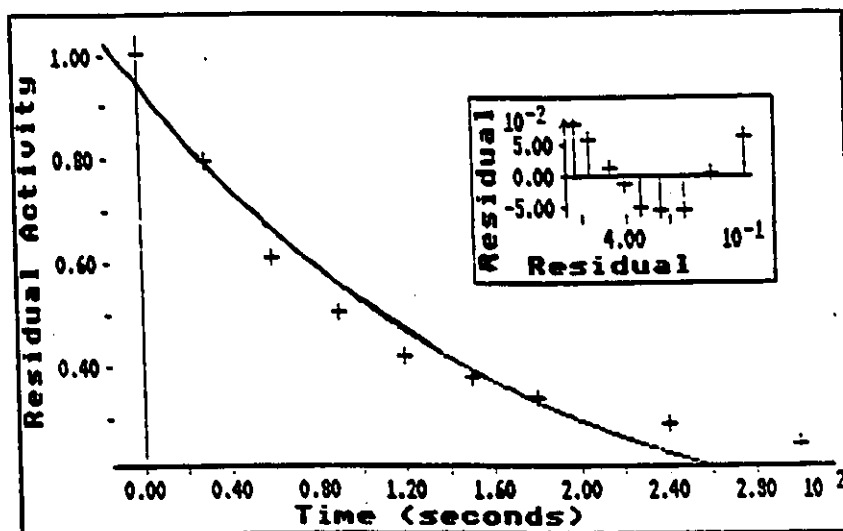


Figure I26 Plot of observed data in Table I26 fit to calculated single-exponential decay curve. Inset: plot of % residual vs. % remaining for experimental values

	Time (seconds)	Residual	Calculated
1	0.00000E+00	1.00000E+00	9.51565E-01
2	3.00000E+01	4.98000E-01	6.16956E-01
3	6.00000E+01	4.98300E-01	4.00009E-01
4	9.00000E+01	1.93900E-01	2.59350E-01
5	1.20000E+02	1.44600E-01	1.68152E-01
6	1.50000E+02	1.25700E-01	1.09023E-01
7	1.80000E+02	1.18900E-01	7.06859E-02
8	2.40000E+02	1.11000E-01	2.97142E-02
9	3.00000E+02	1.15000E-01	1.24910E-02

Table I27 Observed and calculated fractional remaining activity data vs. time used for single-exponential decay analysis: [HRP] = 100nM; [H₂O₂]=0.5mM; [phenol]=1.0mM. Initial value (A) = 96.29 ± 0.076.

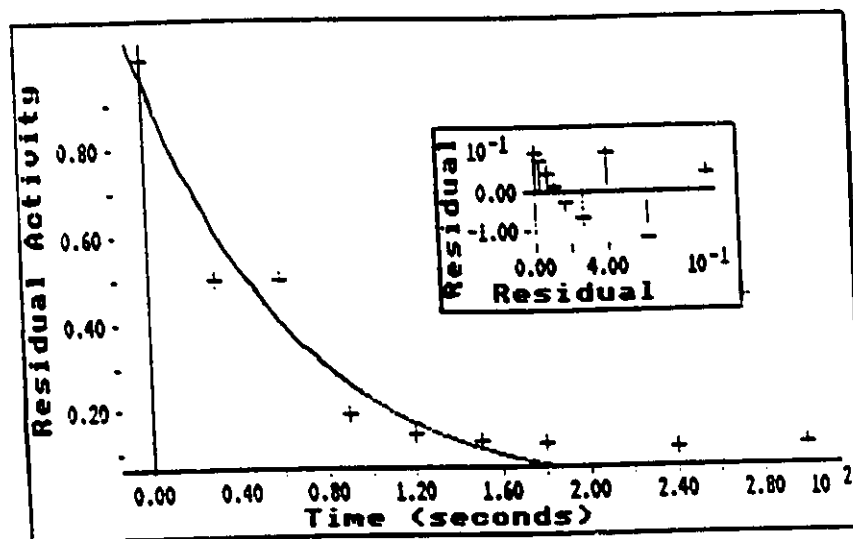


Figure I27 Plot of observed data in Table I27 fit to calculated single-exponential decay curve. Inset: plot of % residual vs. % remaining for experimental values

	Time (seconds)	Residual	Calculated
1	0.00000E+00	1.00000E+00	8.99598E-01
2	3.00000E+01	3.05300E-01	5.06954E-01
3	6.00000E+01	2.08700E-01	2.85686E-01
4	9.00000E+01	2.33100E-01	1.60994E-01
5	1.20000E+02	1.97100E-01	9.07255E-02
6	1.50000E+02	1.82500E-01	5.11269E-02
7	1.80000E+02	1.75400E-01	2.88117E-02
8	2.40000E+02	1.55200E-01	9.14976E-03
9	3.00000E+02	1.28800E-01	2.90570E-03

Table I28 Observed and calculated fractional remaining activity data vs. time used for single-exponential decay analysis: [HRP] = 100nM; [H₂O₂] = 0.5mM; [phenol] = 2.0mM. Initial value (A) = 89.95 ± 0.138.

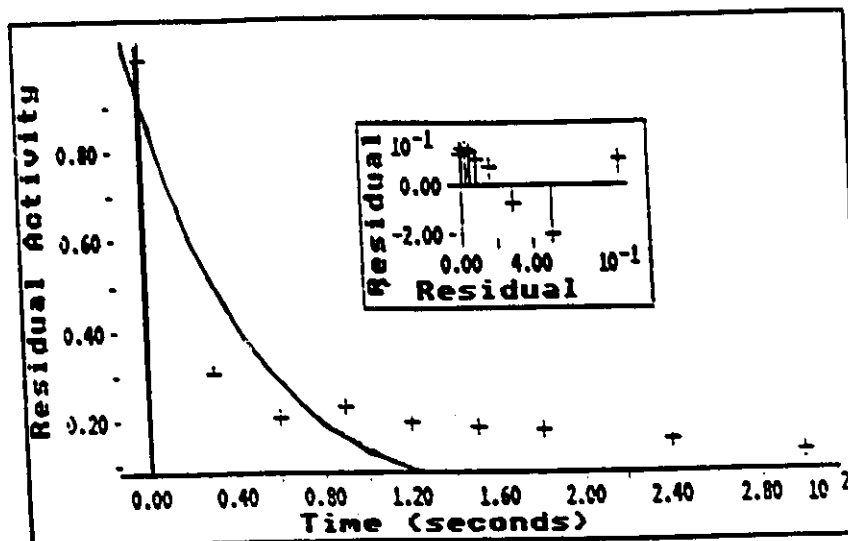


Figure I28 Plot of observed data in Table I28 fit to calculated single-exponential decay curve. Inset: plot of % residual vs. % remaining for experimental values

	Time (seconds)	Residual	Calculated
1	0.00000E+00	1.00000E+00	1.00480E+00
2	3.00000E+01	9.46300E-01	8.96303E-01
3	6.00000E+01	8.06000E-01	7.99518E-01
4	9.00000E+01	6.76000E-01	7.13184E-01
5	1.20000E+02	6.07300E-01	6.36173E-01
6	1.50000E+02	5.41000E-01	5.67478E-01
7	1.80000E+02	4.88400E-01	5.06201E-01
8	2.40000E+02	4.16000E-01	4.02782E-01
9	3.00000E+02	3.78000E-01	3.20492E-01

Table I29 Observed and calculated fractional remaining activity data vs. time used for single-exponential decay analysis: [HRP] = 100nM; [H₂O₂]=1.0mM; [phenol]=0.2mM. Initial value (λ) = 100.48 ± 0.0257.

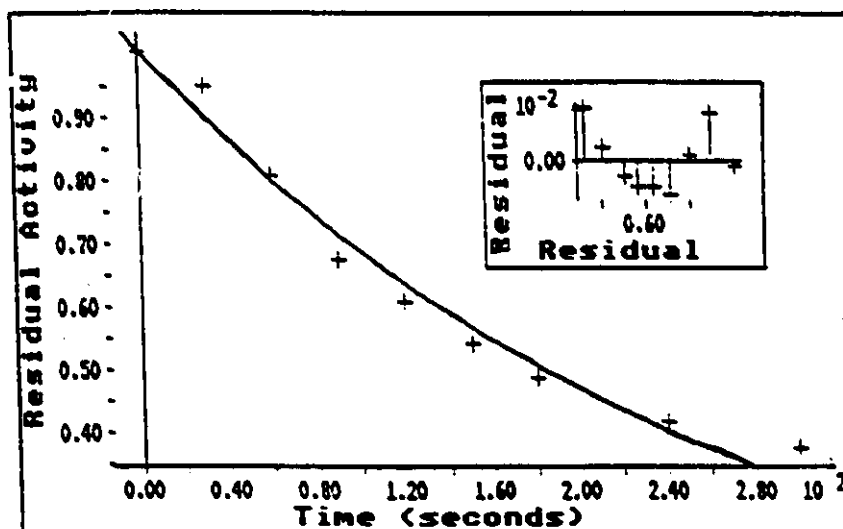


Figure I29 Plot of observed data in Table I29 fit to calculated single-exponential decay curve. Inset: plot of % residual vs. % remaining for experimental values

	Time (seconds)	Residual	Calculated
1	0.00000E+00	1.00000E+00	9.90388E-01
2	3.00000E+01	6.36000E-01	6.33442E-01
3	6.00000E+01	3.75300E-01	4.05143E-01
4	9.00000E+01	2.39300E-01	2.59125E-01
5	1.20000E+02	1.68300E-01	1.65734E-01
6	1.50000E+02	1.21000E-01	1.06001E-01
7	1.80000E+02	1.04000E-01	6.77974E-02
8	2.40000E+02	7.04000E-02	2.77342E-02
9	3.00000E+02	4.96000E-02	1.13453E-02

Table I30 Observed and calculated fractional remaining activity data vs. time used for single-exponential decay analysis: [HRP] = 100nM; [H₂O₂]=1.0mM; [phenol]=0.5mM. Initial value (A) = 99.91 ± 0.021.

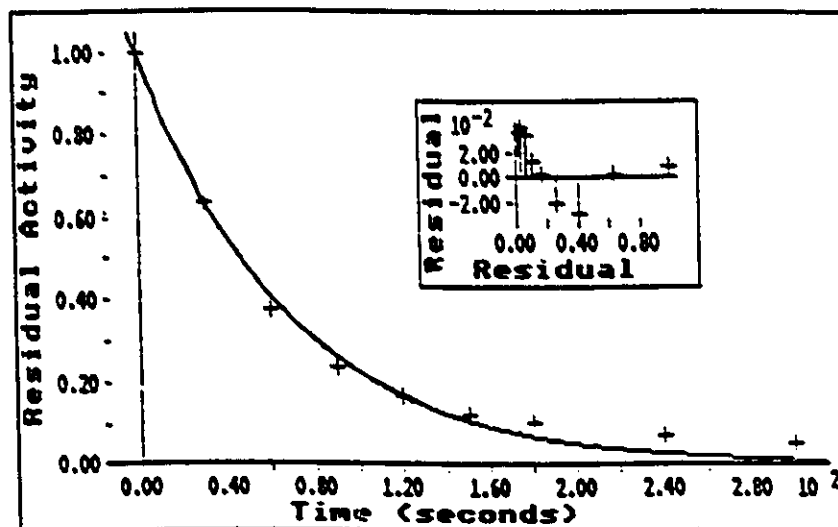


Figure I30 Plot of observed data in Table I30 fit to calculated single-exponential decay curve. Inset: plot of % residual vs. % remaining for experimental values

	Time (seconds)	Residual	Calculated
1	0.00000E+00	1.00000E+00	9.89538E-01
2	3.00000E+01	5.34000E-01	5.48229E-01
3	6.00000E+01	2.84100E-01	3.03733E-01
4	9.00000E+01	1.63200E-01	1.68276E-01
5	1.20000E+02	1.06000E-01	9.32291E-02
6	1.50000E+02	8.29000E-02	5.16513E-02
7	1.80000E+02	6.67000E-02	2.86161E-02
8	2.40000E+02	4.38000E-02	8.78356E-03
9	3.00000E+02	2.60000E-02	2.69606E-03

Table I31 Observed and calculated fractional remaining activity data vs. time used for single-exponential decay analysis: [HRP] = 100nM; [H₂O₂] = 1.0mM; [phenol] = 0.75mM. Initial value (A) = 98.95 ± 0.026.

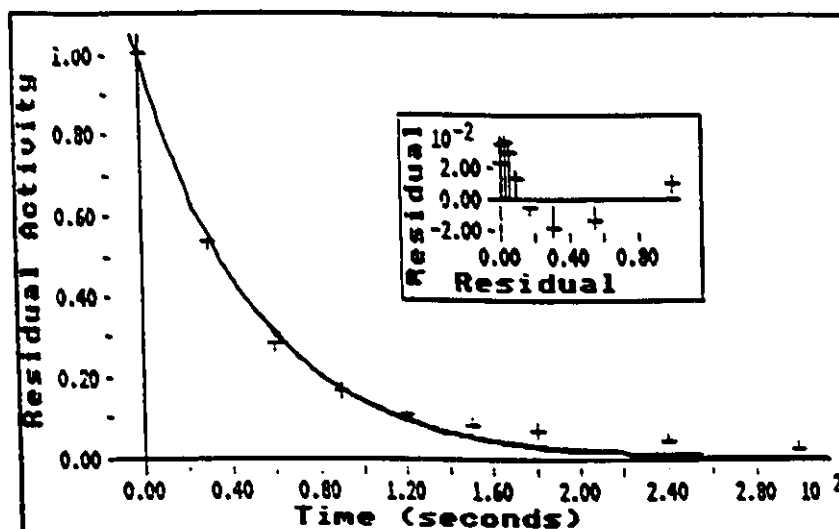


Figure I31 Plot of observed data in Table I31 fit to calculated single-exponential decay curve. Inset: plot of % residual vs. % remaining for experimental values

	Time (seconds)	Residual	Calculated
1	0.00000E+00	1.00000E+00	9.89418E-01
2	3.00000E+01	4.27000E-01	4.53228E-01
3	6.00000E+01	1.92000E-01	2.07613E-01
4	9.00000E+01	1.17400E-01	9.51023E-02
5	1.20000E+02	7.90000E-02	4.35640E-02
6	1.50000E+02	5.30000E-02	1.99556E-02
7	1.80000E+02	3.90000E-02	9.14117E-03
8	2.40000E+02	2.39000E-02	1.91812E-03
9	3.00000E+02	1.61000E-02	4.02486E-04

Table I32 Observed and calculated fractional remaining activity data vs. time used for single-exponential decay analysis: [HRP] = 100nM; [H₂O₂]=1.0mM; [phenol]=1.0mM. Initial value (A) = 98.94 ± 0.026.

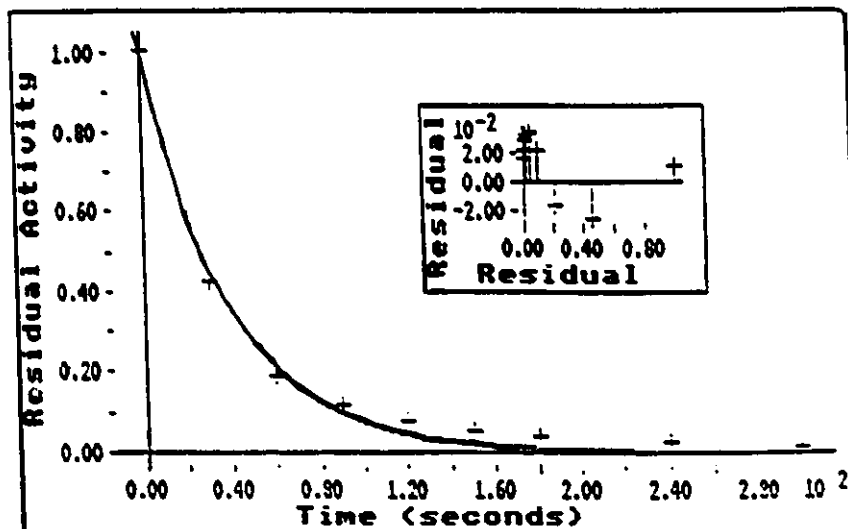


Figure I32 Plot of observed data in Table I32 fit to calculated single-exponential decay curve. Inset: plot of % residual vs. % remaining for experimental values

	Time (seconds)	Residual	Calculated
1	0.00000E+00	1.00000E+00	9.97714E-01
2	3.00000E+01	2.38400E-01	2.53901E-01
3	6.00000E+01	8.20000E-02	6.46133E-02
4	9.00000E+01	4.30000E-02	1.64430E-02
5	1.20000E+02	2.60000E-02	4.18445E-03
6	1.80000E+02	1.31000E-02	2.70991E-04

Table I33 Observed and calculated fractional remaining activity data vs. time used for single-exponential decay analysis: [HRP] = 100nM; [H₂O₂]=1.0mM; [phenol]=2.0mM. Initial value (A) = 100.91 ± 0.027.

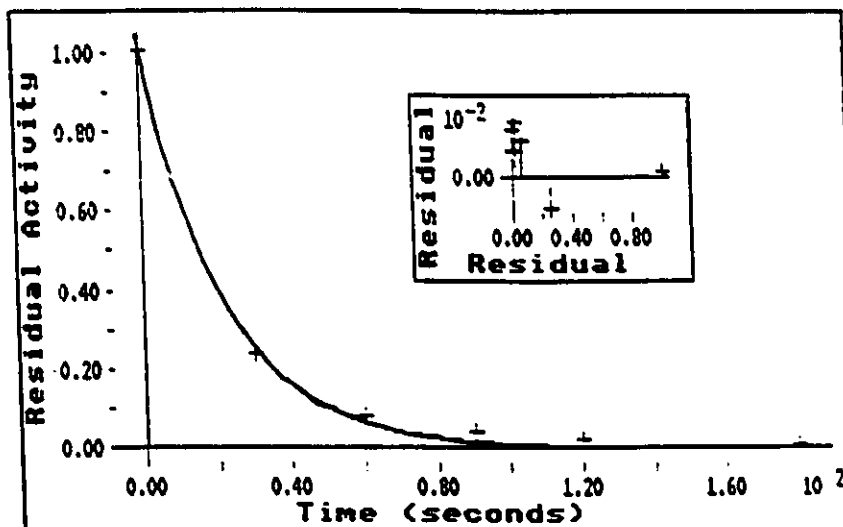


Figure I33 Plot of observed data in Table I33 fit to calculated single-exponential decay curve. Inset: plot of % residual vs. % remaining for experimental values

VITA AUCTORIS

NAME: Kathy Baynton

PLACE OF BIRTH: Chatham, Ontario; 1966

EDUCATION:

BSc. (Honours), Biology: 1986-1990
University of Windsor, Windsor, Ontario.

A.H.T. Diploma: 1984-1986
St. Clair College of Applied Arts and Technology,
Windsor, Ontario.

Ontario Secondary School Honours Diploma: 1979-1984
Chatham Collegiate Institute
Chatham, Ontario.

WORK/RESEARCH EXPERIENCE:

07/92-present	Department of Chemistry and
06/89-09/90	Biochemistry/Civil and Environmental
06/88-09/88	Engineering, University of Windsor, Windsor, Ontario:

RESEARCH ASSISTANT

01/92-06/92	Groupe de Cancérogénèse et Mutagénèse Moléculaire et Structurale, I.B.M.C. du C.N.R.S., Université Louis Pasteur, Strasbourg, France.
-------------	--

VISITING RESEARCHER

AWARDS: Natural Sciences and Engineering Research Council,
Canada (NSERC): 04/91-04/92

Rotary Club Tuition Award: 09-04/89-90; 90-91